

SOUTHWEST RESEARCH INSTITUTE®

Internal Research and Development 2013

The SwRI IR&D Program exists to broaden the Institute's technology base and to encourage staff professional growth. Internal funding of research enables the Institute to advance knowledge, increase its technical capabilities, and expand its reputation as a leader in science and technology. The program also allows Institute engineers and scientists to continually grow in their technical fields by providing freedom to explore innovative and unproven concepts without contractual restrictions and expectations.

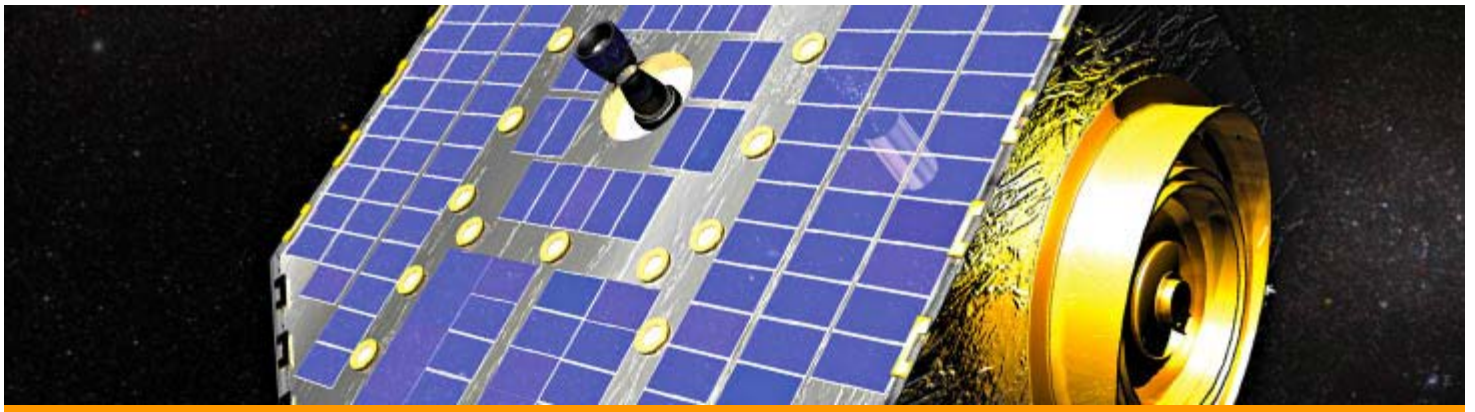


- Space Science
- Materials Research & Structural Mechanics
- Intelligent Systems, Advanced Computer & Electronic Technology, & Automation
- Measurement & Nondestructive Evaluation of Materials & Structures
- Engines, Fuels, Lubricants, & Vehicle Systems
- Geology & Nuclear Waste Management
- Fluid & Machinery Dynamics
- Electronic Systems & Instrumentation
- Chemistry & Chemical Engineering

Copyright© 2014 by Southwest Research Institute. All rights reserved under U.S. Copyright Law and International Conventions. No part of this publication may be reproduced in any form or by any means, electronic or mechanical, including photocopying, without permission in writing from the publisher. All inquiries should be addressed to Communications Department, Southwest Research Institute, P.O. Drawer 28510, San Antonio, Texas 78228-0510, action67@swri.org, fax (210) 522-3547.

SOUTHWEST RESEARCH INSTITUTE®

SwRI IR&D 2013 – Space Science



- Capability Development and Demonstration for Next-Generation Suborbital Research, 15-R8115
- Development of a Comprehensive Two-Dimensional Gas Chromatography and Mass Spectrometry Research Thrust at SwRI, 15-R8223
- Polar Regolith Environment Molecular Impact Simulation Experiment (PREMISE), 15-R8241
- Capability Development for Modeling Small Icy Satellites in the Solar System, 15-R8319
- Capability Development for Modeling Small Icy Bodies in the Solar System, 15-R8323
- Capability Development of Type II Supernova Models, 15-R8333
- Carbon Foils Properties for Space Plasma Instrumentation, 15-R8340
- TALS (Tactical Aerobotic Launch System) Evaluation and Demonstration, 15-R8346
- Fostering International Collaborations for Auroral Imaging at the European Incoherent Scatter Radar Facilities, 15-R8350
- Validating CSSS model to Investigate Slow Solar Wind Origins, 15-R8373
- Field Test of Detection and Characterization of Subsurface Ice Using Dielectric Spectroscopy, 15-R8374
- Development and Demonstration of Computer Vision Software for Solar Transient Events, 15-R8390
- Optimization of Charge Couple Device Readouts for Particle Detection, 15-R8404

SOUTHWEST RESEARCH INSTITUTE®

SwRI IR&D 2013 – Materials Research & Structural Mechanics



- Formation Impact Study of Lithium-ion Battery Capacity, Cycle Life, and Safety, 03-R8277
- Corrosion Measurements in Fuel Systems, 18-R8203
- Development of Novel Silicon Clathrates for Energy Harvesting and Storage, 18-R8279
- Fretting and Flow Assisted Corrosion Effects on Nitinol Stents for Biomedical Use, 18-R8282
- Large-Area Synthesis of Graphene for Electronic Devices, 18-R8303
- Development and Demonstration of Erosion Prediction Capabilities for Oil and Gas Industry Applications, 18-R8338
- Design, Analysis and Instrumentation of a Full-Scale Reusable Landmine Test Rig, 18-R8383
- The Development of a Dynamic Finite Element Model of the Temporomandibular Joint (TMJ) and Study of Joint Mechanics, 18-R8386
- MicroCT Investigation of Relationships in Bone-cartilage Structure, 18-R8399
- Develop Method for Hydriding Fuel Cladding and Characterize Influence of Hydriding on Mechanical Behavior, 20-R8269
- Development of Ni-Cr-Si Coatings to Resist Type II Hot Corrosion, 20-R8377

SOUTHWEST RESEARCH INSTITUTE®

SwRI IR&D 2013 – Intelligent Systems, Advanced Computer & Electronic Technology, & Automation



- Evaluating the Efficacy of a Criteria Model for Selecting Mobile Augmented Reality as a Learning Tool, 09-R8200
- High Fidelity Physics-Based Simulation of Construction Equipment, 09-R8365
- Adaptation Layer for SpaceWire Plug and Play Protocols, 10-R8216
- 3D Imaging for Behavior Classification, 10-R8221
- Special Purpose IP Routing, 10-R8243
- Secure Mobile Applications for Corporate Travelers, 10-R8244
- Investigation into Techniques for Detecting Negative Obstacles 10-R8278
- Detection of Malware on Vehicular Networks, 10-R8281
- Advanced Situational Awareness Experiment, 10-R8284
- Robotic Part Handling for Unstructured Industrial Applications, 10-R8301
- Traffic Signal Interface Concepts, 10-R8320
- ROS-Industrial® Strategic Technology Development, 10-R8335
- Feasibility Study for Embedded Software Control of Flexible RF Filters, 10-R8356
- Dynamic Real-Time Lane Modeling, 10-R8361
- Robotic Part Handling of Unstructured Materials: Semi-Random Component Pick and Place for Assembly, 10-R8369
- Control of Laser Coating Removal Process, 10-R8385

- Phasor Measurement Units Time Synchronization Attack, Detection, Protection and Control, 10-R8393
- Wireless Protocol Fuzzing Framework, 10-R8401
- Efficient Methods for Uncertainty Propagation in Computational-Fluid-Dynamics-Based Fire PRA, 20-R8271

SOUTHWEST RESEARCH INSTITUTE®

SwRI IR&D 2013 – Measurement & Nondestructive Evaluation of Materials & Structures



- [Next-Generation Neutrally Buoyant Sensors, 10-R8274](#)
- [Guided Wave Imaging Technology Development, 18-R8289](#)
- [EDAS-MS Upgrade and Demonstration Program, 18-R8367](#)

SOUTHWEST RESEARCH INSTITUTE®

SwRI IR&D 2013 – Engines, Fuels, Lubricants, & Vehicle Systems



- Severe Downsizing of a Three-Way Lean NO_x Trap (3wLNT) Diesel Engine, 03-R8293
- Diesel Cold Start Emission Control Research for 2015-2025 LEV III Emissions, 03-R8299
- D-EGR WGS Catalyst Development and Optimization, 03-R8326
- Development of Advanced Analysis of Aluminum Cylinder Heads, 03-R8364
- Development of a Methodology to Generate On-Board Diagnostic Threshold Selective Catalytic Reduction Catalysts for Heavy-Duty Diesel Applications, 03-R8376
- Investigation of an Oleophobic Coating Effect on Gasoline Direct Injection (GDI) Engine Components to Reduce Carbon Deposits, 08-R8362



- Integrity Management of Nuclear Power Plant Components Subjected to Localized Corrosion Using Time-Dependent Probabilistic Model, 20-R8267
- Development of an Integrated Numerical Framework for Tsunami Hazard Assessment at Nuclear Installations, 20-R8268
- Soil-Structure Interaction Assessment of New Modular Reactors, 20-R8270
- Chemical-Based Tertiary Oil Recovery from Carbonate Rocks, 20-R8348
- Integrated Physical Analog and Numerical Modeling of Geologic Structures, 20-R8368
- Hypothesis Testing for Subfreezing Mass Movements, 20-R8407



- [An Experimental Facility and Analytical Methodology for Determining Frequency-Dependent Force Coefficients of Foil Gas Bearings, 18-R8189](#)
- [A Comprehensive Approach to Predicting Vortex-Shedding-Induced Pulsation Amplitudes in Piping Systems, 18-R8325](#)
- [Improvement of Wet Gas Compressor Performance Using Gas Ejection, 18-R8327](#)

SOUTHWEST RESEARCH INSTITUTE®

SwRI IR&D 2013 – Electronic Systems & Instrumentation



- [Alternative Advanced Electronic Countermeasure Techniques, 09-R8349](#)
- [GPS-denied Localization System, 10-R8248](#)
- [Microwave Methods for Enhanced Combustion in Natural Gas Engine Applications, 10-R8408](#)
- [Development of a Wireless Power Transfer Technique for Quick-Charging Inaccessible Electronic Devices, 14-R8363](#)
- [Scaling Kinetic Inductance Detectors \(KIDs\), 15-R8311](#)
- [Capability Development for Extreme Ultraviolet Imaging and Calibration, 15-R8322](#)

SOUTHWEST RESEARCH INSTITUTE®

SwRI IR&D 2013 – Chemistry & Chemical Engineering



- Develop Transplantable Vascularized Cell Constructs to Accelerate Wound Healing, 01-R8214
- Metabolomics of Radiation Exposed Rats, 01-R8259
- Combined Laser and Medicated Scar Therapies, 01-R8276
- Applied Dermal Delivery Nano-Formulations, 01-R8321
- Photoresponsive Polymeric Composites Utilizing UV Light Harvesting from Upconverting Nanoplatelets, 01-R8334
- A New Generation of Bone Cements/Grafts Based on Magnetic Calcium Phosphate Nanoparticles (MCP NPs) Using a Magnetic Field-Triggered-Polymerization (MFTP) Process, 01-R8370
- Drug-loaded Magnetic Calcium Phosphate Nanoparticles (MCP NPs) for Cancer Therapy, 01-R8400
- Determination of PAHs in the Rubber by GC/MS, 08-R8402

2013 IR&D Annual Report

Capability Development and Demonstration for Next-Generation Suborbital Research, 15-R8115

Principal Investigator

S. Alan Stern

Inclusive Dates: 01/01/10 – Current

Background — Research applications for new-generation suborbital vehicles include microgravity sciences, space life sciences, Earth and space sciences, land use, education and public outreach (EPO), technology development and space systems development and demonstrations (including TRL raising). The primary research advantages of these vehicles include more frequent access to the space environment, lower launch cost compared to conventional sounding rockets, capability for human operator presence, better experiment affordability, gentler ascent and entry compared to sounding rockets, extended periods of turbulence-free microgravity and increased time in the 250,000 to 400,000 ft (80 to 120 km) region of the atmosphere (the "Ignorosphere").

Approach — SwRI's long-term business interests in these vehicles are:

- To exploit them for planetary, microgravity, aeronomical and auroral research.
- To provide research-related common systems (flight computers, data recording racks, etc.) and payload integration services to NASA and/or vehicle providers.
- To provide instrumentation, payload specialists and flight project expertise to research groups, both domestic and overseas, working in this area.

Therefore, the overarching objective for this project is to put SwRI in the lead of the burgeoning suborbital research field using next-generation, manned vehicles by becoming one of the first, and quite possibly the first, organization to fly payloads with research payload specialists on these vehicles. This will open up to SwRI a series of new business opportunities including funded research projects, hardware development projects, ground and flight system task order contracts associated with next-generation suborbital work, and providing payload specialists for next-generation suborbital flights.

Accomplishments — Accomplishments on this project for this year include:

- Met with flight providers XCOR and Virgin Galactic to obtain flight integration timelines and experiment documentation flight requirements (February 2013).
 - Requested and received flight integration requirements documents and initiated work to complete these documents.
 - Clarified crew training requirements with both XCOR and Virgin Galactic.
 - Checked out all three SwRI flight experiments after more than a year in storage.
 - Reported on the progress of SwRI's commercial suborbital program at the NSRC-2013 meeting (250+ participants).
 - Attended September 2014 meeting in Mojave, Calif., for Virgin Galactic flight customers.
 - Presented three public talks on the SwRI Suborbital Program at local clubs/organizations.
 - Attended an invited panel presentation and discussion on the SwRI Suborbital Program at Spaceup Houston 2013 Commercial Spaceflight event (February 2013).
 - Received the latest version of the XCOR Lynx Payload User's Guide (September 16, 2013 – v.4).
 - Participated in a workshop on planetary science applications in suborbital science at the annual Division for Planetary Sciences meeting held October 6, 2013, in Denver.
-

2013 IR&D Annual Report

Development of a Comprehensive Two-Dimensional Gas Chromatography and Mass Spectrometry Research Thrust at SwRI, 15-R8223

Principal Investigators

[Mark Libardoni](#)

Kristin Favela

Inclusive Dates: 04/06/11 – Current

Background — Volatile and semi-volatile organic compounds are some of the most widely studied samples. Traditional analytical methods rely on single dimension gas chromatography (GC) coupled to selective detectors or mass selective detectors (MS). More recently, the use of comprehensive two-dimensional gas chromatography (GCxGC) as an advanced analytical tool has gained significant popularity for complex sample analysis, target species in a heavy matrix, and screening of difficult samples compounds below traditionally reported LODs. Recent advances to GCxGC instrumentation have made this technique more robust to routine analysis, complex sample screening and the simultaneous quantitative detection of compounds found within. This multi-year project will introduce GCxGC to SwRI and explore the opportunities that make it a viable analytical tool for advanced analysis of complex mixtures, trace level detection of target compounds and future hardware development for space applications.

Approach — The development of a GCxGC thrust at SwRI is divided into two sub-projects. The first is establishing GCxGC as a routine analytical tool, thus increasing the outreach exposure and analytical capabilities of the Institute to provide advanced separation techniques to current and future clients. Application avenues in the field of metabolomics (small molecule metabolites for healthy and diseased states) as well as environmental screening are being investigated and pursued. The second sub-project involves developing advanced GCxGC methodology and space flight hardware. Sample inlet systems, thermal and valve-based modulator development to support portable and flight-ready GCxGC systems as well as advanced detectors are being investigated.

Accomplishments — Researchers successfully demonstrated the use of GCxGC in metabolomic and environmental samples. A GCxGC developmental laboratory has been established where students and scientists are working on advanced methodology and hardware support projects. Both efforts have let to establishing contacts with clients, resulting in collaborative projects.

2013 IR&D Annual Report

Polar Regolith Environment Molecular Impact Simulation Experiment (PREMISE), 15-R8241

Principal Investigators

Edward L. Patrick

Kathleen Mandt

Stephen Escobedo

Joseph Mitchell

Gregory Winters

Gregory Miller

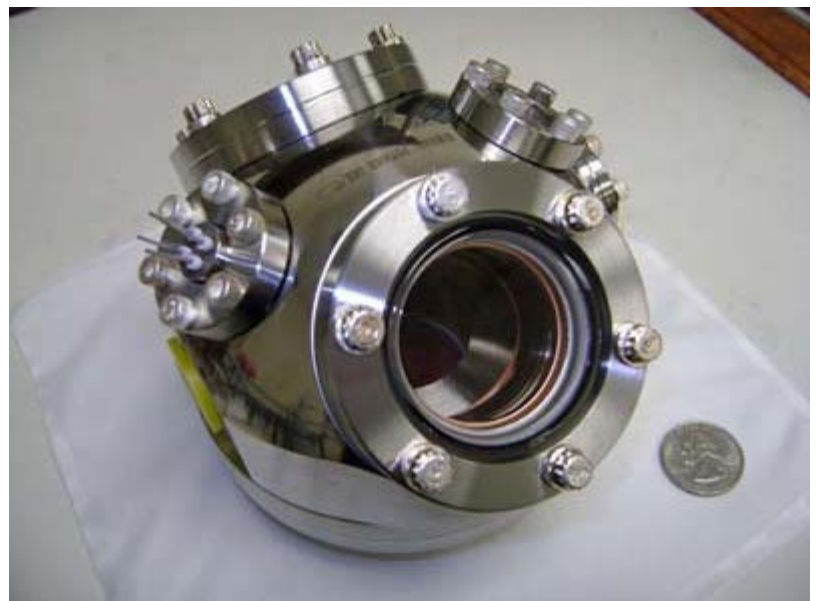
F. Scott Anderson

Inclusive Dates: 07/01/11 – 1/02/13

Background — Evidence for water found in the polar regions of the Moon (LRO/LCROSS) and Mercury (MESSENGER) has triggered a renaissance in the study of these regolith environments. In the case of the Moon, the surface has not been probed by mass spectrometry since the Apollo 17 mission more than 40 years ago. Water at the lunar surface provides an essential natural resource needed for extended human presence and also provides a source for the production of hydrogen (H₂) and oxygen (O₂) for fuel cells or as a spacecraft propellant. The motivation for this project was the interest in simulating the lunar surface environment and how water (H₂O) and other volatiles (CO₂, CH₄, etc.) are trapped there, and also to determine the best sample handling protocol to use at the lunar surface to release those volatiles to a landed mass spectrometer instrument.

Approach — A quantity of JSC-1A lunar soil simulant was deposited into a custom-fabricated, gold-plated copper sample cell and placed within a vacuum system where the simulant was desiccated by bakeout in excess of 100°C and evacuated until a base pressure of 1x10⁻⁸ Torr was obtained. A residual gas analyzer (RGA) quadrupole mass spectrometer (QMS) with 0 to 300 dalton mass resolution was integrated to the system to provide a log of the simulated lunar exosphere appearing above the surface of the simulant. A UV laser was used to test laser ablation of the simulant surface as a means of producing detectable gas plumes at the mass spectrometer. The original intent was to cool the sample cell to cryogenic temperatures to simulate surface

conditions at the lunar poles. However, after exhaustive tests, persistent atmospheric gas peaks appearing in the mass spectrum of the chamber at room temperature led to the conclusion that these gases were evolving from the lunar simulant. Laser ablation was attempted as a means to produce increased signal at the mass spectrometer, but the intensity of the ablation plume was so great as to



Soil Sample Chamber

require abandoning the method. Subsequent inspection of the laser-ablated surface with a flashlight produced an inexplicable jump in background pressure. Despite the presence of persistent gas peaks, pure gases and gas mixtures were introduced to the simulant through a leak valve to produce, in a typical experiment, chamber pressures of approximately 3×10^{-8} Torr for a total of 10 minutes. Some of the gases showed no persistence based upon mass spectrometer scans. However, other gases did show persistence and suggested that adsorption of the molecules took place at the surface of one or more mineral phases in the grains. All of these tests were performed at room temperature, suggesting that an increased residence time exists for some gases within the lunar regolith with a potential for affecting volatile evolution even at temperatures far above those found at the lunar poles.

Accomplishments — Results of tests exposing the simulant to various gases and to photon sources are currently pending publication. A preliminary design for a prototype lunar mass spectrometer was completed to support future lunar mission proposals, and the results have implications for future studies of the lunar surface using mass spectrometers. Results from this experiment supported submission of a proposal to the NASA Research Opportunities in Space and Earth Sciences (ROSES) Lunar Advanced Science and Exploration Research (LASER) program and will also contribute to the submission of another LASER study proposal in February 2014.

2013 IR&D Annual Report

Capability Development for Modeling Small Icy Satellites in the Solar System, 15-R8319

Principal Investigators

[Raymond Goldstein](#)

Daniel Boice

Inclusive Dates: 06/20/12 – 10/20/12

Background — Data from the Cassini spacecraft have transformed our view of the Saturnian system, including its icy satellite, Enceladus. The surprise discovery was the observation of plumes of material being emitted from a region near the south pole of Enceladus, later identified as composed primarily of water with entrained grains, likely of ice and dust. Similarities to activity of comets abound. Almost two-dozen flybys of Enceladus have provided a host of measurements of neutral and ion composition and dynamics in its surrounding environment. Moreover, a detailed understanding of how gas in the plumes and plasma in the environment surrounding Enceladus interact is lacking. SwRI's experience with modeling chemistry in cometary atmospheres allows for a unique quantitative approach to address key issues regarding the plumes of Enceladus and its surroundings.

Approach — The available composition data obtained by the Cassini Plasma Spectrometer (CAPS) during the fifth Enceladus flyby (E5) was analyzed using a chemical dynamics model originally developed for comets to understand the processes that produce the observed ion composition. The combination of this unique data set together with a novel modeling approach originally developed for chemistry in comets has been used to address key outstanding issues regarding this icy satellite. The sophisticated chemical model presents a powerful new tool with which to understand the complexity of the ion-neutral, gas-plasma interactions and to contribute significantly to understanding Enceladus and its surrounding environment.

Accomplishments — Comparisons were made between the new model results and the CAPS data analysis. The model has been enhanced by the inclusion of energetic electrons that surround Enceladus in the E-ring of Saturn as described by Cravens et al. (2011). These hot electrons interact primarily with the plume species via electron impact reactions. Additional electron impact reactions were added to the chemical network of the SwRI code to properly account for them. They produce another source of water group ions and further dissociate the neutral water, resulting in the formation of more H_2O^+ , OH^+ , and O^+ at the expense of H_3O^+ . This results in the improved agreement of the current model with the preliminary model without the hot E-ring electrons (Boice and Goldstein 2010). These results are encouraging even though there is work to be done concerning OH^+ and O^+ . This will make an intriguing issue to be addressed in a proposal submitted to NASA for future work.

2013 IR&D Annual Report

Capability Development for Modeling Small Icy Bodies in the Solar System, 15-R8323

Principal Investigators

[J. Mukherjee](#)

Daniel Boice

W. Huebner

J. Benkhoff (ESA ESTEC)

H. Kawakita (Kyoto Sangyo Univ.)

C. Western (Univ. Bristol)

Chris McKay (NASA Ames)

Inclusive Dates: 07/01/12 – 07/01/13

Background — In 2011, the bright comet Lovejoy made a very close encounter with the Sun, providing a rare opportunity to study the physical properties of sungrazing comets and their coupling to the near-solar environment. Multiple spacecraft observed Lovejoy's perihelion passage at a variety of wavelengths with spatial resolution. There is much to be learned from this and other sungrazers; however, no comprehensive model exists to aid in the interpretation of these observations. Phosphorus is a key element in all known forms of life, and phosphorus-bearing compounds have been observed in space. It is ubiquitous in meteorites, and it has been detected as part of the dust component in comets, but searches for P-bearing species in the ice phase in comets have been unsuccessful.

Approach — The goal of this project is to adapt SwRI's general-purpose simulation code of the physical and chemical processes in comets to study the sungrazing comet Lovejoy and the phosphorous chemistry of comets with implications to astrobiology. The innovative model that results will combine SwRI's codes with two codes supplied by collaborators, extending and enhancing SwRI's existing capabilities. No computer model currently exists that is capable of addressing the key physical processes and conditions that are thought to be relevant in sungrazing comets in a self-consistent manner as well as likely phosphorous chemistry in comets. Software will be developed that facilitates the comparison of model predictions with ground-based spectral observations needed to reap the full benefits of the model and foster collaborations with observers. The resulting Universal Virtual Spectrometer (UNIVERS) software will be used to address key science issues.

Accomplishments —

- Developed a comet model for sungrazing comets by including thermodynamic data for cometary dust that undergo sublimation in the extreme thermal environment experienced by a sungrazer and considered secondary ionization and dissociation processes by energetic photoelectrons.
- Created the web interface for UNIVERS on a Linux-based server. Sample model output has been used to successfully test the web interface and different aperture sizes have been implemented for development of the instrument modules.
- Calculated reaction pathways of gas-phase and photolytic chemistry for simple P-bearing molecules likely to be found in comets and important for prebiotic chemistry. The big astronomy news was the surprising discovery of a new sungrazing comet, C/2012 S1 (ISON) that will heighten interest in this work.

2013 IR&D Annual Report

Capability Development of Type II Supernova Models, 15-R8333

Principal Investigator

[Amanda Bayless](#)

Inclusive Dates: 09/17/12 – 01/17/13

Background — An enduring problem in understanding our cosmic origins is to understand the processes by which heavy elements, the building blocks of life and planets, are created and distributed throughout the universe. We now know that many of these heavy elements are created in the final stages of a massive star's life and released into the surrounding environment when the nuclear reactor stellar core explodes as a supernova. These stars were between eight and 100 times the mass of the Sun and release $\sim 10^{51}$ ergs/s, or about the energy of 10^{30} atomic bombs. This is enough energy to create heavy elements through neutron fusion and beta decay. Despite our progress in understanding, the mechanisms by which a star explodes and how the elements are distributed are not well understood. The information we have primarily comes from observations and spectra showing the change in brightness over time and the elemental content at the edge of the supernova. These observations do not give us direct information on the internal processes of the explosion or information about the star that exploded, which are crucial for understanding the life cycle of massive stars. A comprehensive model of the explosion is needed to fully understand how and why the most massive stars end their life catastrophically.

Producing a computer model for supernovae that matches observational data is a very difficult problem. Due to limited computational resources, most numerical models incorporate only one or two of the following critical physical laws: magneto-hydrodynamics, radiative transfer, nuclear processes, or atomic transitions. These limitations are accommodated by making basic uniform assumptions about the dynamics, opacities and wavelength dependencies. Nevertheless, these assumptions frequently affect the accuracy of key parameters, such as the energetics of the supernova and the initial mass, radius, etc., of the star. The mass range alone for a star can vary over a magnitude in parameter space, and often there is no *a priori* information, resulting in an extensive search of parameter space. This search can be months of computing and personnel resources, with no guarantee that the final model fit is a unique solution.

Approach — The proposed solution is to use a modeling code that incorporates all of the critical physics, not just a subset; use a state-of-the-art computational resource required by such a code; and create a database of models from this code, filling a reasonable range of parameter space, to minimize the need for future computational resources. The database of models that will ultimately be created will be quickly searchable, giving an almost immediate, excellent constraint and understanding of supernovae discovered in the future. This database of models will be available publically in the form of a coarse grid in parameter space. The refinement of the model fits using the new code can only occur with SwRI and LANL collaboration.

Accomplishments — The first paper that is a direct result of this effort has been submitted. Four proposals resulted from this work.

2013 IR&D Annual Report

Carbon Foils Properties for Space Plasma Instrumentation, 15-R8340

Principal Investigators

Frédéric Allegrini

Kent Coulter

Inclusive Dates: 10/01/12 – Current

Background — Carbon foils are critical components in many space plasma instruments built at SwRI. They are used to detect particles — ions, electrons, or neutral atoms — that pass through by a coincidence measurement and/or to determine their speed with a time-of-flight (TOF) measurement. There are many effects resulting from the interactions of ions with carbon foils, for example, energy straggling, angular scattering and charge exchange of the ion, and secondary electron emission from the foil. All of these effects have been studied for different parameters, such as ion mass and energy, and for different carbon foil thicknesses. However, there are still significant gaps in the literature and, in particular, for the thin carbon foils used in SwRI's instruments (nominal $0.5 \mu\text{g}/\text{cm}^2$, which corresponds to about 2 to 3 nm). Moreover, the different characteristics of the interactions of ions with carbon foils have been investigated in most cases for only one variable at a time. Little information is found about energy straggling as a function of angular scattering or charge state of the particle after passing through the foil. This project is about measuring these effects and the relationship between them.

All these effects scale with foil thickness, which is why SwRI uses the thinnest practical foils to mitigate the impact of the unwanted effects (e.g., energy straggling, angular scattering) on the performance of its instruments. Ultra-thin carbon foils are difficult to handle and can have intolerable defects (e.g., pinholes, tears). A small increase in thickness reduces the amount of defects and can make a big difference in the handling and robustness of the foils. It is not clear what the impact of a small increase of thickness has on the unwanted effects and on the amount of defects. This project is also about acquiring data to better guide the choice of foil thickness. This will help in selecting the optimal foil thickness for future designs of space plasma instruments.

Approach — The project had four objectives:

- Measure energy loss of ions as a function of exit angle and charge state for different species, energies, and foil thicknesses.
- Measure angular scattering of ions as a function of incident energy and foil thickness for different species.
- Measure foil composition and surface properties using X-ray photoelectron spectroscopy, Fourier transform infrared spectroscopy, Raman spectroscopy and energy dispersive spectroscopy.
- Measure carbon foils resistance to static pressure.

Accomplishments — The experimental setup for the first objective is functional and data is being taken. In particular, the energy straggling was measured as a function of angle for hydrogen ions passing through a nominal $1 \mu\text{g}/\text{cm}^2$ carbon foil. Significant progress was also made on the other objectives. The scattering angle distribution was measured for different species (H, He, C, N, O, Ne, and Ar) in the energy range from 1 to 50 keV for different foils thicknesses between 0.5 and $2.5 \mu\text{g}/\text{cm}^2$. The surface properties of a couple of foils were measured using the techniques listed above. And the resistance to static pressure of about 25 carbon foils of different thicknesses was measured. The project is currently on-going and all objectives are being pursued.

2013 IR&D Annual Report

TALS (Tactical Aerobotic Launch System) Evaluation and Demonstration, 15-R8346

Principal Investigators

[William D. Perry](#)

David Lopez

Michael L. Fortenberry

Inclusive Dates: 10/10/12 – 02/10/13

Background — The process for inflating and launching most Lighter-than-Air (LTA) systems presently requires a large paved or grassy area that is clear of obstructions, where the hull can be unpacked and laid out in preparation for inflation. This process typically must be conducted inside a very large hangar or outdoors under very low wind conditions since these hulls can be several hundred feet in length and made from very lightweight material. Inflating and launching takes time, leaving the hull at risk of damage from wind gusts. Usually it requires large handling equipment, along with an experienced launch team to get the LTA system launched without damage. Most military applications would prefer to deploy LTA systems quickly from remote unimproved sites, with minimum personnel with limited training. This is not possible using current inflation and launch processes.

SwRI devised the Tactical Aerobotic Launch System (TALS) concept for rapidly launching LTA systems from a self-contained package that provides inflation, stabilization, protection and finally release. TALS can be operated by a small team and will provide remote-controlled or autonomously launching of LTA systems on command. The concept is adaptable to launching balloons, airships and aerostats. In February 2012, SwRI completed an internal research project to develop this concept to address the need for a method of quickly launching LTA vehicles. Under project 15-R8226, the concept for the TALS was completed along with a working 35-percent scale demonstration model. The TALS demonstrator was tested extensively in the laboratory to verify function of the control system and software, but the team only conducted two field tests under light wind conditions. While these tests were mostly successful with only a few problems, it was clear that the system was not ready to be demonstrated and additional testing and refinements were needed. This project was awarded in October 2012 to fund additional testing and preparation for an on-site demonstration.

Approach — The goal of this project was to refine the TALS hardware and software in preparation for a demonstration of the systems. A series of lab and field tests would be conducted to evaluate the performance under a range of conditions, resulting in changes to the system to improve the reliability and performance.

This project was conducted in three phases:

- Upgrade the TALS based on results of earlier field tests.
- Conduct additional tests under a variety of wind conditions and refine TALS based on the results.
- Conduct demonstration for representatives of the military.

The figure below shows the automated inflation and launch sequence during the TALS demonstration.



TALS Demonstration of an Automated Inflation and Launch of an Airship

Accomplishments — Under this project, TALS was upgraded and 20 laboratory tests and 4 field demonstrations of the TALS were conducted. A TALS demonstration video was produced and distributed. This project allowed for additional field testing under a variety of wind conditions. It also allowed the TALS operations to be refined to reduce the risk of problems during the formal demonstration. An on-site live demonstration of the 35-percent scale TALS for representatives from the Department of Defense encompassing the U.S. Army Space and Missile Defense Command, Defense Advanced Research Projects Agency and the Office of the Secretary of Defense. The live demonstration was canceled due to travel restrictions for DOD personnel resulting from the "sequester." A video of the TALS demonstration was distributed to the DOD representatives and was received with great interest. SwRI was asked to submit an estimate for building and demonstrating a full-scale TALS.

2013 IR&D Annual Report

Fostering International Collaborations for Auroral Imaging at the European Incoherent Scatter Radar Facilities, 15-R8350

Principal Investigators

[Robert G. Michell](#)

Marilia Samara

Inclusive Dates: 11/15/12 – 03/15/13

Background — The primary objective of this project is to demonstrate the observational capability and to organize the needed collaborations across several different countries to prepare a strong NSF Science Across Virtual Institutes (SAVI) proposal. The main science driving the collaboration revolves around imaging the auroral fine structures visible at the EISCAT radar sites and how the optical structures relate to features observed in the radar data. This is being used as a seed topic to demonstrate the advantages of such global collaborations on a single campaign relating to a specific science topic.

Approach — The main approach included several steps. In the first step, two imagers were set up at the Tromso EISCAT Radar site in Norway and operations were coordinated with the European EISCAT radar users. A dedicated observing campaign was then conducted from Tromso in mid-January, where SwRI researchers were on site to change settings and filters to optimize the scientific return and also to determine real-time the best conditions for using the allotted radar time. SwRI was granted 24 hours of dedicated time on the EISCAT radars. In addition, researchers operated other imagers in Alaska to observe the global nature of the aurora, as the EISCAT sites are located approximately 12 hours different from Alaska, making observations possible on opposite sides of Earth.

Accomplishments — Initial analysis has yielded many very good examples of auroral events over the EISCAT radars. SwRI is collaborating with several scientists in Tromso on data analyses. In addition, researchers gained experience using the software for analyzing the radar data, which is different from the NSF-operated radars. A white paper was submitted to NSF outlining SwRI's idea for a SAVI proposal, and SwRI is awaiting their response and comments for submitting a full proposal.

2013 IR&D Annual Report

Validating CSSS model to Investigate Slow Solar Wind Origins, 15-R8373

Principal Investigators

Bala Poduval

Craig E. DeForest

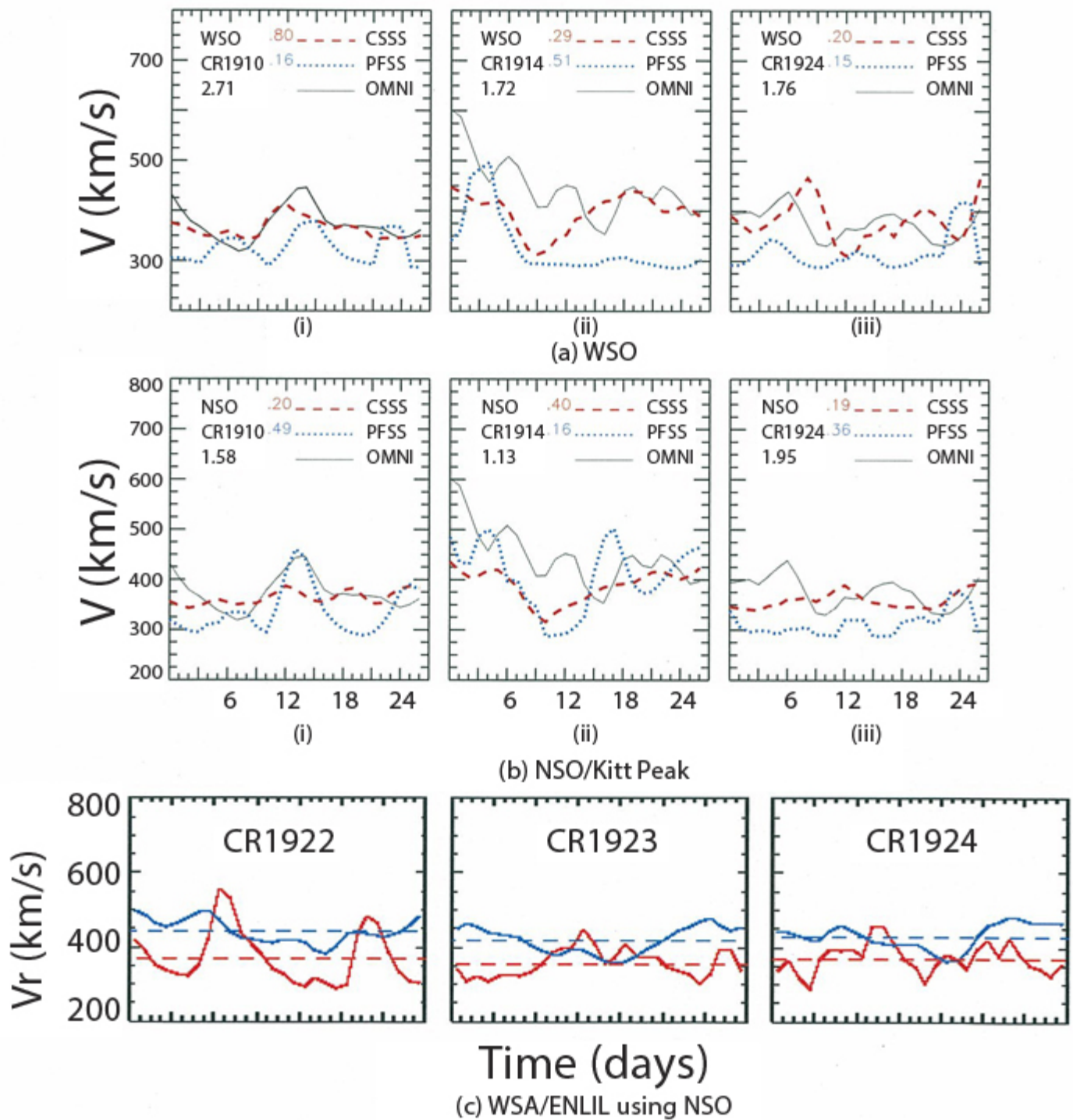
Inclusive Dates: 02/18/13 – 06/18/13

Background — The existence of the solar wind — the supersonic expansion of corona out into the heliosphere — was established more than a half-century ago. Still, the nuances of the mechanism that gives rise to the two distinct components with differing physical properties, the slow and the fast winds, are not completely understood. The fast wind has been identified as emanating from the coronal holes, but the origin of slow solar wind remains controversial and is the most debated topic in solar physics. Fluctuations in solar wind, termed space weather, triggered by solar transient events cause magnetospheric and ionospheric disturbances leading to disruption and damage to electrical and electronics systems on Earth. Monitoring space weather and making accurate forecasts well ahead of time is required to protect them. WSA-ENLIL, the two-part space weather prediction model, is the state-of-the-art prediction scheme. The semi-empirical WSA (Wang-Sheeley-Arge) model provides an approximate outflow as the inner boundary condition for ENLIL, a sophisticated three-dimensional magnetohydrodynamic (MHD) model that predicts space weather conditions in the near-Earth environment. However, because of discrepancies between the predictions of WSA and the observed solar wind, there are ongoing efforts to improve the inner boundary conditions for ENLIL. The CSSS (Current Sheet Source Surface) model has been shown to perform better than the WSA model and will be a better alternate for driving ENLIL.

Approach — To validate the CSSS model, the predicted solar wind was compared with the observed solar wind near Earth's orbit. For the solar wind predictions, the inverse correlation between solar wind speed and the flux tube expansion (FTE) factor was used and is defined as:

$f = (R_{Sun}/R_{ss})^2 * (B_{r(phot)}/\{B_{r(ss)}\})^2$, where R_{Sun} is the radius of the Sun, R_{ss} is the radius of the source surface, and $B_{r(phot)}$ and $B_{r(ss)}$ are the magnetic field on the photosphere and the source surface. The validated CSSS model was then used to investigate the slow solar wind-pseudostreamer (regions of close magnetic field configuration between open field regions of like polarity) association.

Accomplishments — Flux tube expansion was computed at the source surface and a best-fit curve was obtained, $v_{sw} = af^2 + bf + c$, where v_{sw} is the solar wind speed and f , the flux expansion factor. The coefficients a , b and c are 90.1, -473.2 and 808.2, respectively. The CSSS model (dashed line, left panels) predicts the solar wind with greater accuracy, by nearly a factor of two, than the WSA model (dotted line, right panels) as shown in the illustration, for selected Carrington rotations (CR) as marked. Here the solid line depicts the observed solar wind speed. The correlation coefficients between the observed and predicted speeds are shown inside each panel. Using the validated CSSS model, the slow solar wind-pseudostreamer relationship was studied by inverse mapping the observed slow solar wind to the source surface and obtaining the magnetic configuration of the corresponding region. Results showed about 70 percent of the slow solar wind in the range 350 to 450km/s was found to correspond to pseudostreamers, while about 30 percent was traced to the center of a unipolar open field region, which was unexpected. To pursue this aspect further a proposal has been submitted to NASA.



Observed solar wind speed in comparison with speed predicted by the CSSS (red dashed lines) and PFSS (blue dotted lines) models, using WSO (panel a) and NSO synoptic maps (panel b). The WSA/ENLIL predictions (blue lines) in comparison with observed (OMNI: red lines) solar wind speed is depicted in panel c; see text for details.

2013 IR&D Annual Report

Field Test of Detection and Characterization of Subsurface Ice Using Dielectric Spectroscopy, 15-R8374

Principal Investigators

[Robert E. Grimm](#)

David E. Stillman

Inclusive Dates: 03/12/13 – 07/12/13

Background — Measuring ice content in permafrost is important to understanding the impact of permafrost melting on the global carbon inventory and the ecology of polar regions. There is further value to civil engineering by assessing the risk to structures due to frost heave and bulk ice melting. Furthermore, non-invasive instruments can measure the heterogeneity of subsurface ice on Mars and in some permanently shadowed craters on the Moon. Geophysical methods are used in permafrost and ground ice, but are inaccurate or incomplete because none exploit the unique properties of ice. The objective of this project was to sense the orientational polarization or dielectric relaxation of ice, as it is distinct and has been well characterized in the laboratory as functions of crystallization state and soluble and insoluble impurities. However, this property of ice had never been measured in the field, let alone used as a basis for subsurface imaging.

Approach — Using a state-of-the-art field instrument purchased last year by SwRI, the first *in situ* measurements were performed to detect subsurface ice and characterize its distribution in and around the U.S. Army Permafrost Tunnel in Fox, Alaska. An approach was established for data assessment and processing, imaging and ice quantification.

Accomplishments — Excellent agreement was found in the overall spectral signatures between field and laboratory measurements. A low-frequency branch is dominated by the "DC" resistivity of the sample, and a high-frequency branch shows decreasing resistivity and changing phase characteristic of the dielectric relaxation of ice. The surface survey parallel to a prior SwRI "DC" survey over the tunnel showed comparable overall layering, but low-frequency resistivities lower by a factor of ~5 in the new survey relative to the old. This can be attributed to subsurface temperatures ~1°C higher beneath the snowmobile path on which the new survey was performed. Surveys on the walls of the tunnel showed much higher resistivities appropriate to ice at temperatures of –3 to –5°C. Images correlated well with regions of higher and lower ice content based on visual classification and sampling. Quantitative mapping, however, remains imperfect due to uncertainties in temperature and the low spatial density of data that could be collected in the allotted time. These issues are being addressed in a follow-on internal research project involving a much more comprehensive field investigation near Tok, Alaska.

2013 IR&D Annual Report

Development and Demonstration of Computer Vision Software for Solar Transient Events, 15-R8390

Principal Investigators

Bala Poduval

Craig E. DeForest

Inclusive Dates: 04/01/13 – Current

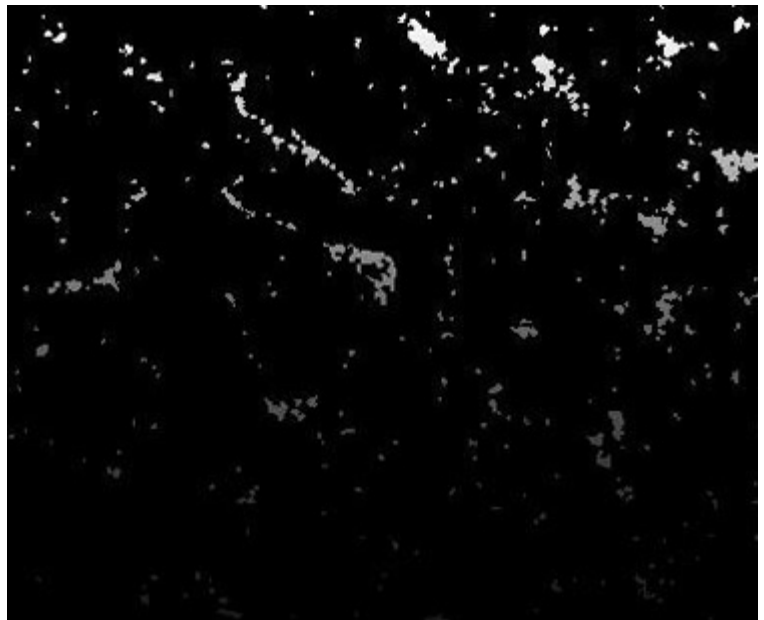
Background — Solar corona exists at a million degree Kelvin (K) above the photosphere, the visible surface of the Sun, which is only 6,000 K. This apparently paradoxical phenomenon, known as coronal heating, is one of the most controversial topics in solar physics. Magnetic reconnection, manifesting as small- and large-scale explosive and eruptive phenomena, is the most viable mechanism for coronal heating. The role of small-scale events such as microflares in coronal heating is poorly understood mainly because of a lack of an unbiased tool for characterizing large populations and a lack of observations across the wide temperature regimes of the corona. The Atmospheric Imaging Assembly (AIA) telescope onboard the Solar Dynamics Observatory (SDO) observes the solar atmosphere in visible (4500 Å), ultraviolet (1600 and 1700 Å), and extreme ultraviolet (94, 131, 171, 193, 211, 304, and 335 Å) wavelengths, covering temperature regimes from 5,000 K to 20,000,000 K. Studying microevents in multiple wavelengths will reveal their evolution in these temperature regimes and clarify the physics.

Approach — The project goal is to develop a computer vision code, Automated Microevent-finding Code (AMC), for automatically detecting and characterizing thousands of microevents and transient features in the AIA images without human bias. AMC will be used for a proof-of-concept study addressing a 60-year-old mystery central to solar physics: Can microflares account for the high temperature of the solar corona? AMC will have other applications in solar physics (e. g., implications of small-scale eruptive events such as miniature CMEs, jets, and plumes) and in planetary sciences (for example, the turbulent eddies in the Jovian atmosphere).

To develop AMC, the SWAMIS vision code for magnetic feature tracking is being modified. However, identifying transient brightenings requires a set of selection criteria and threshold values completely

different from those for magnetic feature tracking. Also, discriminating the events from other brightenings and dynamics of the corona is a challenge, as the AIA images are high resolution and high cadence. The microevents detected in each wavelength will be associated in multiple wavelengths.

Accomplishments — A test-version of AMC was developed that is capable of identifying the microevents in AIA 1600 Å data and associating them in multiple frames of the time series. A sample of the identified features is shown in the illustration. The image shown is a small slice of the original image of size 4096 x



Microevents identified in 1600 Å data observed by SDO/AIA telescope on February 8, 2013.

4096 pixels. Here, the small, irregular bright spots are the microevents detected using the AMC. Thirteen frames were used to define and detect these features.

2013 IR&D Annual Report

Optimization of Charge Couple Device Readouts for Particle Detection, 15-R8404

Principal Investigators

[Robert G. Michell](#)

Jason L. Stange

Inclusive Dates: 07/01/13 – Current

Background — The objective of this effort is to design and build electronics for reading and controlling a commercial charge couple device (CCD), such that the response to ions and electrons of different energies can be quantified and the trade-offs and limitations can be determined for use in particle detecting instruments. CCDs are primarily used to detect photons, but there is great potential in using them for detecting electrons and ions. The detecting ability, or quantum efficiency (QE), of CCDs is typically well characterized for photons of different wavelength, but little is known about the QE of CCDs for detecting electrons and ions. For example, using CCDs in an electron spectrometer would have many advantages over a traditional MCP-based detector, including the ability to operate in poor-vacuum conditions, and it can be made smaller and use less power.

Approach — The technical approach centers on developing the electronics needed for reading and controlling a CCD and the testing of a commercial CCD for particle detection. The electronics are being developed using a commercially available CCD. Two options are being investigated within the parameter space of possible electronics designs for reading and controlling a CCD: using analog electronics for doing most of the signal processing before converting to digital and immediately converting to digital and then using a field-programmable gate array (FPGA) to directly process the digital signals. Once operational, the CCD and readout electronics will be used to characterize the detector response to electrons and ions of different energies. The parameter space and trade-offs needed can then be quantified to enable the use of CCDs for detecting elements in a range of different particle detecting instruments, including electron and ion spectrometers, ion mass spectrometers, Faraday cups, neutral particle detectors and optical imaging in the infrared, visible and ultraviolet.

Accomplishments — The electronics board for housing the CCD and the front end electronics are being designed. The design will be finalized soon, so the board can be ordered and fabricated. The CCD has been ordered and received from E2V, model number CCD47-20. The CCD requires several different voltages to operate and these will be generated by another electronics board, for which the design is nearly finished and will also be fabricated soon. Plans for the next quarter include building and testing the CCD housing and control board, building and testing the power board and investigating the use of Peltier coolers for cooling the CCD to reduce noise.

2013 IR&D Annual Report

Formation Impact Study of Lithium-ion Battery Capacity, Cycle Life, and Safety, 03-R8277

Principal Investigators

Jeff Q. Xu

Robert Smith

Jayant Sarlashkar

Vikram Iyengar

Inclusive Dates: 01/01/12 – Current

Background — A "stable" surface film is formed on graphite electrodes upon the first charging of lithium-ion battery cells. This is called formation, which is a critical step during the battery manufacturing process. The formation of this solid electrolyte interface (SEI) layer passivates the graphite surface against further solvent decomposition. The SEI acts to decelerate the cell aging process and improve performance. To date, much of the SEI formation process is still not fully understood and the process is not well monitored during the formation step. Therefore, a direct and effective approach is needed for monitoring the formation process to develop effective and efficient formation protocols.

Approach — The objective of this project is to develop and evaluate the static and dynamic formation protocol impacts to lithium-ion cell performance such as capacity and cycle life. The approach is to leverage the thermal characteristics of the cell produced when the battery cell is under the first charging or formation cycle. By comparing various thermal or heat profiles at different formation rates, one or more clear voltage transition points can be identified as reference points to guide the changes of formation rates. Figure 1 illustrates this approach.

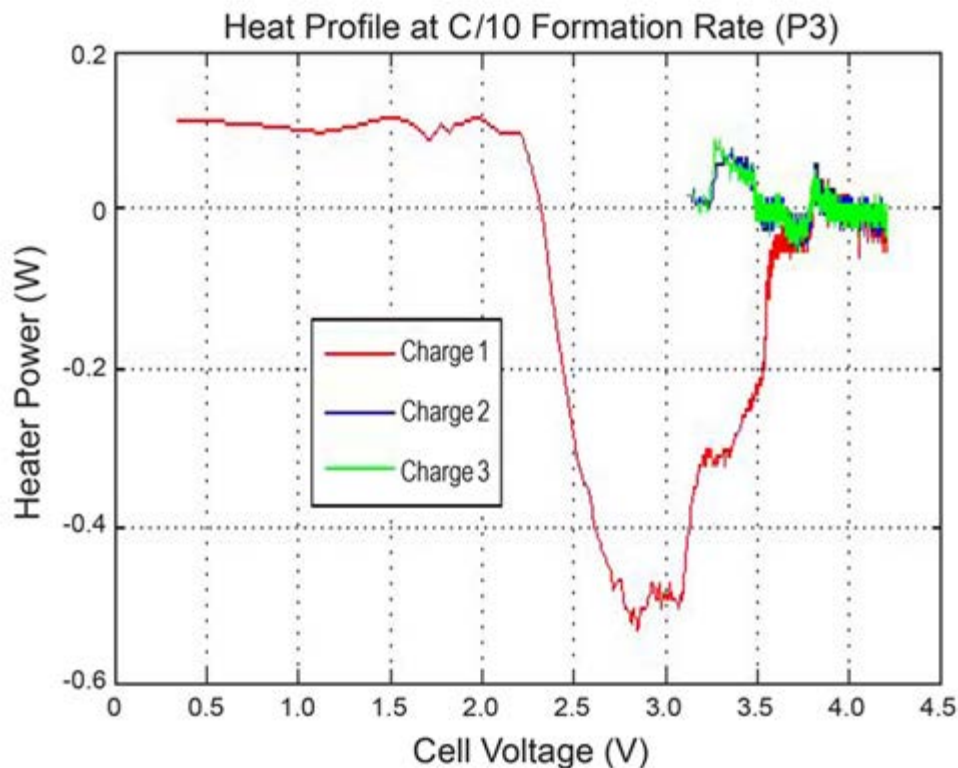


Figure 1. Net heater power change as a function of cell voltage during C/10 formation rate

Accomplishments — Use of a heat profile measurement/analysis tool during the cell formation stage can offer insight for developing a suitable dynamic formation protocol for any type of graphite anode chemistry-based lithium-ion cell and potentially can be used for silicon or carbon silicon alloy-based anodes. The cells formed using the dynamic formation protocol have proved that thermal or heat measurement is effective during the study. The project was able to identify a specific voltage window that is most important to form an SEI layer effectively by using dynamic charge currents to allow reactions to take place with reduced battery cell degradation. A flexible formation current could be adopted to expedite the process. This tool can be applied to investigate novel electrolyte composition and additive functions, electrode material selection and formulation to the improvement of battery capacity, cycle life and safety. Figure 2a and 2b are examples of the experimental setup.

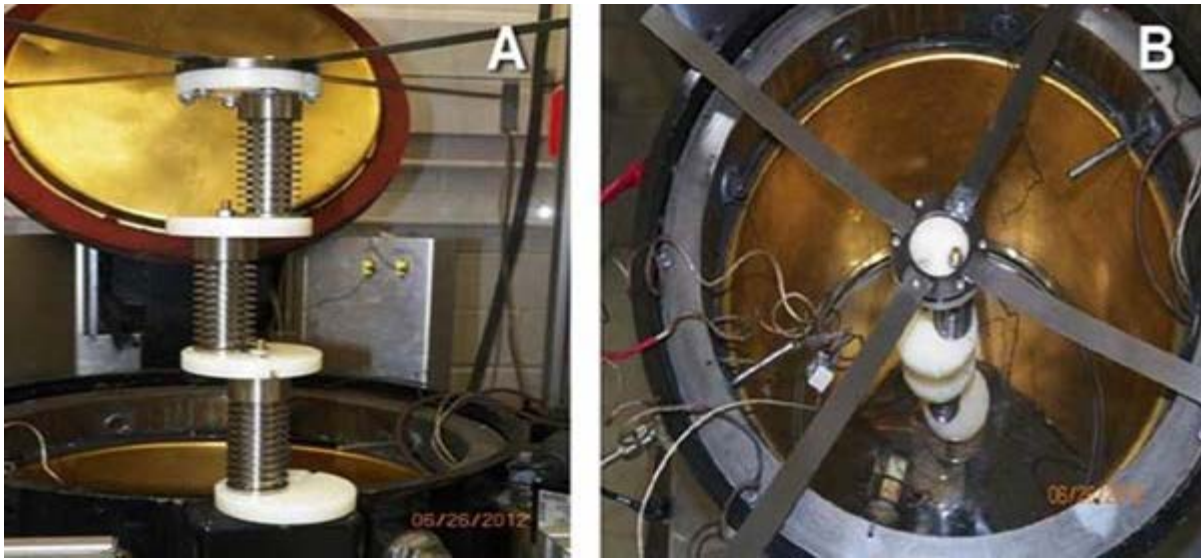


Figure 2. Example of experimental setup for one kind of specific battery

2013 IR&D Annual Report

Corrosion Measurements in Fuel Systems, 18-R8203

Principal Investigators

James F. Dante

Gary Bessee

Inclusive Dates: 01/01/11 – 01/01/13

Background — Corrosion in engines and underground fuel storage tanks has become a widespread problem in recent years. This appears to be related to the introduction of ultralow sulfur diesel fuel (ULSD). However, corrosion in fuel is difficult to study due to its low conductivity, making *in situ*, real-time conventional electrochemical techniques impractical. Another technical issue is the phase instability of ethanol/gasoline blends, such as E10, in the presence of water. As low as 0.5 vol% water in the dispensing line can cause phase separation leading to severe corrosion and off-spec blend. This phenomenon has been found to be very sensitive to the composition of the blend, water content and temperature, but no operating boundaries for phase stability have been established. No confirmed root cause has been established to explain the corrosion failures observed in the field.

Approach — The objectives of the project are to validate a method for measuring corrosion rates in fuel systems, investigate the effect of dew points, water content and fuel chemistry on the corrosivity of ULSD, and determine the parameters leading to phase separation in ethanol/gasoline blends. Multielectrode array sensor (MAS) technology will be used to measure corrosion rate in fuels. MAS allows measurement of corrosion rates in thin electrolyte layers, such as ones forming in fuel. Carefully selected model fuels will be used to investigate the environmental effects that increase the corrosivity of ULSD compared to other diesel fuels. Two approaches will be employed to study the phase separation of ethanol/gasoline blends. Thermodynamic calculations will first be carried out using a mixed solvent electrolyte model to define parameter boundaries of phase instability. Then, the corrosion properties of different blends will be measured using the MAS technology.

Accomplishments — The final report was submitted in December 2012. The summary of findings is as follow:

- An increase in the aggressiveness of surrogate gasoline was linked to ethanol additions using MAS.
- In diesel fuel systems, corrosivity is governed by the aggressiveness of water contaminants. A decrease in pH to a value of 5 has the largest effect on corrosivity.
- No difference was found in the corrosivity of LSD and ULSD fuels under the conditions tested. The corrosivity of a diesel/water mixture is increased when the diesel fuel is first filtered. This may be the result of the removal of corrosion inhibitors (among other constituents) for the filtered fuel. Note that after filtering, the difference between the corrosivity of the two types of fuels is still indistinguishable. Also note that we have not studied the ability of these fuels to support microbiological growth.
- For temperatures below 40°C, there is no difference in the ability of LSD and ULSD to hold water for diesel fuels tested. Filtering the fuel removes polar molecules resulting in a decrease in the ability of the fuel to hold moisture and thus promoting phase separation. Filtering has the same effect on both the LSD and ULSD fuels tested here.
- While the corrosivity of the diesel fuels tested here are primarily a function of contaminant water chemistry, aggressiveness of gasoline containing ethanol is at least in part a function of the corrosivity of ethanol.
- The MAS probe in its current configuration was unable to detect the onset of phase separation from

gasoline blends or contaminated diesel fuels although it was very successful in measuring corrosion processes.

2013 IR&D Annual Report

Development of Novel Silicon Clathrates for Energy Harvesting and Storage, 18-R8279

Principal Investigators

Kwai S. Chan

Michael A. Miller

Inclusive Dates: 01/01/12 – 07/01/13

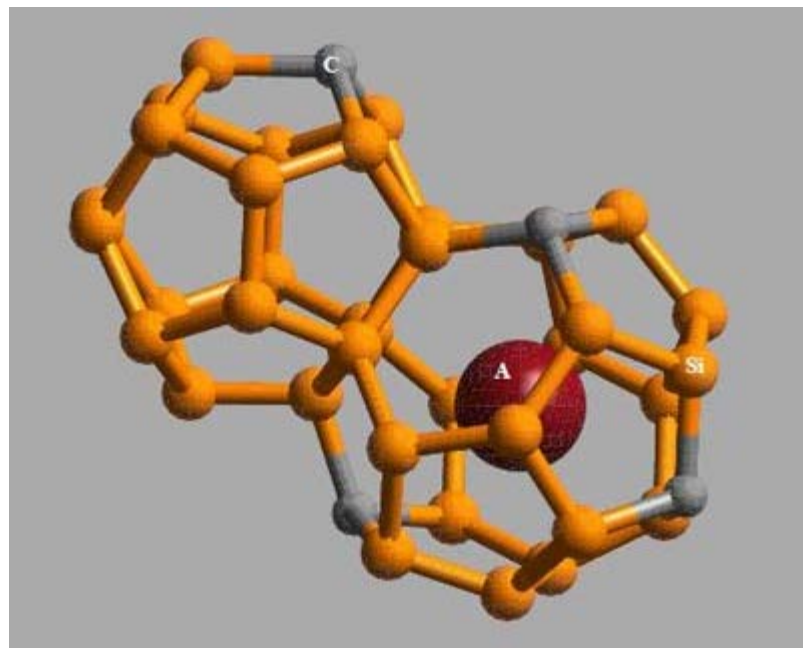
Background — Solid-state thermoelectric devices (TEDs) exhibit many attractive features for electrical power generation compared to traditional fuel-combustion systems, which include extraordinary long life, no moving parts, no emissions and high reliability. To this end, the Type I and II clathrates of silicon and germanium alloys are attractive thermoelectric (TE) materials because they can be engineered to exhibit high thermal power, high electrical conductivity and low thermal conductivity by scattering phonons without interrupting electron conduction. Despite these attributes, the figure of merit of current silicon clathrates is still below that of existing TE materials based on rare-Earth elements and needs further improvement for industrial applications.

Approach — The objectives of this research project are to:

1. develop novel silicon clathrates by substituting clathrates framework and guest atoms using small-sized atoms,
2. characterize the thermoelectric properties,
3. develop a first-principles computational approach for modeling the effects of small-atom interactions, and
4. design and demonstrate a multilayered TED using the novel TE material.

An innovative direct synthesis method and a traditional arc-melting method are used to synthesize Type I metal-silicon clathrates with small-sized atom substitution on the Si framework and guest-atom insertion within the cage structure. The thermoelectric properties of metal-silicon clathrate compounds in bulk and layer forms will be characterized with and without compressive stress. A computational methodology will be used to develop an understanding of the effects of small-atom substitution and encapsulation within the cage structure on the thermoelectric properties and to design the desired multilayer architecture for optimum thermoelectric properties.

Accomplishments — A first-principles computational approach was used to design new silicon-based clathrates using small-sized atoms such as C or N as substitution atoms on the framework that is



Hybrid carbon-silicon Type I clathrate framework with guest atom A inside the cage structure designed via first-principles computations. Similar structures were designed and synthesized by substituting Si framework atoms with nitrogen atoms.

stabilized by alkaline or alkaline earth guest atoms, A, inside the cage structure of the framework, see illustration. Several hybrid carbon-silicon clathrates and one hybrid carbon-nitrogen clathrate were synthesized and confirmed by experimental techniques. First-principles computations indicated that new clathrate materials can be tailored to exhibit a wide range of electronic properties and have potential as either electronic or thermoelectric materials. Two patent applications related to the hybrid carbon-silicon and carbon-nitrogen clathrates are pending.

2013 IR&D Annual Report

Fretting and Flow Assisted Corrosion Effects on Nitinol Stents for Biomedical Use, 18-R8282

Principal Investigators

Elizabeth Trillo

Erica Macha

James F. Dante

Xingguo Cheng

Inclusive Dates: 01/01/12 – Current

Background — Nickel-titanium alloys, also referred to as nitinol, have been used for many years as a biomedical stent material to repair damaged vessels. Although there have been marked improvements in the design of stents and nitinol processing, the number of stent failures has remained high (up to 32 percent). Failure of a stent is considered to be a fracture of the stent support system and/or corrosion on the stent that results in nickel ion release, which is toxic to the body. A common procedure is to overlap stents to accommodate a longer damaged vessel length. This introduces a fretting scenario. A combination of fretting along with flow-assisted corrosion and pulsatile effects, as well as pH of the local wound site are potential performance issues in the *in vivo* condition that have not been accounted for in the literature. The proposed research looks to understand these combined effects on nitinol stents.

Approach — There are three major objectives of this effort:

1. Determine the effect of biological fluid flow on the corrosion behavior of nitinol stent material,
2. Determine the combined effects of fretting and biological fluid flow at a lower pH conditions, and
3. Assess the biocompatibility of nitinol stents using endothelium cells after flow and fretting/flow testing.

A test apparatus will be built to simulate the combined effects of fretting and flow conditions in simulated biological solutions. The corrosion potential during fretting and flow are to be recorded for up to three months. Lower pH solution tests will be performed to determine how the corrosion behavior will change when the material is near inflamed tissue or crevice areas. After testing, the stent surface morphology will be examined by Micro-CT, scanning electron microscopy (SEM) and auger spectroscopy. Cyclic polarization testing will be performed to determine general and localized corrosion effects. Nickel-ion concentration measurements will be obtained from the test fluid during the exposure. In addition, biocompatibility testing will be performed to see if there is cell adhesion and proliferation on the nitinol stents after exposure.

Accomplishments — A four-channel flow apparatus was used to test four overlapping nitinol stents under a fretting and flow condition. Open-circuit potential measurements were recorded while the system was under a continuous flow of phosphate buffered saline (PBS) solution at a rate of 250 mL/min. The stents were fretted using a four-point bending mechanism that would deflect the stents for 10 minutes three times a week. Changes in the open-circuit potential were noted as well as the time it took to recover to the baseline potential. After a baseline open-circuit potential is reached (four days), the fretting mechanism is activated. A decrease in open circuit during fretting was observed on the stents, but the potential then recovered to the baseline value within minutes. There were also small perturbations in the open-circuit potential noted during testing. During this time the potential showed a sudden drop. These could indicate a potential breach in the surface oxide where corrosion may have occurred.

Cell culture testing using human umbilical vein endothelial cells was performed on one stent after an initial flow/fretting test for a duration of five days. The stent exhibited excellent cytobiocompatibility. Cells were

able to attach and proliferate on the stent after fretting and flow testing.

2013 IR&D Annual Report

Large-Area Synthesis of Graphene for Electronic Devices, 18-R8303

Principal Investigators

Vasiliki Z. Poenitzsch

Thomas Booker

John Harrison

Inclusive Dates: 04/01/12 – 10/01/13

Background — At present, graphene is one of the hottest topics in condensed-matter physics and materials science. Graphene is a monolayer, thick planar sheet of sp²-bonded carbon atoms packed in a two-dimensional (2D) honeycomb lattice. The unique structure of graphene yields extraordinary thermal, mechanical and electrical properties. In 2004, Novoselov and Geim first isolated graphene by cleaving graphite with adhesive tape. Research on graphene has since been a fast-developing field, with exciting properties being confirmed and new concepts and applications appearing at an incredible rate.

Potential applications include field-effect transistors, interconnects, sensors, conducting films, clean energy devices, and conductive reinforced composites. Because of the promising and versatile properties of graphene, Novoselov and Geim were awarded the 2010 Nobel Prize in Physics. Despite intense interest and remarkably rapid progress in the field of graphene-related research, there is still a long way to go for the widespread implementation of graphene. It is primarily due to the difficulty of reliably producing high quality samples, especially in a scalable fashion. This project seeks to help close the chasm between graphene manufacturability and its application. Developing graphene deposition technologies will enable SwRI to provide applied research and development on graphene to a range of clients.

Approach — The primary objective of this project is to establish graphene deposition technologies at SwRI®. The immediate aims of this project are to establish a graphene thermal chemical vapor deposition (CVD) processing technology, develop a novel graphene plasma enhanced CVD (PECVD) processing technology and investigate their electronic application specific performance of produced graphene films. Facilities and expertise to deposit large-area (≥ 1 in.²), high-quality graphene films at SwRI (Figure 1) were established. This new capability will significantly strengthen SwRI's position to provide applied research and development on graphene to a range of clients. An in-house graphene thermal chemical vapor deposition (CVD) technology was developed.

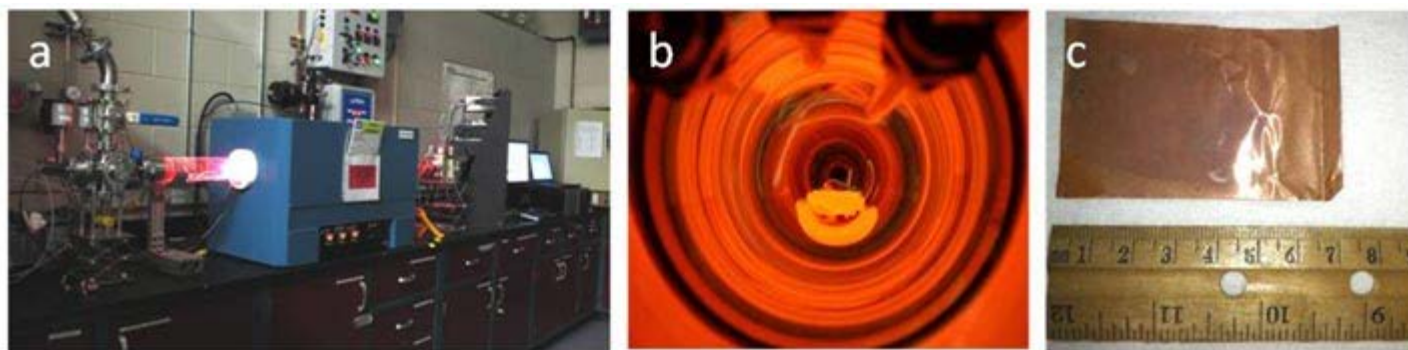


Figure 1. Photographs (a,b) of new thermal CVD chamber running process experiments for producing graphene films and of (c) as-grown film on Cu foil from a graphene deposition process experiment.

Accomplishments — The technology was used successfully to grow pristine, single-to-few layer graphene films using Raman spectroscopy, transmission electron microscopy (TEM), and scanning

tunneling microscopy (STM) (Figure 2). The large area graphene films were successfully transferred from Cu growth substrates to glass and Si wafer substrates (Figure 3). The performance was measured of 94 percent transmittance and 900 to 1,300 ohms/square for transferred SwRI graphene films, which matches that of current state-of-art CVD graphene films. A plasma-enhanced chemical vapor deposition (PECVD) technology was developed using a plasma jet and heating stage (not shown). PECVD growth of graphene films was investigated, but resulted only in the deposition of thin, amorphous carbon films. A PECVD process for growth of vertically aligned carbon nanotubes (CNTs), however, was developed. Preliminary evidence was also obtained for higher pressure PECVD deposition of diamond-like carbon (DLC) films. Altogether, SwRI has built a portfolio that will enable entry into the graphene research arena. While this project focused on graphene, the real benefit of the project was establishing thermal CVD and PECVD processes that have expanded and diversified SwRI's current unique coating capabilities and efforts in nanotechnology.

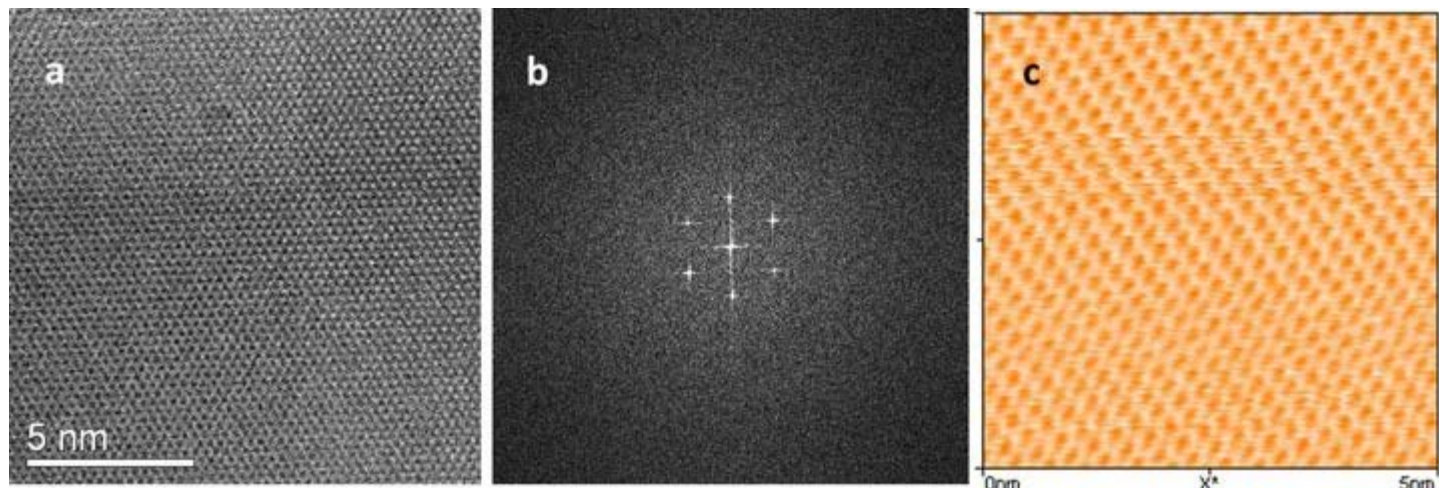


Figure 2. (a) Transmission electron microscopy image showing atomic resolution, (b) diffractogram showing crystalline structure, and (c) scanning tunneling microscopy image showing atomic resolution of pristine, single layer graphene film.



Figure 3. Photograph of 2 in. x 2 in. pristine graphene film transferred to glass substrate. Measured performance of 94 percent transmittance and 900 to 1,300 ohms/square for transferred SwRI graphene films.

2013 IR&D Annual Report

Development and Demonstration of Erosion Prediction Capabilities for Oil and Gas Industry Applications, 18-R8338

Principal Investigators

[Rebecca A. Owston](#)

Steven J. Svedeman

Steven T. Green

Shane P. Siebenaler

Ronghua Wei

Inclusive Dates: 10/01/12 – Current

Background — Equipment erosion is a major problem for the oil and gas industry, resulting in many millions of dollars in capital and labor expenditures each year. In addition to the economic aspects of erosion, safety and environmental risks are also matters of concern. Oil companies and their suppliers recognize the importance of accurate prediction of erosion rates, which allows for design improvements to extend the life of equipment and/or the judicious choice of coatings to reduce wear.

A combination of testing and computational modeling is used for estimating erosion rates. Testing is generally expensive, time-consuming, limited in terms of maximum flow rates/sand concentration that a facility can handle, and frequently employs shear-thinning viscosifier agents to keep the proppant (sand or other solid particles) suspended. Computational modeling of erosion is a low-cost alternative to testing for preliminary design analysis. Current erosion models are generally semi-empirical in nature though, and caution must be exercised in their application to practical cases. From a survey of the literature, only a limited number of computational fluid dynamics (CFD) erosion studies have been conducted on oilfield equipment considering realistic non-Newtonian fluids. These studies generally do not report the functional relationships of their model coefficients or systematically consider the effect of different geometries, sand concentration, flow rates, etc.

Approach — The objective of this project is to develop and demonstrate capabilities for accurate prediction of erosion using a two-fold approach: computational modeling and experimental testing. Data from each area are intended to complement and enhance the value of the other. Specific tasks for the project include:

- Validate common flow-coupled erosion CFD submodels against existing experimental data for low-concentration (<10 percent) proppant flowing through a simple elbow geometry
- Use experimental data obtained as part of this project to extend CFD submodels to include non-Newtonian fluids and high proppant concentrations
- Determine whether scaling of experimental testing is possible with regard to fluid viscosity, flow rate, and/or proppant concentration
- Demonstrate the ability to effectively model erosion in oilfield equipment using CFD

Accomplishments — Based on a literature search, five viable erosion submodels were identified and incorporated into a CFD software package for benchmarking. Benchmark validation was carried out through comparison of elbow-bend simulation results against a corresponding experimental data set from the literature. In general, good qualitative agreement was demonstrated with the model, as shown by the expected "tongue" pattern evidenced in Figure 1. However, quantitative measurement of the penetration rate had a high level of error using default model coefficients. Simple tuning of a single model parameter at a time did not provide good agreement with empirical data over a wide range of flow conditions. This indicates that it may be necessary to incorporate additional variables and/or develop new submodel forms

based on unique dependencies. This will be done in conjunction with experimental results currently being obtained.

The experimental portion of the project has also commenced. Test section parts and target coupons have been designed, fabricated and assembled. A total of six erosion tests have been completed using 316 stainless steel coupons. Variations in flow rates and impingement angles have been examined. Figure 2 shows an example of erosion depth for a coupon tested for 20 hours at flowing conditions of 42 gpm with 0.6 percent sand loading.

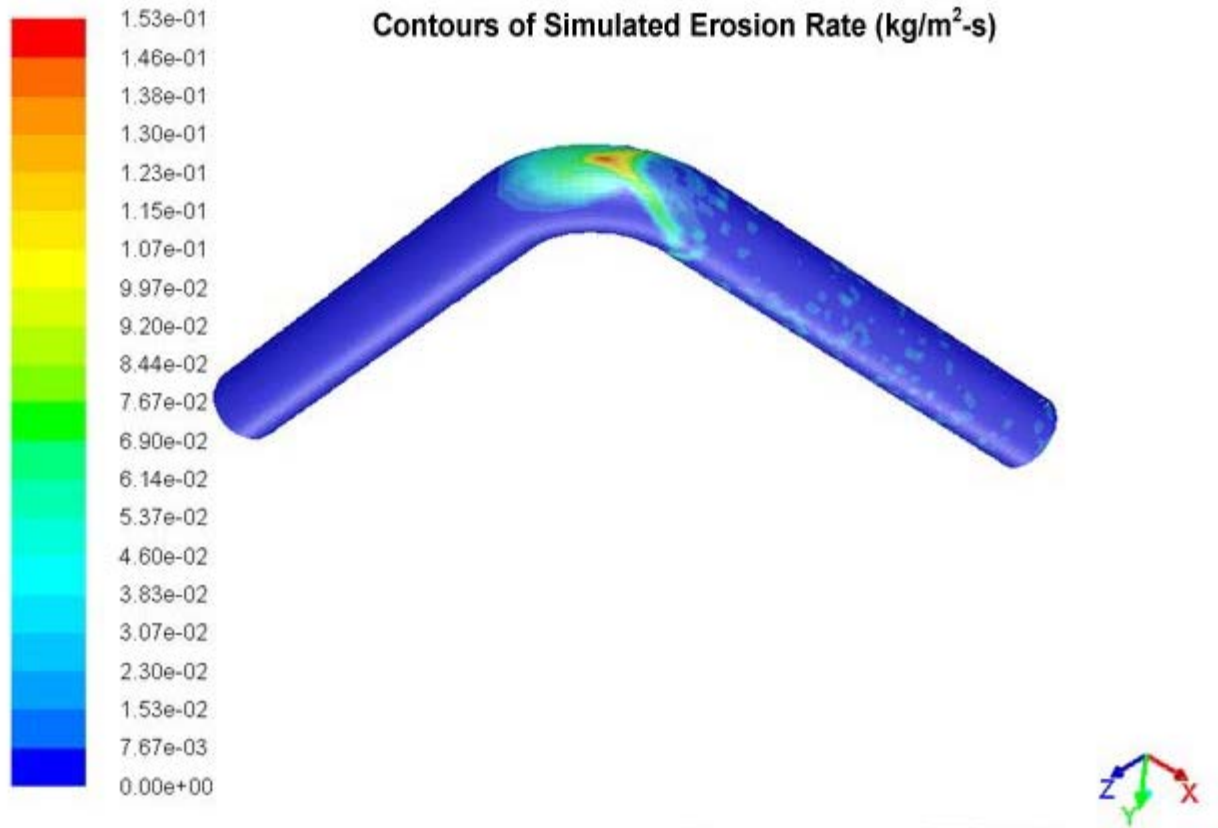


Figure 1. Erosion contours from CFD simulations show the expected “tongue” profile observed experimentally from eroded elbows.



Figure 2. After running in the test rig for approximately 20 hours, the 316 stainless steel coupon shows clear evidence of an eroded indentation at the target face.

2013 IR&D Annual Report

Design, Analysis and Instrumentation of a Full-Scale Reusable Landmine Test Rig, 18-R8383

Principal Investigators

[Carl E. Weiss](#)

Andrew Barnes

Matthew Grimm

James T. Mathis

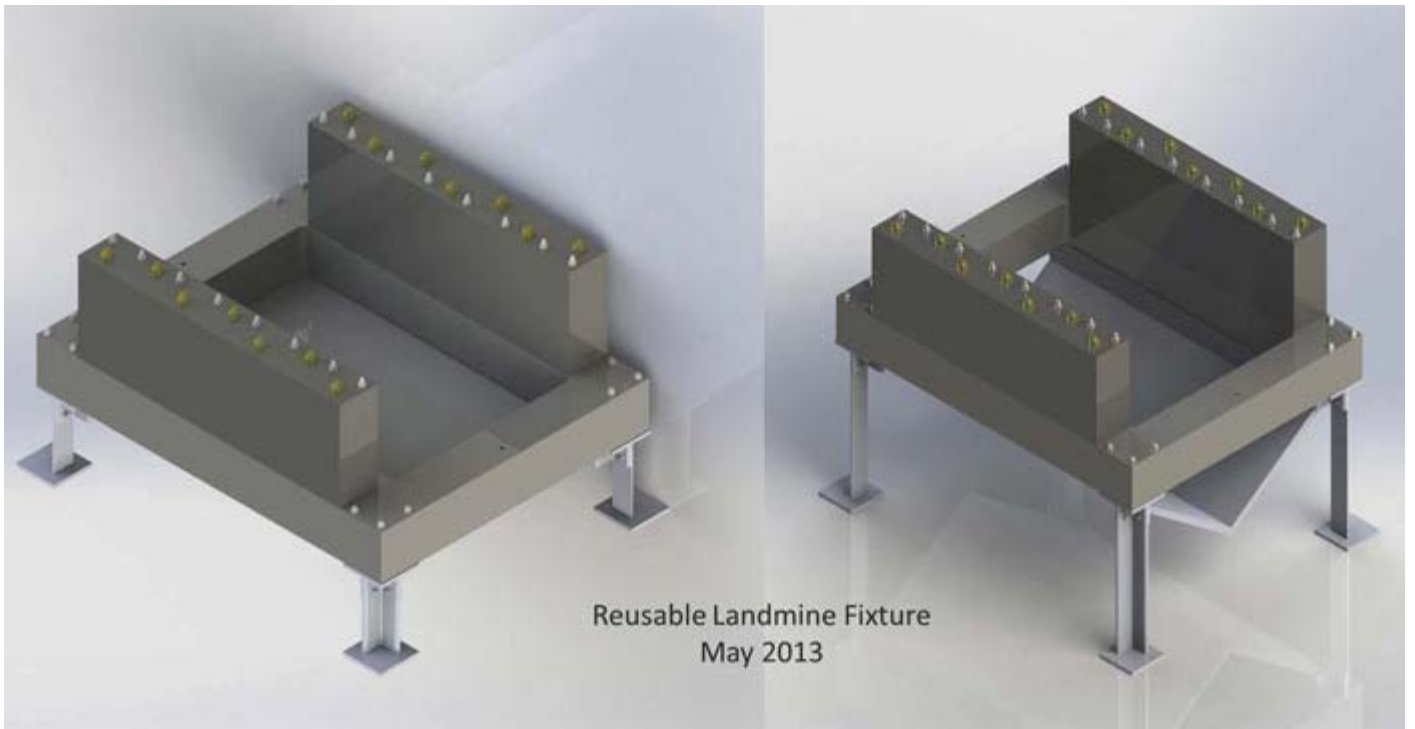
P.A. Cox

Inclusive Dates: 04/03/13 – 08/05/13

Background — SwRI has performed mine blast testing for a variety of clients over the past several years to support the development of mine blast-resistant vehicles. Tests have been performed on full-scale vehicles and on vehicle components. A majority of component tests have been performed on the SwRI Universal Landmine Test System (ULTS), a reusable fixture for repetitive testing with charges up to 12 pounds TNT. This project was conducted to meet client demands to test larger vehicle components without the need to fabricate the full vehicle and to do so with larger charges.

Approach — SwRI had indications that a client would pay for fixture fabrication if SwRI could design a fixture for full-scale testing and demonstrate through numerical simulations that it could survive repetitive testing with charges up to 60 pounds TNT. A quick-look project was used to meet client needs for testing in the fourth quarter of 2013. The test fixture needed weight and size goals to represent a full size vehicle, and strength and durability were overriding concerns. Discussions with existing clients led to a target size of 6 feet by 8 feet and a maximum weight of 32,000 pounds.

Accomplishments — CAD layouts were developed to size the fixture to accommodate a 6-foot by 8-foot test article. Early layouts indicated that the frame must be at least 7 foot by 9 foot in platform. If fabricated from a solid plate, ballast could be cut from the plate center to increase overall fixture weight. Although plates with thicknesses greater than 14 inches were considered for their bending strength and stiffness, a 14-inch plate gave fixture weights that were consistent with the weight goals of the project. A 14-inch thick, SA 516 Grade 70 steel plate, of adequate size, was located in stock. Numerical simulations were performed to demonstrate that a test fixture, cut from the SA 516 Grade 70 steel plate, was adequate to withstand the blast loading from a buried 60-pound TNT charge. The final configuration is shown below. It has been fabricated, and the first client-funded tests have been performed with the fixture.



Reusable Landmine Test Fixture

2013 IR&D Annual Report

The Development of a Dynamic Finite Element Model of the Temporomandibular Joint (TMJ) and Study of Joint Mechanics, 18-R8386

Principal Investigators

[Daniel P. Nicoletta](#)

Travis D. Eliason

Todd L. Bredbenner

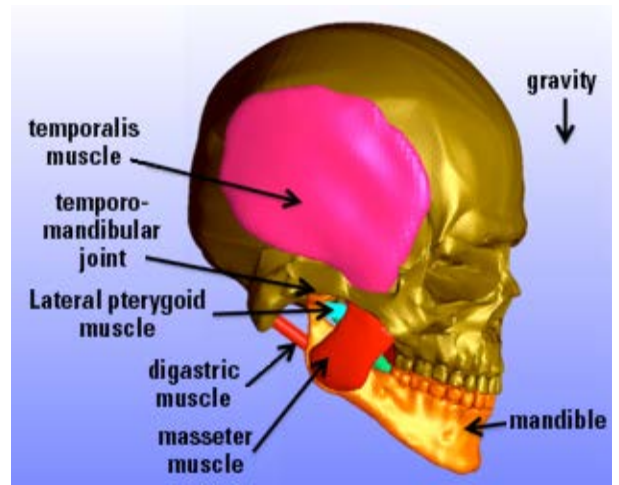
Inclusive Dates: 04/01/13 – Current

Background — Disorders of the temporomandibular joint (TMJ) result in an annual cost of \$4 billion and affect more than half of the population. TMJ disorder (TMD) causes pain in the jaw when speaking or chewing that is often associated with clicking and popping of the jaw and can limit a person's ability to open their mouth. Women ages 20 to 40 are the most prevalent sufferers of TMD. Various studies indicate that women with TMD outnumber men anywhere from 3:1 to 8:1. While the causes of TMJ disorder (TMD) are not completely understood, it is thought that alterations in joint mechanics due to osteoarthritis (OA) or trauma results in degradation and inflammation of the joint soft tissues (cartilage and disc), which then results in pain and limited motion. In addition, displacement of the TMJ disc is also associated with TMD. The dynamic mechanical environment within the TMJ during chewing or clenching is not well characterized because of the complexity of the anatomy and materials. Within the TMJ research community, the question of how soft tissue properties and geometry of the joint affect the mechanical environment has gone unanswered and is the focus of this project.

Approach — The primary objectives of this project are:

- Develop a detailed dynamic finite element model of the TMJ and mandible from head CT scans.
- Determine muscle activation timings and magnitude to achieve dynamic mouth opening and closing using a new a proportional–integral–derivative (PID) controller method.
- Perform sensitivity analyzes of TMJ disc properties to determine the importance of those properties in the resulting forces and stresses of the TMJ during normal mandible movements.
- Implement an element erosion or damage material model for the TMJ disc to investigate the effects of disc degeneration on the muscle forces required for normal mandible movements.
- Develop a statistical shape model of the TMJ coupled with the dynamic finite element model.
- Investigate the effect of gender differences on TMJ stress using the FE-coupled statistical shape model.

Accomplishments — A dynamic finite element model of the skull, mandible, TMJ and musculature has been developed using a generic anatomy database and implemented in an open-source finite element analysis program (FEBio v. 1.5, University of Utah). The model consists of the skull, mandible, upper and lower dentition, and bilateral temporalis, masseter, lateral pterygoid, digastric muscles (see illustration). The skull, mandible and teeth are modeled as rigid bodies while the muscles are modeled using three-dimensional active contraction continuum elements. The material model used for the muscle elements is a transversely isotropic



Dynamic Finite Element model of the skull mandible, TMJ and associated active muscles. In this model, left and right muscle pairs are activated simultaneously using the same activation curve.

Mooney-Rivlin with viscoelasticity. Force is generated along a locally defined fiber axis direction using a modified active contraction model. The muscle material model parameters are taken from the literature. Motion of the mandible relative to the maxilla (skull) is produced by coordinated active, time-varying contraction of opposing muscle groups and is constrained by contact between the mandibular condyle and the temporal bone in the mandibular fossa, contact between the upper and lower dentition, and the constraint supplied by the deformation of the attached musculature.

The initial muscle activations have been determined using a traditional parameter optimization method. The control parameters in this case consist of activation levels for each muscle as a function of time throughout the targeted motion. The muscle activation parameters are determined using a non-linear least-squares (NLS) optimization approach that aims to minimize the difference between an *a priori* determined mandibular motion and the muscle-controlled mandibular motion. Initially, the muscle activation parameters were determined using a simplified model consisting of only two muscles, idealized versions of the masseter and the digastric muscles with a targeted motion of opening and closing the jaw within a three-second time frame. The targeted motion was produced by uniformly rotating the mandible with respect to the maxilla from the initial closed position through approximately 0.3 radians (17 degrees) and back to the closed position. For the NLS optimization, the muscle activation parameters consisted of 7 activation time points for each muscle evenly spaced over three seconds resulting in a total of 14 muscle activation parameters. The left and right muscles were activated equally for both the masseter and the digastric muscles.

A new method for determining muscle activation forces and timings will be developed for this project. This method uses a PID controller interfaced with the finite element model to adjust muscle forces and timings during the simulation in a feedback loop to minimize the error between the model displacement and a predefined displacement curve. The PID controller method can determine muscle activation timings in a single forward dynamics simulation rather than the hundreds or thousands of FE model simulations required using the traditional NLS optimization.

2013 IR&D Annual Report

MicroCT Investigation of Relationships in Bone-cartilage Structure, 18-R8399

Principal Investigators

Todd L. Bredbenner

Daniel P. Nicoletta

Inclusive Dates: 06/26/13 – 10/28/13

Background — Osteoarthritis (OA) is the most common form of arthritis and the major cause of activity limitation and physical disability in older people. Osteoarthritis most often occurs in the hands (at the ends of the fingers and thumbs), spine (neck and lower back), knees and hips. Arthritis causes pain, swelling and reduced motion in joints caused by the breakdown or degradation of the articular cartilage covering the joint surfaces. It is widely believed that OA results from the local mechanical environment of the joint in general, and in the cartilage in particular, in combination with systemic susceptibility to the disease. However, many individuals who do not have these risk factors will go on to develop the disease later in life. This has led to the hypothesis that slight differences in joint mechanics, driven by variability in joint anatomy, along with biological and genetic predisposition, lead some individuals to develop OA while others do not. Previous collaboration with Texas Biomedical Research Institute (TxBiomed) has shown that knee OA occurs commonly and naturally in male and female adult baboons. The roles of cartilage degeneration and the underlying subchondral bone in the onset and progression of osteoarthritis have been the subject of much debate over the past several decades due to the disparate treatment pathways that are associated.

Approach — The objective of this project was to characterize the spatial relationship between cartilage thickness and defects and the composition of the underlying subchondral bone in baboon knees from a small subset of 30 age-matched females: 10 were unaffected by OA, 10 had early stage OA, and 10 had moderate OA disease. The left, distal femur of 30 baboons was imaged using micro-computed tomography (microCT). Bone and cartilage components were identified in the imaging data for each individual and image intensity values in the microCT data for bones were converted to bone mineral density values. Statistical shape and trait modeling methods (partly developed under internal research projects 18-R8039, 18-R8072, and 18-R9541) were used to describe the spatial variation in cartilage thickness and adjacent bone density characteristics for each distal femur.

Accomplishments — SwRI researchers demonstrated their ability to image and characterize knee cartilage and adjacent bony tissue from baboons and, despite small sample sizes, demonstrated the ability to differentiate between OA status using a characterization of the cartilage-subchondral bone interface. The results from this project, along with other data previously collected at TxBiomed (in collaboration with SwRI), form the basis for justifying the baboon as a model of the human osteoarthritic condition and allow the pursuit of targeted funding opportunities within the National Institutes of Health (NIH) and with commercial pharmaceutical and imaging clients. SwRI believes that this now existing body of preliminary data will open up a new area of research that can be applied to pre-clinical drug development, genetic analysis of OA susceptibility, and assessment of osteoarthritis risk, incidence, and progression from clinical MRI and contrast-enhanced CT data. Researchers expect that results obtained from larger sample sizes of distal femurs and proximal tibias, will be proposed in response to a targeted NIH Program Announcement and will further elucidate the effects of OA involvement on the functional behavior of cartilage and the relationship with the adjacent subchondral bone.

2013 IR&D Annual Report

Develop Method for Hydriding Fuel Cladding and Characterize Influence of Hydriding on Mechanical Behavior, 20-R8269

Principal Investigators

Xihua He

Yi-Ming Pan

Kwai Chan

Inclusive Dates: 11/01/11 – 6/27/13

Background — Zirconium-based cladding material exposed to coolant water during nuclear reactor operations could produce hydrogen, and part of the hydrogen could be absorbed into the cladding at concentrations from less than 100 to up to 600 ppm. During extended dry storage, cladding plays an important role in spent nuclear fuel retrievability and confinement and in thermal performance and subcriticality. As the cladding cools during extended storage, the hydrogen inside the cladding may precipitate as hydrides; furthermore, under hoop stresses induced by thermal gradient, both existing and newly formed hydrides may reorient. Depending on their size, distribution, and orientation, these hydrides may lead to premature fracture as a result of hydride embrittlement or delayed hydride cracking. Because the United States is actively considering extended dry storage as an alternative approach for managing spent nuclear fuel and has an increased amount of high burnup fuel as a result of changes in plant operating conditions, there is a strong need for data that can be used to predict the lifetime of cladding. The objectives of this project were to develop methods and identify parameters controlling hydride formation at various hydrogen concentrations, identify conditions when hydrides reorient under stress, and characterize the influence of hydrides and their orientation on mechanical properties.

Approach — The primary objectives of this project were:

- Develop methods and parameters to prepare specimens with various hydrogen concentration levels
- Identify conditions when hydrides reorient under stress
- Conduct mechanical tests to characterize the influence of hydriding on cladding mechanical behavior

Accomplishments — Major accomplishments are highlighted in the following areas.

Four methods have been used to hydride the material: electrochemical method — cathodic charging followed by diffusion annealing; hydrogen charging in a tubular reactor with continuous flow of a mixture of hydrogen-argon gas; hydriding in pure hydrogen in a pressurized vessel; and hydriding in supercritical water at 350°C. All these methods need to be operated for tens of hours and at elevated temperatures. A new method for accelerated hydriding at lower temperature was developed, which involves surface activation by some metal salts, hydrogen storage on surface, hydrogen migration and diffusion, as illustrated in the process in Figure 1.

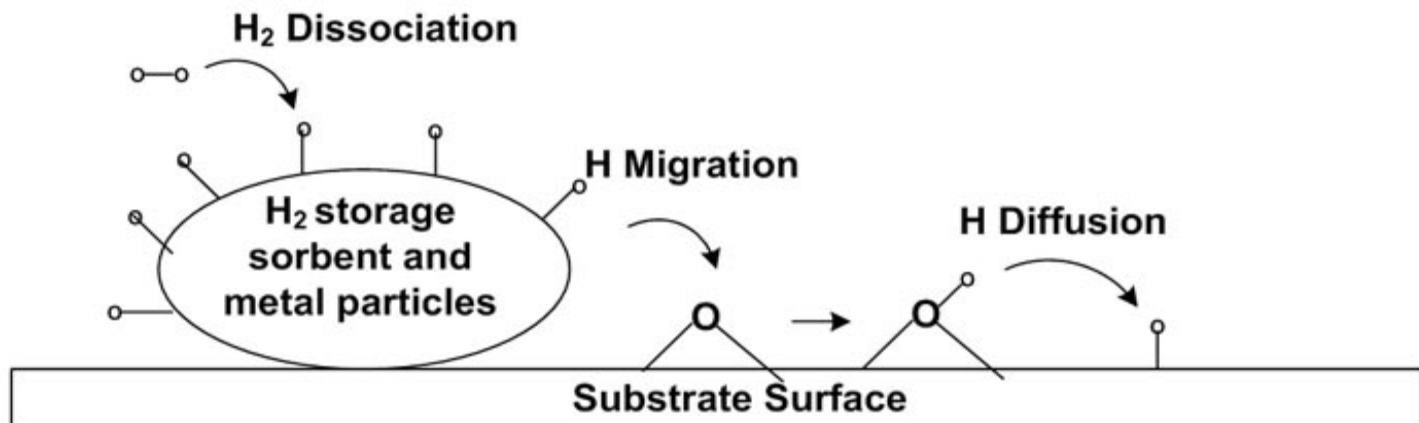


Figure 1. Diagram of the newly developed method for accelerated hydriding at lower temperatures.

Hydride reorientation heat-treatment was performed on hydrogen charged Zircaloy-2 three-point bend specimens at 320 to 350°C for one to two hours, followed by cooling to 200°C. Hydride reorientation occurs in Zircaloy-2 at K levels ranging from 5.5 MPa(m)^{1/2} to 27.4 MPa (m)^{1/2}, and reoriented zone sizes are consistent with a critical hydride reorientation stress in excess of 90 MPa. Reoriented hydrides formed in Zircaloy-2 ranged from submicron-sized to as large as 22 μm.

Fracture testing was conducted on hydride reoriented three-point bend specimens at 200°C in the scanning electron microscope. Reoriented hydrides formed in Zircaloy-2 ranged from submicron-sized to as large as 22 μm. Fracturing of reoriented hydrides of larger sizes (> 10 μm) is more prevalent than that of smaller sizes (< 5 μm). The reoriented hydrides reduced fracture resistance through a void nucleation, growth, and coalescence process at the crack tip, as shown in Figure 2. The resulting crack resistance curves for Zircaloy-2, with reoriented hydrides, decreased from 38 MPa(m)^{1/2} to 21 MPa(m)^{1/2}, with increasing hydrogen contents from 51 wt. ppm to 1,265 wt. ppm, as shown in Figure 3.

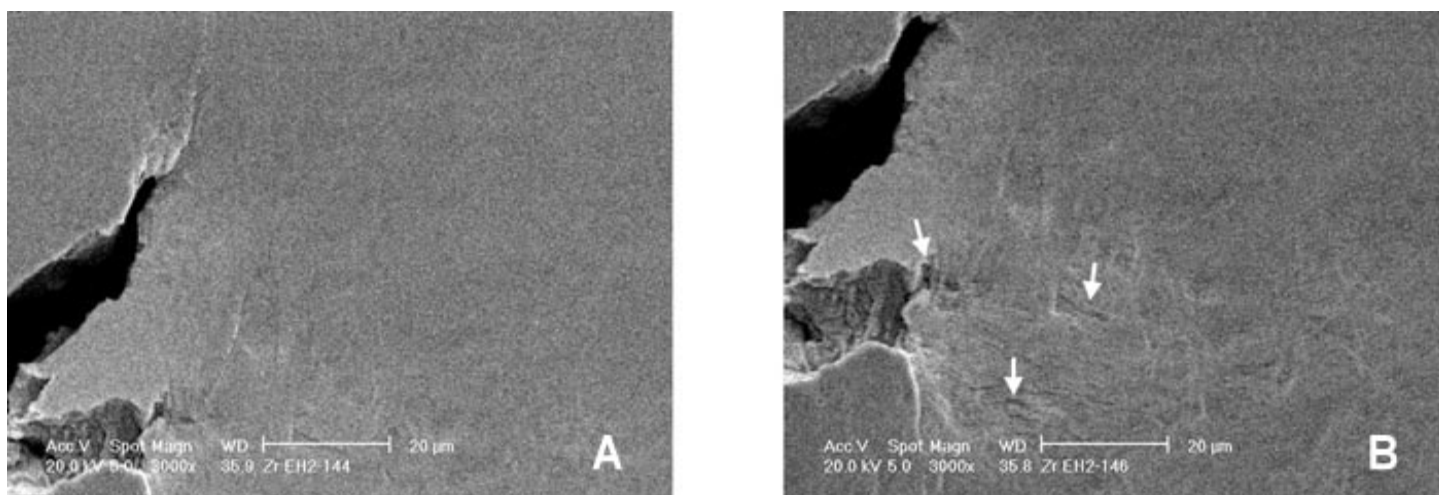


Figure 2. Crack tip fracture process in one specimen after hydride orientation: (a) $K = 20.6 \text{ MPa(m)}^{1/2}$ and (b) $K = 24.7 \text{ MPa(m)}^{1/2}$, showing hydride fracture ahead of the crack tip to form voids that link with the main crack tip.

2013 IR&D Annual Report

Development of Ni-Cr-Si Coatings to Resist Type II Hot Corrosion, 20–R8377

Principal Investigators

Yi-Ming Pan

Ken Chiang

Inclusive Dates: 03/20/13 – 09/14/13

Background — Nickel-based gas turbine material is subject to Type II hot corrosion attack that is manifested by a localized pitting corrosion attack. Hot corrosion is an accelerated, often catastrophic, surface attack of superalloy gas turbine components in the temperature range of 650 to 1,000°C. This type of accelerated attack is considered to be caused primarily by deposits of sodium sulfate (Na_2SO_4), which act as a flux to damage an otherwise protective oxide scale. The Na_2SO_4 can be ingested in the gas turbine intake air or can be produced by a reaction between sodium chloride (NaCl) in the air and sulfur (S) as an impurity in the fuel. The corrosive effect may be further intensified in marine and other industrial turbines where the alloys may be contaminated with other impurities as well as Na_2SO_4 .

The subject of hot corrosion is divided into two sub-types: Type I — high-temperature hot corrosion above about 900°C where pure Na_2SO_4 is above its melting temperature (884°C), and Type II — low-temperature hot corrosion (LTHC) between about 600 and 750°C, where a low melting eutectic such as $\text{Na}_2\text{SO}_4\text{-CoSO}_4$ (melting point 565°C) is formed on the metal surface. The Type I hot corrosion is characterized by accelerated oxidation and sulfide formation in the alloy matrix. Type II hot corrosion is characterized by pitting corrosion. Prolonged exposure of a gas turbine superalloy to low-melting eutectic salts can seriously degrade to the durability of turbine components.

Most conventional protective coatings are based on either alumina (Al_2O_3) formation or chromia (Cr_2O_3) formation for high-temperature oxidation and corrosion protection. Theoretical consideration and laboratory tests indicated that both the alumina-forming and chromia-forming coatings are susceptible to Type II hot corrosion. In this project, a new coating that forms a combination of chromia (Cr_2O_3) and silica (SiO_2) was developed. The oxidation resistance of the coating was demonstrated in furnace testing in air. The Type II hot corrosion resistance of the coating was evaluated in pilot testing in a gas flow environment.

Approach — An innovative coating that resists Type II hot corrosion attack of the disk alloy was proposed and evaluated in this project. The coating is innovative in two aspects: the coating contains only the three elements Ni, Cr and Si, and the coating was deposited at SwRI using the plasma-enhanced magnetron sputtering (PEMS) method. The coating compositions were selected from the single phase field of the Cr-Ni-Si ternary phase diagram. The alloy selected for this study was a superalloy named Alloy 10. The alloy has a composition of Ni-14.9Co-10.2Cr-3.69Al-3.9Ti-1.87Nb-2.73Mo-6.2W-0.9Ta-0.03C-0.03B-0.10Zr in wt. % nominal. Three Ni-Cr-Si coating compositions with silicon concentrations 6 atomic % (at. %), 9 at.% and 12 at.% were selected for development and evaluation. The hot corrosion tests were conducted at the Honeywell facility in Morristown, N.J.

The Ni-Cr-Si coatings were produced by a dual-gun PEMS process. The PEMS technique uses an electron source, such as a hot filament, and a discharge power supply to generate a plasma, in addition to the magnetron plasma, in the entire vacuum system. Using the PEMS technique, the measured ion flux to the sample surface can be up to 25 times higher than without the filament generated plasma.

Accomplishments — A new Ni-Cr-Si coating that resists Type II hot corrosion was developed in this

project. Four Ni-Cr-Si coating deposition runs were completed using the plasma-enhanced magnetron sputtering process in a vacuum chamber. The coating microstructure was characterized, and a uniform, compact and adherent coating was produced. High-temperature oxidation resistance of the coating was evaluated in air at 700°C. The oxide morphology was examined using optical metallography and scanning electron microscopy with associated energy dispersive X-ray analysis. After exposure to 700°C for 40 hours in air, the coating surface formed a thin (0.5 µm) chromia and silica-rich layer, which acted as a barrier to resist high-temperature oxidation of the remaining coating and the substrate.

The Type II hot corrosion resistance of the Ni-Cr-Si coating processes was evaluated in the Honeywell Morristown hot corrosion pilot testing facility. In the Type II hot corrosion test, a salt paste consisting of 60 wt.% Na₂SO₄ and 40 wt.% MgSO₄ was deposited on the coated surface. The Type II hot corrosion exposure conditions involved a flowing gas consisting of a mixture of SO₂/air with a gas flow rate of two liters (L)/min of air and 2.6 mL/min SO₂. Temperature was measured by thermocouples in the furnace prior to testing and controlled by standard furnace thermocouples. The samples were exposed to the hot corrosion conditions at 700°C for 24 hours. Under these hot corrosion test conditions, the uncoated Alloy 10 formed numerous corrosion pits with pit depths up to 50 µm. With the Ni-Cr-Si only approximately 1 µm of the coating was consumed to form the protective barrier layer. The Alloy 10 substrate was totally protected against Type II hot corrosion.

2013 IR&D Annual Report

Evaluating the Efficacy of a Criteria Model for Selecting Mobile Augmented Reality as a Learning Tool, 09-R8200

Principal Investigator

Jenifer Wheeler

Inclusive Dates: 01/03/11 – 11/23/12

Background — Mobile devices are becoming increasingly important and strategic components in the delivery of learning content. To a large degree, this is driven by the ubiquity of these devices, as well as the increasing capabilities of the technology. Thus far, most mobile-learning applications have focused on the delivery of training content and courses. Mobile devices are now capable of supporting a wide range of content delivery including applications such as simulations and Mobile Augmented Reality (MAR). While anecdotal evidence indicates strong potential for using mobile platforms in training and performance support, more empirical data is needed to begin truly defining the best use for this technology. For instance, when is it most appropriate to use MAR for learning as opposed to alternatives such as 2D animation or 3D simulation? Understanding the criteria for selecting MAR will aid in its effective application, as well as the application of other approaches.

Approach — This research effort consists of the following phases:

1. Develop and analyze selection criteria for a MAR learning application based on human performance and learning theories.
2. Design a task for study that is tailored to the MAR selection criteria. That is, based on the criteria, design a task that is optimally suited for a MAR application.
3. Implement two different mobile learning solutions (i.e. 3D simulation and MAR) that are each intended to teach or support the task created.
4. Collect and analyze data from three different groups of participants, each using a different mobile learning application (and a control group), to perform the task to draw conclusions regarding the validity of the selection model as well as key usability insights for each type of solution.



Mobile augmented reality enhances task performance

Accomplishments — The project team developed a criteria model for selecting mobile augmented reality as a learning delivery tool based on skill type, task characteristics and task execution variables. This model was used in the selection of the Soma cube puzzle as a study task. MAR and 3D applications were developed to teach and provide practice for the assembly of the Soma cube. A study was conducted to compare participants' ability to assemble the Soma cube after learning and practicing with the MAR application, the 3D application, or no mobile application (control group). Results suggest that the MAR

group was able to assemble the cube more quickly than the other groups.

2013 IR&D Annual Report

High Fidelity Physics-Based Simulation of Construction Equipment, 09-R8365

Principal Investigators

Warren Couvillion

Brian Fisher

Ryan Logan

Inclusive Dates: 01/07/13 – 05/07/13

Background — Recognizing the value of construction equipment simulators, the U.S. Army put out a request for proposals for a program with the potential to develop up to 592 construction equipment virtual trainers (CEVT) simulating five different types of construction equipment. SwRI construction equipment simulators have many of the basic requirements for the draft System Requirements Document (SRD) released for the potential RFP, but significant advances to equipment/terrain modeling and 3D rendering techniques are necessary to meet the full set of requirements. SwRI's construction simulators were made using SwRI's Graphics Interface Library (Grall). Grall became dated and more expensive to maintain and extend than to replace. The CEVT SRD requires a significant increase in visual and physical modeling fidelity beyond the capabilities of Grall and SwRI's current simulators. The objective of this research was to obtain the necessary information required to reduce uncertainty in future development of the existing simulators. To fulfill this objective, SwRI systematically investigated and evaluated commercial game engines in two primary areas – equipment modeling and dynamic terrain.

Approach — Before this effort, it was determined that the two best options for game engine evaluation were Unity and Havok. The engines were evaluated by attempting to model an excavator and dynamic, diggable terrain using both engines.

Accomplishments — Using Unity, a simple application was built that simulates an excavator digging in the ground. The PhysX engine was used to model the vehicle dynamics, and digging



Figure 1. The Unity and Havok game engines were used to model an excavator to provide a basis for comparisons of these commercial products.

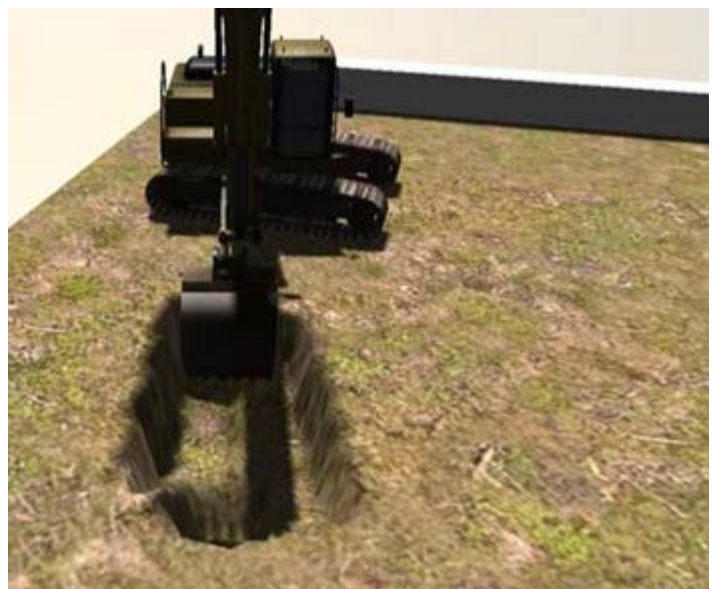


Figure 2. The game engines' assessments included investigation of dynamic terrain capabilities.

was accomplished by modifying the Unity terrain height-map. Points on the height map were modified based on their proximity to the bucket of the excavator. This approach worked, but may be impractical on a large scale. The Unity terrain, while modifiable, is optimized based on the assumption that it will rarely change. The approach used for this study may not be expandable to a large-scale terrain that could be modified at any point. Using a trial version of the Havok physics engine, an existing tank demo was modified to add an articulated arm and bucket to the tank body. The Havok physics engine also uses a heavily optimized height map to model terrain, but it cannot be modified during run-time using Havok physics calls. Havok does include classes for their graphical editor that do allow the terrain to be edited. Fortunately, the classes used to modify terrain within the Havok editor can also be used during simulations. It was determined that the Unity engine is both cheaper and easier to use than the Havok engine. It also has a large user community, allowing access to many sample projects and code. While the capabilities are not as substantial as Havok's, the ability to quickly define and test approaches interactively in the Unity editor is a major plus. Unity is the more cost-effective game engine for commercial applications such as SwRI's current equipment simulators. However, a large military effort may require Havok. While the learning curve is significantly steeper, having full access to the source code will make it easier to interface with other existing software such as after-action review and/or scenario-generation tools. The ability to load and modify large terrain databases, such as those used in military simulators, and the ability to more easily integrate military networking protocols to support joint exercises will be a significant consideration.

2013 IR&D Annual Report

Adaptation Layer for SpaceWire Plug and Play Protocols, 10-R8216

Principal Investigators

[Paul Wood](#)

Carlos Quiroz

Allison Bertrand

Sue Baldor

Inclusive Dates: 04/01/11 – 09/30/12

Background — Two plug and play (PnP) protocol options for SpaceWire (SpW) exist – one defined by the U.S. Air Force Research Laboratory (AFRL) and one developed by the European Space Agency (ESA). The ESA Spacecraft Onboard Interface Services (SOIS) protocol aims to work within the framework of the SpaceWire standard, blending PnP structures into existing SpaceWire features and retaining protocol-level support for legacy devices. The AFRL space plug-and-play architecture (SPA) protocol is geared more towards agility and adaptability to provide generalized support for more kinds of devices and networks (including blended networks of SpaceWire and other protocols). This effort investigated whether a common interface could be developed using a PnP adaptation layer to interact through both variants of plug and play, and a simulated SpaceWire Network Attached Storage (NAS) device was used as a challenge task. The project was extended to examine feasibility of performing OPNET Modeler simulation that integrated a SPA implementation.

Approach — The approach was to build a lightweight implementation of various components of the system combined with existing hardware and software so that experiments could be conducted. Using experience from the first half of the project, additional work was performed to better understand an actual SPA implementation to perform experiments in a combined simulation of the SPA with OPNET. A test bed was assembled using available SwRI resources. The test bed consisted of a SpaceWire network with two routers and Linux computers. An adaptation layer for the PnP capability was defined and implemented. A SPA middleware implementation developed by Utah State University was acquired from AFRL and ported to the physical system. Simulated producer, consumer, and NAS applications were written. The USU SPA was successfully operated using the test bed in both a raw mode and with the adaptation layer in place for the simulated applications. No ESA reference implementation was available; thus, a second SPA implementation was acquired from Broad Reach Engineering (with AFRL support). This implementation proved to be too different in its hardware and software interfaces to be practical to port to the test bed. The implementation was analyzed and it was determined, in principle, that it should be usable with the adaptation layer. The project was extended to investigate the feasibility of combining an OPNET simulation with an actual SPA implementation. The USU SPA V9.1 was used and it was verified that a simulation was feasible using OPNET co-simulation and a custom controller program external to OPNET. The external program provided an interconnect between the SPA executables and the OPNET internal model.

Accomplishments — This work showed that an adaptation layer was feasible to add to existing PnP implementations. The addition of the adaptation layer to the USU SPA implementation was straightforward and effective. A lightweight NAS was built, along with producer and consumer applications, which were connected using the adaptation layer and the USU SPA. The adaptation layer impact on system performance was negligible. A second SPA implementation was analyzed. This implementation was not directly operable on the underlying hardware. This version, however, would have been compatible with the adaptation layer. Also, although no reference implementation of the ESA approach existed, the adaptation layer concept was workable for that environment as well. Finally, in the project extension, it was shown that the SPA could be successfully integrated with the OPNET Modeler. The ability to perform software-in-

the-loop (SIL) simulation (for example, the SPA) is an enabling factor in performing very high fidelity simulations of SpW networks.

[2013 IR&D](#) | [IR&D Home](#)

2013 IR&D Annual Report

3D Imaging for Behavior Classification, 10-R8221

Principal Investigator

Chris Lewis

Inclusive Dates: 04/01/11 – 10/01/12

Background — This research developed an automated behavior recognition capability, which uses a very low-cost, 3D color sensor for observing the motion of people. The system uses a variety of state-of-the-art machine-learning techniques to estimate which of the trained behaviors is being performed. Several training tools were also developed that allow the system to be easily customized for a variety of applications. A novel feature derived from raw motion measurements was developed and shown to discriminate well between exercise behaviors. This feature, called a Motron, is constructed from natural cluster centers in data vectors containing position and velocity measurements of the subject. A new clustering algorithm was also developed and shown to be useful for both analysis and for accurately modeling sampled data.

Approach — The techniques were implemented under ROS (Robot Operating System), which is an open-architecture, publish-subscribe, system integrating driver for common sensors and machine-learning tools into a convenient development environment. ROS nodes were developed for training classifiers, analyzing clusters in data and for estimating behaviors in real time.

Accomplishments — A novel motion descriptor, called a Motron, was developed. The descriptor is formed from natural clusters in pose measurements. Histograms of observed Motrons over a time window were shown to be both salient and computationally inexpensive features for classifying behaviors in real-time. In addition, a novel cluster analysis algorithm was developed that automatically determines both the number of clusters and models for those clusters in arbitrary high-dimensional data. Results from this

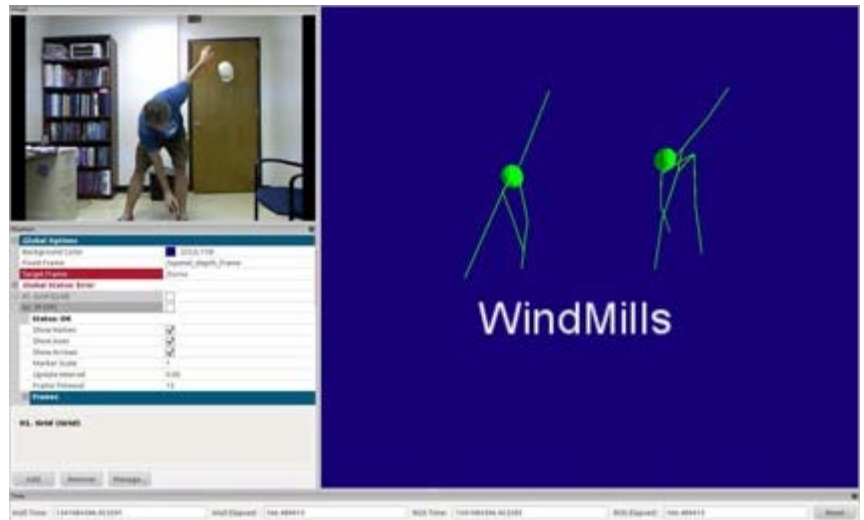


Figure 1. A real-time behavior recognition system is trained to recognize motions. This system relies on natural clusters in the complex motion measurement data. A novel cluster analysis algorithm, having wide applicability, finds these natural clusters in high-dimensional data.

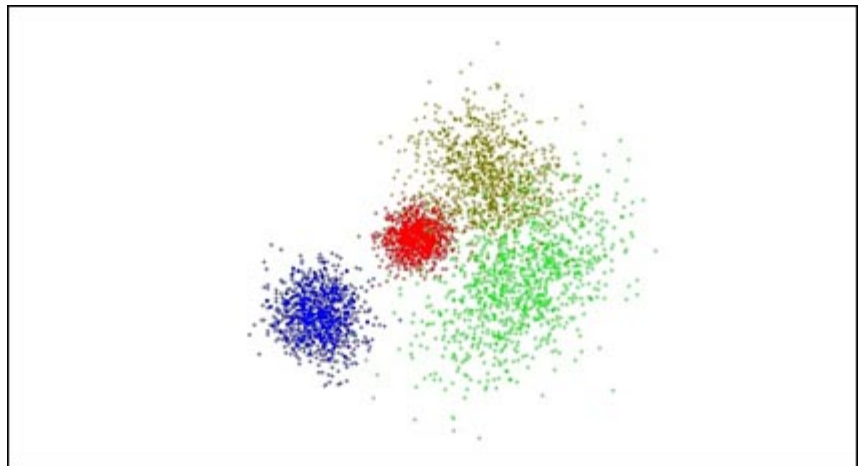


Figure 2. The image shows a two-dimensional slice of clusters found in twelve-dimensional data having significant overlapping distributions.

project have been employed on projects for the National Institute of Standards and Technology, and for the Office of Naval Research.

2013 IR&D Annual Report

Special Purpose IP Routing, 10-R8243

Principal Investigators

[Myron Moodie](#)

Todd Newton

Ben Abbott

Patrick Noonan

Inclusive Dates: 07/01/11 – 12/31/12

Background — Network solutions permeate all domains, from our homes and cars, to industry and space. The success of networking stems from the growth and standardization of the Internet Protocol (IP), which provides a universal open transport. The openness of this protocol makes it such that multiple vendors have fielded interoperable devices. Almost every company has network closets filled with blue boxes (Cisco® routers) and every home has a network connection that includes a router and wireless access point. This openness in standardization comes with a cost. Special purpose and flexibility beyond the envelope of support is very hard to reach. For example, simply adjusting a home router to better handle overload in the Voice over IP scenario is a serious challenge. Consequently, most networks are only used in their default settings with performance accepted and the functionality left as a mystery. The ubiquitous nature of networks has led to a desire to leverage networking technologies in special communications arenas. Unfortunately, not all of these scenarios are well served by “default-setting” networking. At times, for the small volume specialized scenarios, the existing vendors are unwilling or unable to adapt or adjust their products. For example, Cisco has no business interest in providing specialized product markets smaller than 100s of millions of dollars.

Approach — A framework was developed for rapid development and deployment of special purpose IP routers. This was achieved by adjusting settings on standard routers (rather than using the typical “default settings”) and combining with embedded computer nodes. The embedded computer nodes can leverage knowledge about the inner workings of the commodity devices and manipulate data flows such that the overall specialized scenario needs are achieved. The approach to this project was to research, define and characterize the virtual router concept and to evaluate its suitability to solving the types of problems similar to flight test telemetry networks. This required evaluating open-source router source code to determine portions that can be leveraged for creating the router virtualization and adding the distributed concepts necessary to implement a virtual router. A series of challenge problems was developed to evaluate the virtual router concept. Baseline performance was measured using standard routers with both default and optimized configurations. The virtual router was evaluated using the same challenge problems and compared to the baseline performance. The virtual router implementation was successively revised and reevaluated to determine performance gain over baseline.

Accomplishments — A number of open-source routing packages were evaluated to determine which looked most promising for a starting point in developing the virtual router concept. Standard and modified router implementations were built based on several of these packages. The virtual router architecture was augmented using distributed physical network interfaces under the control of a central control node. A combination of open source software capabilities not originally designed for routing applications was leveraged to enhance the scalability and flexibility of the virtual router approach. A laboratory environment was established by implementing multiple virtual router nodes using a combination of SwRI network lab resources. The main test bed setup consisted of nodes distributed within an SwRI building, inside a residence in San Antonio, and in a hotel room in Pennsylvania. Network performance was measured across these three networks under varying network load conditions both with and without the virtual router. The project demonstrated that with a few modifications in limited locations to existing networks

better control of network data can be maintained through the existing network infrastructure, allowing for improvements in efficiency and performance between congested networks.

2013 IR&D Annual Report

Secure Mobile Applications for Corporate Travelers, 10-R8244

Principal Investigators

Sean C. Mitchem

Sandra Dykes

John Whipple

Inclusive Dates: 07/11/11 – 10/11/12

Background — Southwest Research Institute and its clients are seeing a surge in employee use of personal mobile devices for company business. Smartphones and tablets raise new security issues because they are often owned by employees and contain a mixture of personal and company information. The prevalence of this trend is illustrated in the fact that a new term has been coined to describe it: BYOD, for Bring Your Own Device. Small mobile devices are more likely to be lost or stolen, exposing sensitive company and client data. Malware risks are amplified because mobile devices connect to the Internet directly rather than from behind corporate firewalls and intrusion protection systems. Safeguarding mobile devices will require developing innovative security technologies that address these new usage patterns and device characteristics.

Approach — This project addressed multiple aspects of mobile device security, with a focus on the following areas:

- Malware threats to mobile devices
- Secure coding methodologies for mobile applications
- Data protection and user authentication utilizing device sensors
- Mobile device management systems trade space analysis
- Mobile applications for corporate travelers

The approach combined web research, literature reviews, interviews with commercial companies, in-house testing of mobile device management systems, developing internal mobile apps for research and testing purposes, and experimentation, depending on the task being accomplished.

Accomplishments — The project produced two white papers: “Malware Threats for Mobile Devices” and “Secure Coding for Mobile App Development.” The first is a general assessment of malware-related threats to mobile devices and secure protection provided by the iOS and Android operating systems. The second paper targets software developers and was intended to provide a primer on best practices for writing secure mobile applications. The research on mobile device management systems leveraged the information from these white papers to assess current solutions. This study produced a technology trade report that describes options and provides recommendations for enterprise organizations. Additionally, the project team produced the article “Mobile Applications Security: Safeguarding Data in a Mobile Device World,” published in the March/April 2012 edition of *CrossTalk, The Journal of Defense Software Engineering*.

Aspects of this research required developing real applications to test understanding and validate new approaches. The applications were developed as deployable apps, useful to Institute employees while on travel. The mobile traveler apps were developed for iOS and Android and consist of Mobile SwRI WebID, SwRI Traveler and Group Text Emergency Notification. The most innovative result of this project is in the area of sensor-based authentication. The motivation was to make authentication easier for users without reducing data protection, effectively balancing risk and usability. Sensors on mobile devices provide measurements of device orientation, touch pressure, touch size and other data. In Sensor-Based Authentication, machine-learning methods were used to train a detector on sensor data. The model can

then be applied to verify a user's identity and detect imposters. Data was collected from 15 volunteers who entered practiced text (e.g., a password) and free-form text. In both cases, the average classification accuracies were more than 99 percent. These results are striking for a preliminary study and indicate that the approach should be pursued further. In a related approach called State-Based Authentication, sensor data was combined with system state to determine the required level of authentication. System state determines how easily sensitive areas of memory can be accessed. Sensors determine whether an attacker may be in possession of the device. For example, sensors can detect whether the device has been laid down since the last password entry. If sensor data guarantees that the owner has maintained possession, then no password is necessary. If not, then the device state is used to determine whether the user must enter a strong password or simple PIN.

In summary, this project has provided a deep understanding of the security issues unique to mobile devices. The white papers and reports will be made available to all SwRI divisions, improving the Institute's knowledge and capabilities in this area. Research results for user authentication will provide a foundation for pursuing externally funded research.

2013 IR&D Annual Report

Investigation into Techniques for Detecting Negative Obstacles 10-R8278

Principal Investigators

Steven W. Dellenback

Jason Gassaway

Richard Garcia

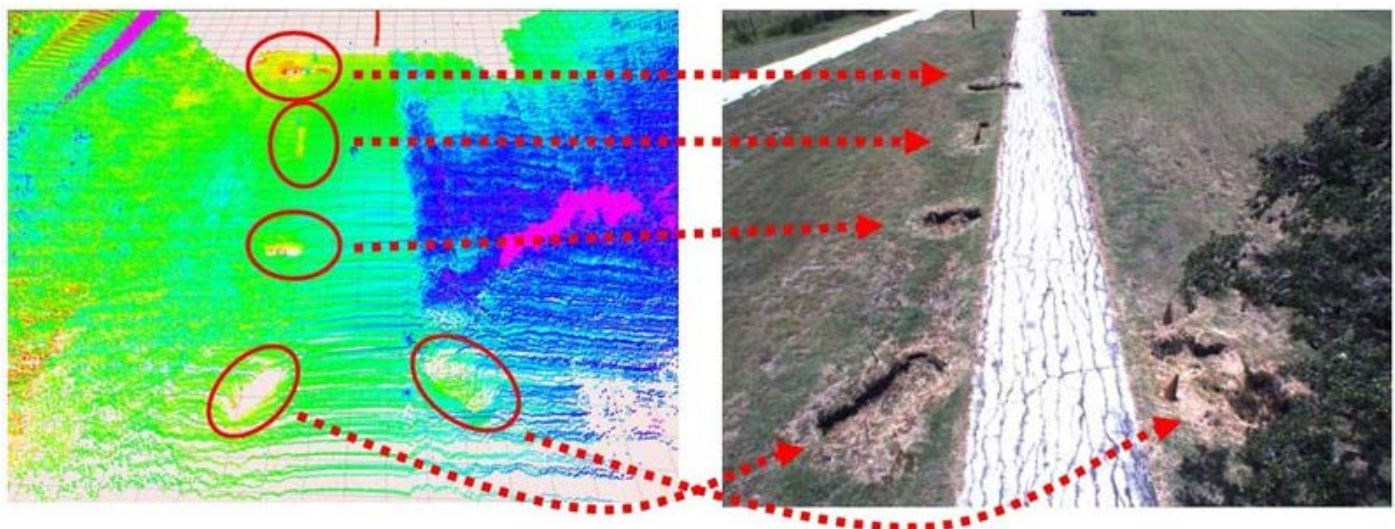
Inclusive Dates: 01/01/12 – 01/12/12

Background — The U.S. military has repeatedly stated the single most complex, unresolved issue in the Unmanned Ground Vehicle (UGV) community is the detection of negative obstacles (these are holes, troughs and anything that does not reflect or is difficult to observe). In most cases, it is simply a geometry problem because the angle in which sensors can detect a hole is not acute enough until the vehicle is too close to do anything about it.

Approach — The goal of this project was to develop techniques that facilitate the detection of “negative obstacles” for UGVs. Negative obstacles are very difficult to identify from a traditional UGV platform moving at a significant speed because the elevation of the sensors does not provide a field-of-view (FOV) that can identify the obstacle in enough time to perform avoidance maneuvers. Techniques currently used are to place downward looking sensors at the front of the vehicle and have a FOV that is measured in a small number of meters with a UGV moving at a very slow rate of speed. This effort investigated the use of sensors that will be located above the vehicle using an airborne platform.

Accomplishments — The following activities were completed:

- Designed and fabricated a mast structure to allow the sensors to be located 12 meters above a HMMWV.
- Designed an algorithm framework that implements a pipeline processing framework composed of the following steps: data collection, localization, filtering, analysis and detection.
- Implemented algorithms to capture data from both LIDAR and a camera attached to the mast. The sensors capture scans of the negative obstacle test area while mounted to the mast and the results provide highly reliable identification of negative obstacles. The following figure depicts how the detection efforts were implemented.



SwRI researchers developed a set of algorithms for use by an airborne sensor that uses LIDAR and vision data to detect holes and depressions not normally detectable by vehicle sensors.

[2013 IR&D](#) | [IR&D Home](#)

2013 IR&D Annual Report

Detection of Malware on Vehicular Networks, 10-R8281

Principal Investigators

[Mark J. Brooks](#)

Marisa C. Ramon

Tam T. Do

Nakul Jeirath

Inclusive Dates: 01/01/12 – 01/01/13

Background — Computers are becoming increasingly prevalent in modern automobiles. By some estimates, even low-end automobiles contain 30 to 50 of these computers, also known as electronic control units (ECUs). ECUs control everything from the in-vehicle entertainment systems (infotainment systems) to the electronic braking system to the engine fuel-air mixture. A recent trend in the industry is the introduction of wireless technologies such as cellular, Bluetooth and even Wi-Fi into the vehicle. Given the increasing sophistication and connectivity, the modern automobile is fertile ground for the same sort of malware and malicious attacks that are associated with traditional personal computers.

Approach — The objective of this project was to demonstrate the feasibility of vehicle malware and to evaluate its associated impacts on the vehicle network, with the end goal of developing a vehicle malware detection system.

To execute the project, the following tasks were performed:

- **Test Bed Development:** A vehicle and multiple infotainment ECUs were obtained to perform experiments and testing.
- **Vulnerability Analysis and Exploit Discovery:** The vulnerability analysis and exploit discovery task tested the infotainment platform and a subset of its threat vectors for specific vulnerabilities.
- **Malware Detection Methodology Research:** The malware detection methodology research task included developing a software tool, Automotive Tool for Reverse Engineering, Analysis, and Detection (autoTREAD™). This tool allowed the monitoring of effects due to Controller Area Network (CAN) injection, such as volume control, seatbelt chimes and other CAN signals, and allowed for developing detection techniques.
- **Algorithm Testing and Performance Measures:** The detection algorithms of the autoTREAD™ software were created during the malware detection task and tested in the algorithm testing and performance measures task. Also in this task, statistics were recorded to verify performance of the algorithms and allow room for algorithms enhancements.



Figure 1. SwRI's Vehicle Security Test Lab

Accomplishments — As a result of this investigation, SwRI has developed autoTREAD™, a tool for reverse engineering CAN signals, sniffing CAN traffic, and detecting injected CAN signals. The algorithms developed detected injected signals very well, detecting purely periodic injected CAN signals indicating

false positive rates of 0.3 percent and true positive rates of 98.8 percent. The algorithm detecting periodic event signals for steering wheel column button pushes achieve a rate of 60 to 65 percent true positive detection with only about a 2 percent false positive indication.

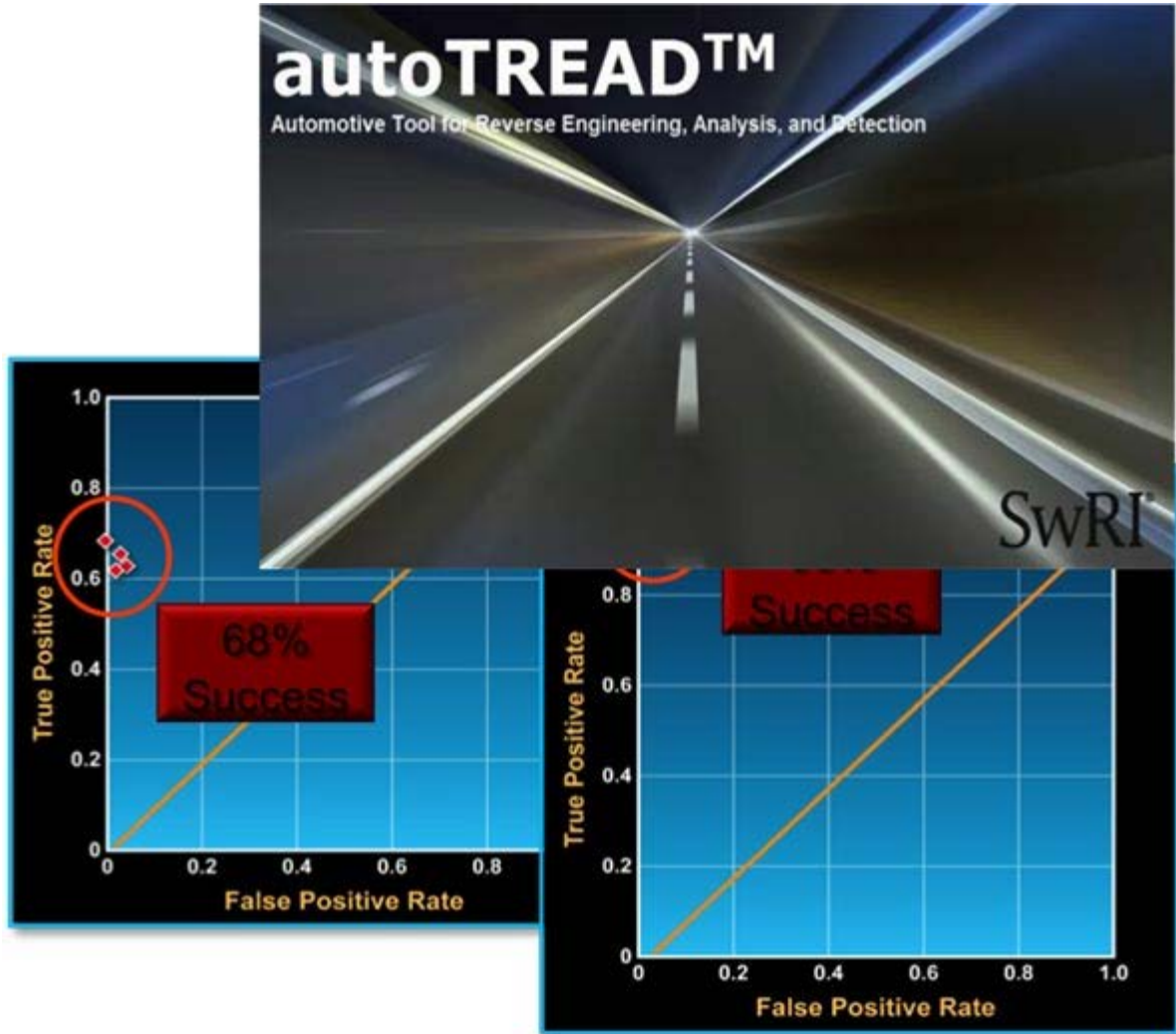


Figure 2. The SwRI-developed autoTREAD reverse engineers CAN signals, sniffs CAN traffic and detects injected CAN Signals.

2013 IR&D Annual Report

Advanced Situational Awareness Experiment, 10-R8284

Principal Investigator

Michael S. Moore

Inclusive Dates: 12/27/11 – 01/01/13

Background — Southwest Research Institute has supported the U.S. Army Program Executive Office for Command, Control, and Communications Tactical (PEO C3T) in developing the Vehicular Integration for C4ISR/EW Interoperability (VICTORY) architecture since 2008. This architecture provides a foundation-enabling sensor and weapon-system interoperability on military tactical vehicles. The VICTORY architecture will provide a core vehicle network that will enable interoperability between systems on the vehicle. Leveraging the VICTORY integration and adding an extra-vehicle mesh network to also share data between the vehicles will enable new situational awareness applications.

Recognizing this potential, SwRI conducted an initial internal research project (10-R8107), resulting in new technologies. One technology receives first-hand observation inputs from multiple, disparate sensors on the vehicles and coordinates between the vehicles to develop an overall view of the local operational picture. It applies heuristic algorithms that correlate the information from the various sensors and automatically applies reasoning that is currently done manually by the soldiers. The goal is to create more actionable information for soldiers. As an example, sensors that are currently fielded have high false alarm rates and, as a result, are often disabled by frustrated soldiers. The Advanced Situational Awareness (ASA) technology should reduce the false alarm rates by correlating information from multiple sensors and from other vehicles. The second technology integrates the operational picture with real-time battle maps and video streams, creating fused views with the goal of providing relevant, timely information to the soldier in simple views.

Approach — The technology developed in the prior project was evaluated in a laboratory setting. This current project is integrating experimental systems on three vehicles and executing experiments in military-relevant scenarios. The feedback obtained from the experiments is being used to adjust the approaches in the correlation and visualization tools and increase their relevance to soldiers. The objective is to quantitatively and qualitatively measure the effectiveness of the ASA technologies and mature the algorithms to meet warfighter needs. Toward this objective, SwRI is collaborating with the Army's Night Vision and Electronic Sensors Directorate (NVESD), which supports the Army Deployable Force Protection (DFP) program. They have teamed with SwRI to integrate the ASA systems with DFP systems, develop military relevant scenarios, and execute experiments.

Accomplishments — An ASA demonstrator vehicle was integrated with a variety of sensors, cameras, and displays to evaluate the technologies. The demonstration vehicle was used in conjunction with two VICTORY-enabled HMMWVs and a stationary Tactical Operations Center (TOC) to develop and test ASA technologies at SwRI. These platforms are integrated via a Extra Vehicle Mesh Network (EVMN), which enables sharing relevant situational awareness information. This shared information is presented to users on an integrated mapping application, "augmented reality" video overlays, and tabular user interfaces.

SwRI then teamed with NVESD after completion of initial ASA technologies testing at SwRI in a weeklong exercise at Camp Roberts, Calif. The SwRI/NVESD team integrated a DFP-VICTORY-ASA experimental system, including three VICTORY and ASA-enabled vehicles (the demonstration vehicle and two HMMWVs), an experimental TOC, and a large-scale DFP network. Extensive experiments were conducted, and data and feedback were collected. Lessons learned from that exercise were used to evolve and mature the ASA technologies.

As a direct follow-on to this research, SwRI received funding from NVESD in FY2013 to integrate a "mobile sensor platform," consisting of an all-terrain vehicle (ATV) (Polaris RZR), a VICTORY network implementation, and a "platoon level interoperability" package. Platoon level interoperability is the newest incarnation of the ASA concept and concentrates on coordination between VICTORY-enabled vehicles and sharing and correlating data from distributed mobile sensors. SwRI integrated the mobile sensor platform with the NVESD integrated sensor architecture (ISA), which is used to integrate DFP systems that protect forward operating bases, and delivered the vehicle in November 2013. Additional follow-on work in FY2014 is planned. This work will extend the platform with additional capabilities and support a demonstration including the ATV mobile sensor platform and the ASA demonstration vehicle. The demonstration is tentatively planned for January 2014 at a location in Mississippi.

[2013 IR&D](#) | [IR&D Home](#)

2013 IR&D Annual Report

Robotic Part Handling for Unstructured Industrial Applications, 10-R8301

Principal Investigator

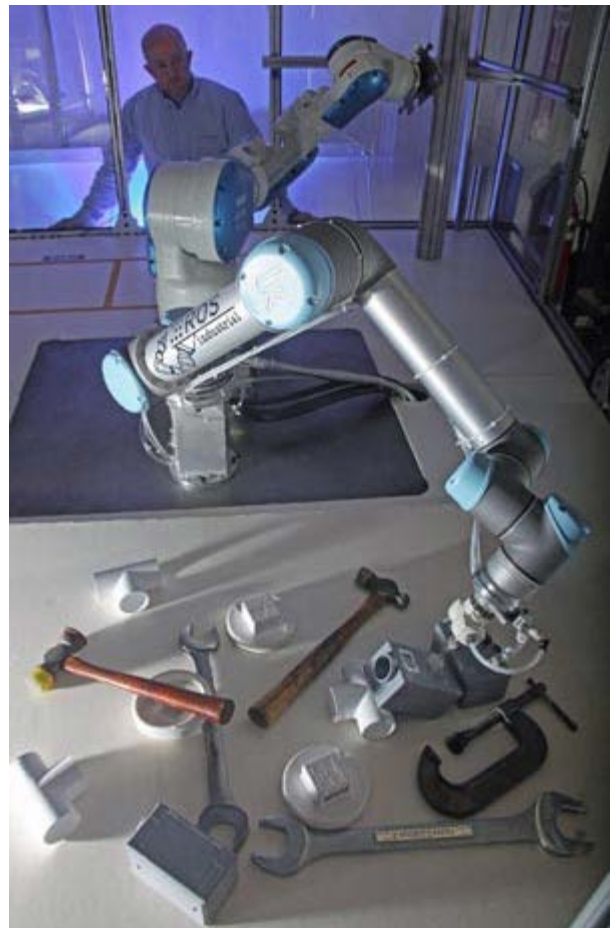
Clay Flannigan

Inclusive Dates: 04/01/12 – 03/01/13

Background — Recent developments in 3D sensor technologies, adaptive robotic grippers and advanced perception and planning algorithms are rapidly advancing the use of robots in complex and dynamic environments. Traditional industrial application of robots requires that parts be precisely located using dedicated fixtures so that there is little uncertainty in the location of the workpiece and condition of the workspace. More advanced industrial robotic systems use 2D or 3D vision sensing to handle minor variations in part locations. However, there are large classes of problems where high part variability or dynamic environments prohibit rigid fixturing methods and confound commercially available vision solutions. An example application is sorting residential recyclables, where there is an almost infinite variability of parts to be manipulated. Aerospace manufacturing is another market that is challenged by high-mix, low-volume processes.

Approach — SwRI is the founder of an open-source software framework for industrial robotics called [ROS-Industrial](#) that builds upon the work of the huge community of robotic researchers using the [Robot Operating System \(ROS\)](#). The current research is extending the ROS-Industrial program through investigation of perception, motion planning and grasp planning methods to address unstructured manipulation. Specifically, PrimeSense structured light sensors are used for colorized, 3D-range image acquisition. Object recognition and pose estimation algorithms have been developed that use the color 3D data to identify objects in cluttered environments. Both vacuum and adaptive finger grippers were employed for grasping. Motion planning objectives included generating efficient and collision-free motion even in dynamic or complex scenes.

Accomplishments — For relatively simple geometric objects, bin picking was successfully demonstrated, including cases where multiple classes of objects were randomly sorted. For more complex objects types, typical of those in manufacturing operations, multiple algorithms were developed and tested for object segmentation and pose estimation. Depending on the optical characteristics of the object and the environment, the algorithms used shape cues, color cues, image texture cues or combinations of the



SwRI has developed multiple perception and planning approaches to address manipulation in cluttered, dynamic, or unstructured environments. The figure shows a demonstration cell that was capable of sorting multiple object classes from a cluttered pile.

three. For highly cluttered scenes, heuristics were developed to singulate parts so that recognition algorithms could be more effectively applied. The results show that certain classes of problems are tractable for industrial application, especially those where parts have salient optical or geometric features. Each application poses unique challenges that must be considered for perception and grasping solutions.

2013 IR&D Annual Report

Traffic Signal Interface Concepts, 10-R8320

Principal Investigator

[Tucker Brown](#)

Inclusive Dates: 07/16/12 – 01/16/13

Background — SwRI is the Florida Department of Transportation (FDOT) and Texas Department of Transportation (TxDOT) software developer for the SunGuide® and Lonestar Advanced Traffic Management Systems (ATMS), respectively. SunGuide and Lonestar provide Traffic Management Center (TMC) operational automation functionality to monitor conditions on freeways and react to changing conditions and incidents by alerting freeway users through messages on signs and dedicated radios as well as dispatching incident response vehicles. During normal operations, incidents inevitably occur on the freeway and they often result in partial blockage of the freeway. In these cases, traffic is often entirely or partially routed off the freeway and onto arterials, e.g. frontage roads and other secondary roadways. The Traffic Signal Control System's (TSCS) timing plans on the arterials are tuned for normally occurring traffic conditions and do not automatically react to this additional traffic. FDOT and TxDOT, as well as other potential DOT users of SunGuide and Lonestar, have expressed interest in incorporating interfaces to TSCS. Such an interface would provide a DOT operator the ability to issue commands to a TSCS to run pre-defined signal plans on the arterials better suited to the additional traffic load. The purpose of this research was to investigate and develop an abstraction reflecting the common elements of TSCS interfaces and then develop and integrate a prototype into the Florida solution, thus improving SwRI's competitive position.

Approach — The approach for this effort was broken into three phases. The first phase was to identify systems of interest and then collect and analyze available documentation for each of the subject systems. The second phase was to develop general interface concepts and a design to accommodate the differences between the systems. This design included the definition of an operator Graphical User Interface (GUI) and isolated interface specifics to facilitate expansion of the software to accommodate all systems at a later time. The third phase was to develop a rudimentary prototype interface to a selected TSCS.

Accomplishments — During the course of the project, a prototype system based on the defined interface abstraction, including functionality to retrieve and display TSCS status, as well affect TSCS status, was designed and built. A vendor system and an SwRI proprietary system were then able to interface with the new abstraction and control multiple types of signal controllers from the same seamless interface. In addition to the proof-of-concept system, there has been interest from FDOT on improving the prototype system. The most meaningful accomplishment will be the potential of the prototyped traffic signal system to generate new clients.

2013 IR&D Annual Report

ROS-Industrial® Strategic Technology Development, 10-R8335

Principal Investigator

Shaun Edwards

Inclusive Dates: 09/17/12 – Current

Background — In a previous internal research effort, SwRI worked closely with Robot Operating System (ROS) developers at Willow Garage to develop an open source ROS-Industrial software stack (software suite) to support the use of [ROS for industrial applications](#). The technology developed under this previous effort brought the use of powerful ROS capabilities, such as advanced perception and path/grasp planning, to industrial robotics applications.

Since the completion of the previous project, the [ROS-Industrial open-source program](#) has attracted significant interest in the industrial robotics community. Two examples of this interest are the growth of the open-source development community and the formation of the [ROS-Industrial Consortium](#). The open-source community has grown to include a worldwide network of commercial, independent and government labs working toward a common goal of enabling advanced industrial robotics and automation through open-source development. The ROS-Industrial Consortium was formed and its first membership meeting was held in March 2013. The goal of the consortium is to provide commercial investment and input into the ROS-Industrial program. Specifically, the consortium will jointly fund technology development through [focused technical projects](#).

The objective of the ROS-Industrial Strategic Technology Development effort is to continue technology development, expanding the capabilities of ROS-Industrial, while supporting the consortium and open source community.

Approach — The approach of the ROS-Industrial technical effort is to expand its capabilities through continued software development both at SwRI and through external development teams, as well as demonstrate real-world applications. Specifically this effort will:

- Provide guidance to the ROS-Industrial open source community, outlining developmental efforts for external teams.
- Expand the ROS-Industrial driver set, providing compatibility and interoperability with major industrial robot vendors.
- Integrate advanced path planning and perception algorithms with a focus on those that are useful in industrial applications, such as machining and painting.
- Demonstrate ROS-Industrial in multiple real-world applications through cooperation with commercial companies.

The software developed under this effort will be released open source under the [ROS-Industrial program](#).

Accomplishments — The project has completed the following milestones:

- The ROS-Industrial software has grown, with many contributions coming from external development teams in the open-source community.
- The ROS-Industrial software now supports most major industrial robot vendor platforms. This [capability was demonstrated](#) at the Automate tradeshow in early 2013.
- Integration of ROS-Industrial with the [MoveIt Library](#), which provides advanced path planning capabilities with close integration of 2D/3D perception.



Video: The ROS-Industrial program recently celebrated its one-year anniversary. This video montage shows the results of programs from around the world using ROS-Industrial.

2013 IR&D Annual Report

Feasibility Study for Embedded Software Control of Flexible RF Filters, 10-R8356

Principal Investigator

[Levi Blackstone](#)

Inclusive Dates: 12/21/12 – 04/21/13

Background — As part of a Defense Advanced Research Projects Agency (DARPA)-funded project, Southwest Research Institute (SwRI) previously teamed with a small business to create a controller algorithm for a new type of tunable radio frequency (RF) filter. During this work, the need to develop a rapid-prototyping capability for embedded control systems was recognized. The purpose of this internal research was to improve these capabilities internally, and to investigate possible implementation approaches for the control algorithm resulting from the previous project.

Approach — A hybrid feed-forward/feedback controller model was developed in a graphical modeling environment. This modeling environment enabled the controller algorithm to be deployed to a microprocessor or field programmable gate array (FPGA) on an accompanying hardware platform. This setup provided the flexibility necessary to investigate multiple deployment strategies without requiring significant rework of the model code.

Using models derived from a hardware characterization, the feed-forward portion of the control algorithm was implemented in a microprocessor. This approach was sufficient to demonstrate basic control capability, enabling a user to select a desired center frequency and tuning the filter appropriately. This level of control provided reasonable results for static frequencies at ambient temperature.

Due to the early prototype status of the customer-provided hardware, SwRI did not receive a functioning feedback sensor early enough to include it in this feasibility study. By including a feedback sensor in the filter control setup, it should be possible to greatly increase the stability of the system across a variety of operating conditions.

Accomplishments — The experience gained from this research should improve SwRI's rapid-prototyping capability for embedded control systems. Although hardware delays impacted the intended scope of this project, the prototyping setup was sufficiently flexible to allow parts of the system to be simulated in the absence of hardware.

Follow-on work has already been awarded based partly on results from this research, and work will be continued in collaboration with the small business and a major defense contractor. This technology has broad applicability in areas such as electronic warfare, radar systems, and cognitive radio, and other entities at SwRI have expressed interest in applying this technology to their own projects.

2013 IR&D Annual Report

Dynamic Real-Time Lane Modeling, 10-R8361

Principal Investigators

[Purser K. Sturgeon II](#)

Richard Garcia

Inclusive Dates: 01/01/13 – 01/01/14

Background — The U.S. Department of Transportation (USDOT) has committed to developing a fully connected transportation system that will enable advanced vehicle safety applications. This work has focused on a number of vehicle-to-vehicle (V2V) and vehicle-to-infrastructure (V2I) applications, such as forward collision warning (FCW), emergency electronic brake lights (EEBL), intersection violation warning, signal phase and timing (SPAT), signal prioritization and pre-emption, blind spot detection/warning and others. Through a number of prototypes and proof-of-concept test-beds over the last six years, it has been accepted that existing map solutions are not adequate for the real-time needs of these applications. They either lack the lane-level resolution required for vehicle safety applications or are cost-prohibitive, requiring precise road surveys or extensive vehicle sensor packages. As a result, the application prototypes up to this point have been reliant on confined test scenarios in which vehicle paths are either straight lines or follow constant, large-radius curves, limiting their applicability and usability in real-world environments.

Approach — Vehicles equipped with U.S. DOT connected vehicle hardware broadcast positional data 10 times per second in a basic safety message (BSM), which is designed to be used for V2V safety applications onboard vehicles. SwRI has developed processes to passively collect these BSMs through roadside equipment and a set of learning algorithms that use the information contained in the BSM to produce a local map of the roadway at an accuracy level of individual lanes. Once this map has been generated, it can be shared back to vehicles in the local area to increase their safety application's accuracy and to reduce false positive warnings. In addition, if a change occurs in the lane structures, such as a portion of one or more lanes becoming unusable due to an accident or debris, the map will automatically update once a sufficient number of vehicles have avoided the location. This method uses the behavior of vehicles themselves to determine the dynamic structure of the local roadway and enables an efficient and rapid method for keeping the map up-to-date.

Accomplishments — SwRI has developed a set of software tools that enable the passive collection of vehicle BSMs to be converted into a high-fidelity, lane-level model of the local roadway structure. These algorithms utilize the behavior of vehicles, as evidenced by their driven paths, to infer the details of lane structure, which have the potential to change due to a construction lane closure, a collision or an obstruction caused by debris. Once the lane-level map has been reduced to a minimum set of GPS points, it is shared back to the local vehicle population, and represents the most up-to-date information on the structure of the local lanes in near real-time.

2013 IR&D Annual Report

Robotic Part Handling of Unstructured Materials: Semi-Random Component Pick and Place for Assembly, 10-R8369

Principal Investigator

[Christina Gomez](#)

Inclusive Dates: 02/01/13 – 06/01/13

Background — Industrial robots have been used for decades in manufacturing for high-volume, repetitive tasks, or tasks where required precision is beyond human capabilities. However, in factories today there remain countless "dull" jobs, those repetitive tasks that defy automated solutions largely due to high cost of the dedicated equipment required to untangle, sort, singulate, feed and pre-position components for assembly or other subsequent operations. Flexible industrial robotic solutions are needed to handle unstructured production/assembly applications. The need for robotic part handling for unstructured industrial applications is diverse. Small- and medium-sized manufacturers need robotic systems that can easily be "re-trained" to handle a variety of parts due to the low volume, small batch nature of their manufacturing processes. One such manufacturer provided parts for testing to improve a process of grabbing the part from the floor to place it into a fixture with pins for further processing. The objective of this research was to investigate methods to robotically manipulate specific client-supplied parts in typical industrial scenarios that include bin containment, unstructured emplacement and accurate placement.

Approach — Building on a previous internal research project (10-R8301) software developed for unstructured grasping was expanded to be more reliable and was combined with a new capability for precise placement. A Universal UR5 robot was used with a three-fingered gripper and a 3D camera (Asus Xtion) to pick commercially supplied parts from a bin into a fixture. Additionally a FARO portable coordinate measuring machine was used to measure the pose of the parts at several stages of the pick and place routine. Previous work from the ROS (Robotic Operating System) and ROS-Industrial was leveraged for both perception and motion planning. The results using only a 3D camera were not consistent enough to ensure accurate placement, so a secondary 2D camera (Allied Vision Technologies Prosilica GigE) was added to extract a more accurate pose estimate.

Accomplishments — In this work, SwRI attempted to narrow the focus of a specific part-handling application. As a result, the robot was able to recognize learned objects and accurately estimate their pose in cluttered environments and researchers could measure the pose error from the perception system(s). The methods used for 3D recognition are complex, computationally intensive and can still be considered too fragile for reliable industrial use. With a more compliant gripper, the 2D recognition pose result would be sufficient for accurate placement on the pin fixture every time.

2013 IR&D Annual Report

Control of Laser Coating Removal Process, 10-R8385

Principal Investigators

Michael P. Rigney

Thomas G. Whitney III

Michael O. Blanton Jr.

Inclusive Dates: 04/01/13 – Current

Background — The use of high-power lasers for coating (paint) removal from aircraft surfaces offers a significant improvement in process efficiency and reduction of both consumables and waste streams relative to alternate approaches (chemical stripping, media blasting). The ability of lasers to quickly ablate paint from surfaces comes with the challenge of controlling laser power to achieve selective coating removal; that is, removal of top coat(s) while leaving the primer layer. SwRI has a long history in the design and deployment of large robotic systems employing media-blasting for coating removal from military fighter aircraft. This research, combined with SwRI's capabilities in precision mobile robot systems will support development of coating removal systems for military and commercial transport aircraft.

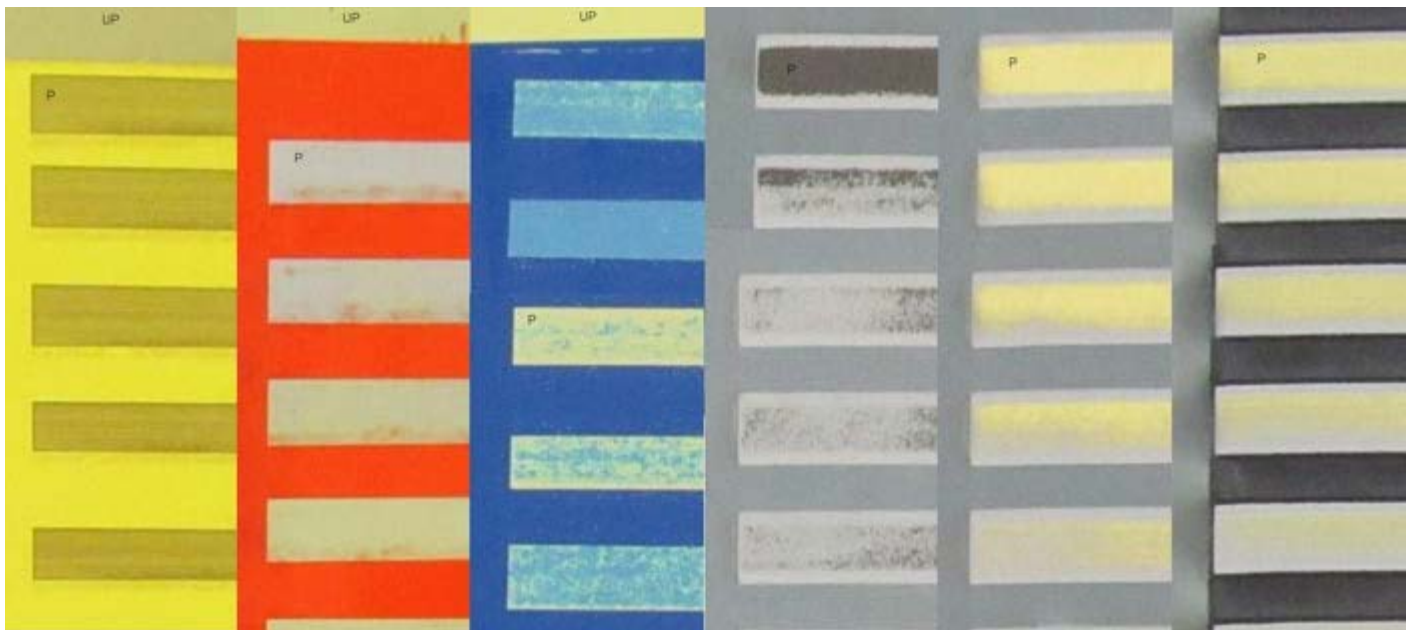


Figure 1. Test panels processed using a prototype laser coating removal scanner.

Approach — The objective of this research is to implement a coating removal state classifier that supports selective coating removal. Application challenges and risks include wide variation in coatings and substrates (thickness, color, laser ablation response), subtle differences between some coatings and substrates, a laser ablation process that exposes a mixture of top coat and the underlying material (coating or substrate) within the incremental regions that must be

sensed, the presence of combustion products in the sensed region, and a high process cycle rate (300 Hz).

Accomplishments — Paint system specifications (top coat(s) and primer combinations) currently used in military and commercial aircraft fleets were tabulated. Test panels for several military and commercial paint systems were fabricated or procured. A portion of the test panels were processed using a prototype laser coating removal scanner (Figure 1). An open-loop laser modulation waveform was

implemented to produce a range of coating removal states for use in control system development. A high-speed imaging system was configured to image the aircraft surface in synchronization with the laser ablation process (Figure 2). Image data from the open-loop stripped panels was acquired and used to develop, train and test coating removal state classifiers. Classifier performance and feature computational burden were evaluated to down-select features and select classifiers providing optimal performance.

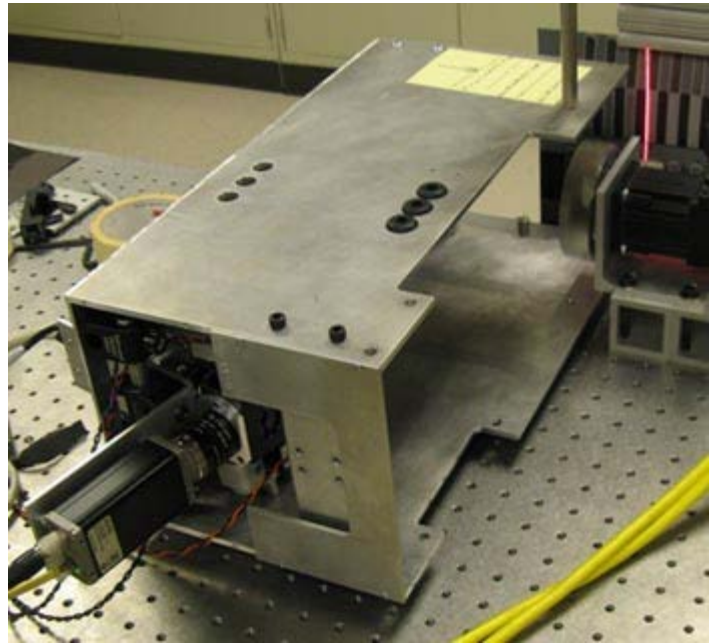


Figure 2. High-speed imaging system for imaging the aircraft surface and laser ablation process.

2013 IR&D Annual Report

Phasor Measurement Units Time Synchronization Attack, Detection, Protection and Control, 10-R8393

Principal Investigators

[Gerardo Trevino](#)

Ben A. Abbott

Inclusive Dates: 05/28/13 – 09/28/13

Background — Phasor Measurement Units (PMUs) are data acquisition devices that measure electrical waves on the electrical grid and share a time source. PMUs provide initially unavailable information to help manage and improve power systems. Advances in technology allow PMUs to provide extremely accurate synchronized phasor (representation of a sinusoidal function) measurements (synchrophasors) from across the power system to enable new decision-making capabilities to help improve system reliability. PMUs currently collect data from substations and other locations within the grid to evaluate its past behavior. PMUs have been used recently to manage the Bulk Electric System (BES) consisting of generators, substations, and 100kV and higher voltage transmission lines. PMU time synchronization is critical to the correct operation and maintenance of the grid operations. Typically, clock synchronization accuracies on the order of a few microseconds are necessary for the proper BES management function. Global Positioning System technology is currently used to provide the common time source; however, an attacker could jam GPS, or worse, spoof it, resulting in potential grid destabilization.

Approach — The goal of this project was to develop SwRI's understanding of its potential client's needs and commercialization limitations while setting up the groundwork for the development of GPS-spoofing detection technologies and providing a viable solution. The technical approach had five tasks:

- Define experiments and evaluation approach
- Design attack and defense algorithms
- Design and implement prototype system
- Whitebox space attack experiments
- Evaluate results and report

Accomplishments — The project produced algorithms and methodologies and an invention disclosure (in progress) to detect and fight through GPS attacks. These results were presented at the Worldwide Graphical System Design Conference and at the North American SynchroPhasor Initiative (NASPI) in August and October 2013, respectively. Additionally, a budgetary estimate has been submitted to a commercial client to further develop the technology and integrate it into their product line. There have also been several business contacts with different companies with interest in this research including a research and development institution from Mexico where this PMU technology is currently being used more aggressively to operate the electrical grid.

2013 IR&D Annual Report

Wireless Protocol Fuzzing Framework, 10-R8401

Principal Investigators

[Joseph G. Loomis](#)

Russell K. Barker

Tam T. Do

Inclusive Dates: 07/01/13 – 10/31/13

Background — Wireless embedded systems are becoming increasingly prevalent in the world. Manufacturers are integrating wireless protocols into their designs so that they become part of the "Internet of things." Wireless protocols such as ZigBee, Bluetooth, and Bluetooth Low Energy (BLE) can be found in devices ranging from home thermostats to cell phones. The protocols are used to provide information and control that in today's threat-heavy world need to be secure. This means that security is increasingly becoming a primary concern for many of the companies that utilize wireless protocols. One common method of assessing the security of a protocol is through fuzz testing or "fuzzing." Fuzzing is a technique in which the input to a system is changed repetitively and in unexpected ways to see how the system reacts for the purpose of identifying vulnerabilities that have not been discovered through normal system testing. This technique has been used to test Transmission Control Protocol/Internet Protocol (TCP/IP) network software and has been adapted by Southwest Research Institute and others to test the application layer of wireless embedded systems. However, to date there has been limited work in fuzzing the intermediate and lower layers of wireless protocols; but, more specifically, no generalized approach has been developed that is readily adapted to multiple protocols.

Approach — This research is investigating approaches to fuzzing the intermediate and lower layers of wireless protocols, with specific attention to developing a generalized and adaptable approach that can be realized using low-cost, off-the-shelf tools, and that is readily adapted to multiple protocols. To achieve this, two likely approaches are being investigated: open system interconnection (OSI) stack injection and stack offload. OSI stack injection is a technique where fuzz cases generated by a fuzzing engine are injected into specific layers of the fuzzing device, which will contain an entire protocol stack, through use of an Application Programming Interface (API). The API will be responsible for packet handling between the fuzzing engine and the stack on the fuzzing device. Stack offload is a technique in which low layers of a stack are implemented on a fuzzing device, and the higher layers of the stack are implemented in software on a personal computer (PC). In this technique, fuzz cases, which are still generated by a fuzzing engine, are transferred to the PC where partial packet structure building is done and then passed to the fuzzing device for complete packet encapsulation.

Accomplishments — A test environment was developed and a fuzzing approach was selected for three popular wireless protocols. For Bluetooth and BLE, the stack offload approach will use the Ubertooth One hardware with a Sulley fuzzing engine. For the Zigbee protocol, a Universal Software Radio Peripheral (USRP) radio will be used with a Sulley fuzzing engine. Development of the complete fuzzing framework for BLE is nearing completion, and testing of the different BLE protocol stacks will begin soon.

2013 IR&D Annual Report

Efficient Methods for Uncertainty Propagation in Computational-Fluid-Dynamics-Based Fire PRA, 20-R8271

Principal Investigators

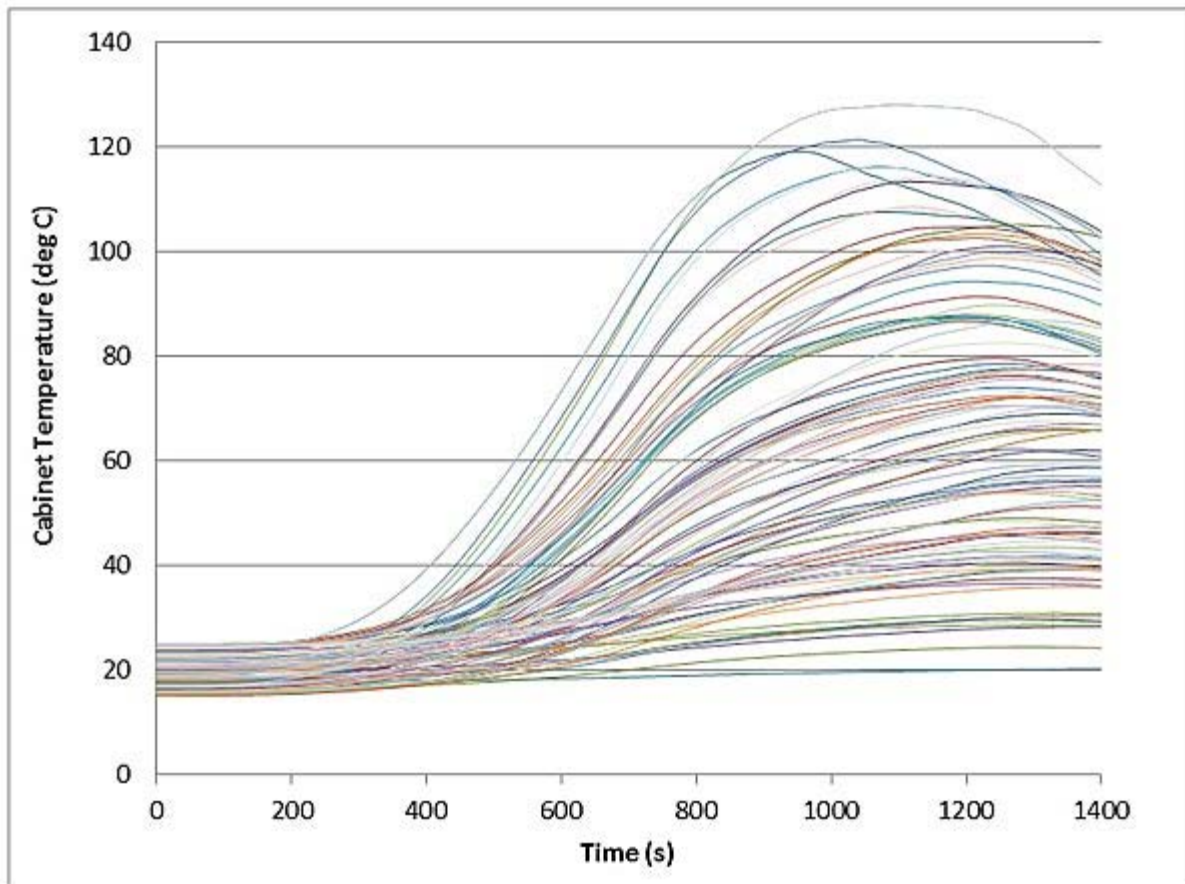
Sitakanta Mohanty

Marc Janssens

Inclusive Dates: 11/14/11 – 12/16/13

Background — U.S. Nuclear Power Plants (NPPs) have recently been allowed to transition from a deterministic fire protection licensing basis to a risk-informed performance-based program. The transition requires a full Fire Probabilistic Risk Assessment (FPRA) to quantify the effect of fire incidents on core damage frequency and large early release frequency. Realistic FPRA involves an accurate evaluation of the performance of critical components for a range of design fires (heat release rates). Ideally, this process heavily relies on the use of computational fluid dynamics (CFD) codes [i.e., Fire Dynamics Simulator (FDS)]. Because CFD codes are computationally intensive (a single run may take days or even weeks), fire modeling is currently limited to point estimates, which do not explicitly account for uncertainties in input parameters and forces the analyst to make conservative assumptions in lieu of full quantification of uncertainty. The traditional Monte Carlo approach for propagating uncertainty requires a large number of CFD simulations (several hundred), which makes uncertainty quantification intractable. There is a strong need for developing an uncertainty quantification method that can propagate uncertainty without sacrificing computational accuracy in FPRA.

Approach — The approach adopted in this project is to propagate input uncertainties in FPRA using a small number of Monte Carlo realizations (a few tens to hundreds as opposed to thousands), which would improve computation time by at least an order of magnitude compared to a pure Monte Carlo method. The methods explored are reliability-based methods that minimize the need for a large number of Monte Carlo realizations to construct a cumulative distribution function (CDF) from the model outputs. The approach involves constructing an approximate CDF from a few Monte Carlo realizations by applying mean value and advanced mean value methods and refining the approximate CDF to the desired level of accuracy by applying an importance-sampling approach. The method involves careful selection of a number of estimation points on the approximate CDF, constructing a CDF through these points, and then repeating the process until the CDF is obtained with the desired level of accuracy for various statistical moments. The results from this method are compared against the regular Monte Carlo method using the stratified sampling method to gauge improvement in computational efficiency. The methods are then tested using a variety of realistic fire scenario examples.



Evolution of temperature in one cabinet from a fire in a neighboring cabinet in the switchgear room. The figure shows 100 of a 1000-realization simulation carried out using a large array of processors on a computer cluster.

Accomplishments — A Monte Carlo (and stratified sampling) FDS model has been developed for benchmarking that will be used once the reliability-based methods are developed. The Monte Carlo FDS code is capable of running the FDS code repeatedly after sampling from input parameter distribution functions (i.e., probability density functions or PDFs), correlating parameters if needed, and propagating one "vector" of input values to a processor on the parallel computer cluster, and collecting FDS code outputs for constructing the model output CDF. An example study of NPP control room abandonment in response to Switchgear Room electric-cable cabinet fire scenario has been explored. Parameters for which uncertainties are to be represented in these test problems and performance function output uncertainties of interest have been identified. Uncertainty is represented via PDFs and propagated through the model for 18 parameters. For a computationally intensive model such as FDS, this is considered to be a relatively large set. Special considerations have been given to time-dependent parameters, such as the heat-release rate curves. Because developing the reliability and Monte Carlo methods requires a large number of trial runs during the model development phase, a faster Monte Carlo CFAST code has been developed to serve as a surrogate for the time-consuming Monte Carlo FDS code. Figure 1 shows a spectrum of temperature evolution curves from which the probability of failure of cables is determined based on a temperature threshold criterion. Reliability-based calculations have been effectively used to extend the failure time prediction to four standard deviations around the mean.

2013 IR&D Annual Report

Next-Generation Neutrally Buoyant Sensors, 10-R8274

Principal Investigators

[Gregory C. Willden](#)

Ben A. Abbott

Ronald T. Green

Inclusive Dates: 12/12/11 – 12/12/12

Background — SwRI had previously developed the award winning Neutrally Buoyant Sensor (NBS) system for automatic mapping of partially water-filled caves and conduits. The technology was successfully adapted for externally funded projects with two government clients; however, newer applications require improved processing capabilities and a more flexible and capable hardware architecture.

Approach — Bringing together rapid prototyping capabilities for quickly building a waterproof housing and a small, powerful, and flexible hardware system enabled the assembly of a toolkit that allows for developing specialized NBS systems to meet potential client needs. Competing constraints that guided the design of the toolkit elements include a low unit cost, having a modular system for rapid development and specialization, employing chirp correlation processing and providing for flexible communication schemes.

Accomplishments — An improved platform for NBS development and specialization was developed. The new components provide higher sampling rates, onboard storage and processing capabilities, as well as rapid prototyped housing components. As part of an externally funded project, the technology toolkit was applied in the creation of a specialized NBS system for mapping and inspecting culvert conduits for a current client (see illustration). Additional toolkit components are being prepared for use in services contracts that are being pursued with a variety of potential clients.



Customer-specific NBS system built from toolkit components.

2013 IR&D Annual Report

Guided Wave Imaging Technology Development, 18-R8289

Principal Investigators

Jay L. Fisher

Adam Cobb

Inclusive Dates: 02/01/12 – 11/01/12

Background — SwRI is a leader in developing and applying ultrasonic guided waves for nondestructive evaluation (NDE), particularly using its magnetostrictive sensors (MsS). One of the limitations of these sensors is that they must be bonded or otherwise well-coupled to the surface of the part being inspected to transfer mechanical wave motion directly to the part. The purpose of this project was to develop specific technical elements needed to advance SwRI's ultrasonic guided-wave technology for inspection of piping and plates, especially for cases where it is not feasible or desirable to bond MsS to the part under inspection. In particular, this project focused on developing electronics that could be used to operate electromagnetic acoustic transducer (EMAT) sensors. These sensors generate the wave motion directly in the part using electromagnetic forces, but they are much less efficient.

Approach — The primary goal was the design of a prototype high-power, low-frequency 2-channel pulser (for direction control or power doubling) and receiver electronics that could be used with new, low-frequency EMAT sensors to generate and receive ultrasonic guided waves. A secondary goal was to implement the beam-forming algorithm, critical to combining data from sensors at multiple positions around the pipe or plate being inspected into SwRI's enhanced data acquisition system (EDAS®). The use of EMAT sensors that can be easily moved across the part surface enables the convenient collection of data for analysis with the beam-forming software.

Accomplishments — The high-power, low-frequency, 2-channel pulser and receiver electronics were developed by modifying an existing single-channel higher frequency design. Each channel provides multi-cycle tone bursts of more than 100 amperes into a 1-ohm load for use with low-frequency EMAT sensors. The two channels are delayed relative to one another to steer or increase the strength of the generated guided wave. The prototype unit will be used on at least one funded project and was the basis for the pulser design used in the MsSR4040SF, a pipeline inspection tool currently under development. The beam-forming algorithms were improved over previous implementations, and clearly improved SwRI's ability to localize flaws in the direction orthogonal to the beam direction. The signal-to-noise ratio (SNR) improvement was dramatic; in the case of a 1-percent cross-sectional area flaw, the SNR increased by a factor of more than four. The beam-forming algorithms were implemented in SwRI's EDAS software. This achievement will allow clients to use the beam-forming tool with existing EDAS analysis tools, including indication marking and reporting tools, for use with conventional (bulk wave) as well as guided wave transducers.



Figure 1. Dual channel pulser/receiver board final design, before installation in enclosure.

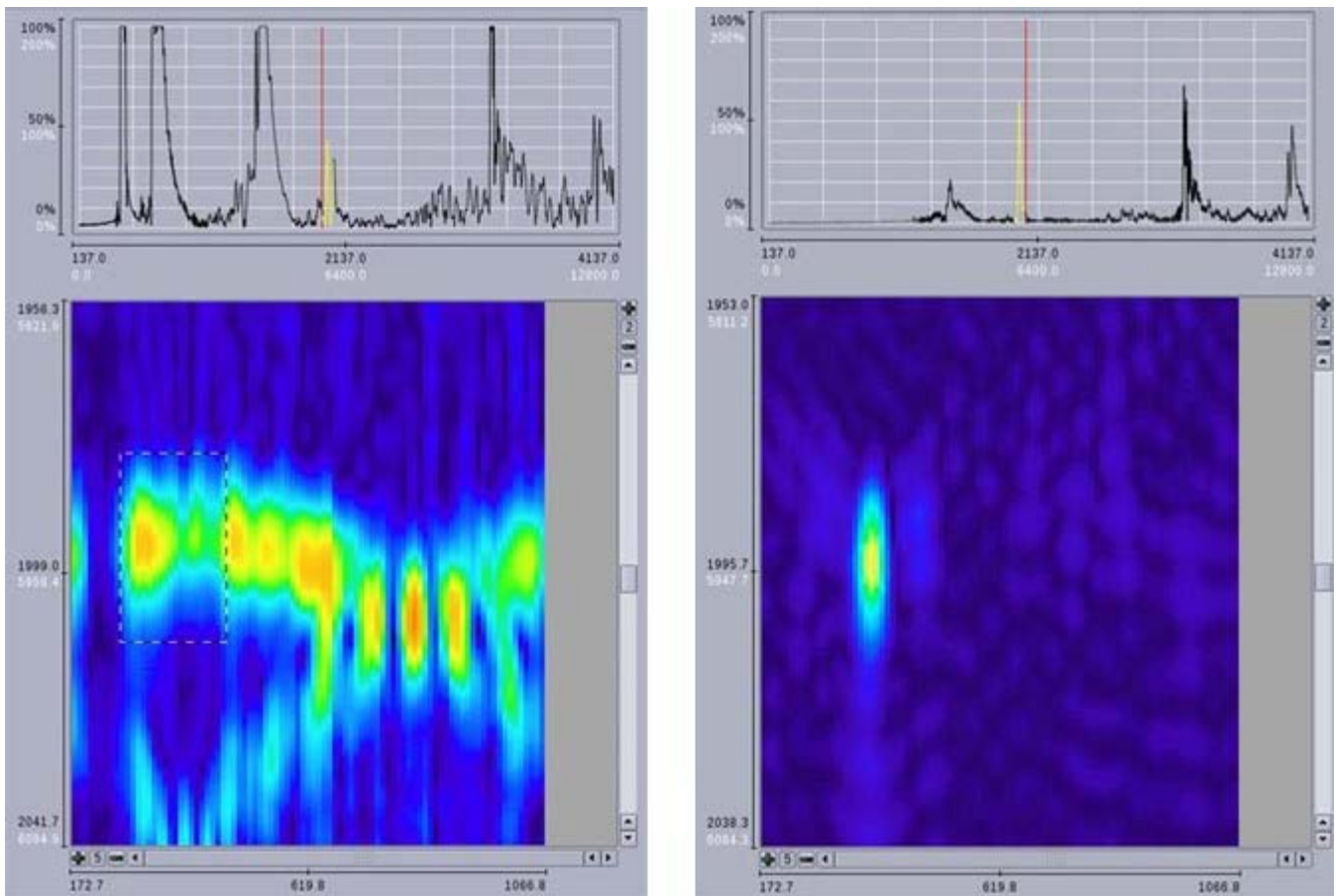


Figure 2.

(Left) Standard EDAS B-scan presentation for data obtained from scanning an MsS sensor circumferentially around a pipe, about 2 m axially distant from the flaw. The horizontal axis is in the circumferential direction, and the vertical axis is the waveform time (axial) direction. Only a small portion of the axial direction is shown in the color image; a complete waveform (A-scan) at one location is shown at the top (only the yellow portion of this waveform is displayed in the image below). The cursor box (rectangle) in the figure identifies the flaw location.

(Right) The pipe data shown after beam-forming is applied. The flaw is localized very well and the SNR is greatly increased. The synthetic waveform shown in the top portion includes the flaw location; the yellow portion of this waveform corresponds to the B-scan window length in the image.

2013 IR&D Annual Report

EDAS-MS Upgrade and Demonstration Program, 18-R8367

Principal Investigators

[Jay L. Fisher](#)

Alan Schaefer

Inclusive Dates: 01/16/13 – 05/16/13

Background — SwRI has supplied EDAS® systems for more than 25 years to provide a highly efficient means of data acquisition and analysis for ultrasonic inspection of nuclear power plant reactor pressure vessels and associated piping. The most recent redesign of EDAS hardware to support these requirements was launched in 2010, with support from SwRI internal research program (project 18-R8163). That redesign (EDAS-MS) was used to manufacture three large systems (two for clients), as well as ensuring that SwRI can support these and other previously delivered systems for years to come. Recently SwRI learned that a client with previous-generation EDAS systems was very interested in obtaining a new inspection system. The client was in the process of evaluating available systems in the market, developing the specifications for their new system, and training their users in a facility that could be rented for a limited time. Therefore, this project was set up to allow the client to evaluate EDAS-MS and its potential for integration with their existing mechanized equipment in the limited time slot that could be made available.

Approach — To allow the client to evaluate the system for their needs, it was necessary to double the number of data acquisition channels from four to eight and to more than double the data acquisition rate per channel, to increase the allowed mechanical scanner speed from 50 mm/second to 250 mm/sec. These improvements were made using existing hardware and by modifying previously developed software.

Accomplishments — The upgraded system was taken to the client site. Tests performed by SwRI personnel and the client resulted in all specifications being met. The client has accepted this system as suitable for use with their next-generation mechanical scanner.

2013 IR&D Annual Report

Severe Downsizing of a Three-Way Lean NO_x Trap (3wLNT) Diesel Engine, 03-R8293

Principal Investigators

[Ryan Roecker](#)

Sankar Rengarajan

Inclusive Dates: 05/01/12 – 12/07/12

Background — Increased cost is driving the diesel engine out of the compact/small car market. SwRI's concept of a three-way lean NO_x trap (3wLNT) diesel engine is a low-cost solution for light-duty diesel OEMs to meet emissions regulations without the need for exhaust gas recirculation (EGR) or an expensive selective catalytic reduction (SCR) system. The aftertreatment is essentially a three-way catalyst with a NO_x adsorbing coating. The 3wLNT is a truly cost-effective solution.

Approach — The 3wLNT engine runs lean at light- to mid-load conditions and stoichiometric at mid to high loads. At lean light-load operation, the aftertreatment is used as a lean NO_x trap. At high loads, the aftertreatment is used as a three-way catalyst by stoichiometric operation. While the concept is certainly cost-effective from a hardware point of view, there are technical challenges in the form of soot production and fuel economy. While it is accurate that stoichiometric engines without significant dilution from EGR have higher fuel consumption on a brake mean effective pressure (BMEP) to BMEP basis, the stoichiometric diesel concept lends itself to significant downsizing potential, which may overcome this deficiency. The down-sizing potential is greater than spark-ignited engines because a stoichiometric diesel engine does not suffer from engine-damaging knock or pre-ignition. The downsizing potential is greater than standard diesel also because there is no need for EGR and excess air. Therefore the 3wLNT concept engine is expected to have lower peak cylinder pressures allowing for higher BMEP levels to be achieved and less demanding turbo-charging requirements.

Accomplishments — Based on the accomplishments and results, the project is defined as a success. The major takeaways from this project are:

- A drivable vehicle that could meet complete light-duty drive cycles with combustion strategies radically different from a conventional diesel engine.
- Severe downsizing potential was proven possible with this kind of combustion strategy. As an example, the curb-side weight of a 2012 Ford F-150 is around 5,333 pounds. This 2.0 L Passat engine was able to drive a Ford F-150 sized vehicle on a chassis dyno over a U.S. Federal Drive Cycle without any limitations.
- Good transient performance as well as drivability was achieved for the heavier vehicle inertia tested on a chassis dyno.
- Fuel penalties between the combustion strategies => lean-burn and lean + stoichiometric combustion were within acceptable ranges.

2013 IR&D Annual Report

Diesel Cold Start Emission Control Research for 2015-2025 LEV III Emissions, 03-R8299

Principal Investigators

[Gary D. Neely](#)

Dr. Jayant Sarlashkar

Darius Mehta

Inclusive Dates: 04/01/12 – 03/31/13

Background — The diesel engine can be an effective solution to help OEMs meet the 2017-2025 U.S. EPA and National Highway Traffic Safety Administration light-duty greenhouse gas and fuel economy standards, especially for larger segment vehicles. However, in this same timeframe, very stringent emission standards will be phased-in (EPA Tier 3 and CARB LEV III), which pose a significant challenge for the diesel engine due to the difficulty in obtaining rapid emissions control with aftertreatment following a cold-start. Therefore, a cost-effective approach is needed for a diesel to obtain rapid emission control following a cold-start to meet future emission regulations.

Approach — The goal of this project was to develop and evaluate a novel diesel cold-start emissions control strategy. The strategy comprises multiple engine tuning improvements to increase exhaust gas temperature without increasing hydrocarbon (HC) emissions and replacing the standard close-coupled diesel oxidation catalyst (DOC) with a state-of-the-art Lean NO_x Trap (LNT). The goal of the strategy was to achieve rapid HC and NO_x control during the first hill of the FTP75, which is necessary to meet future emission standards. An illustration of the various technologies that comprised this strategy is shown in Figure 1.

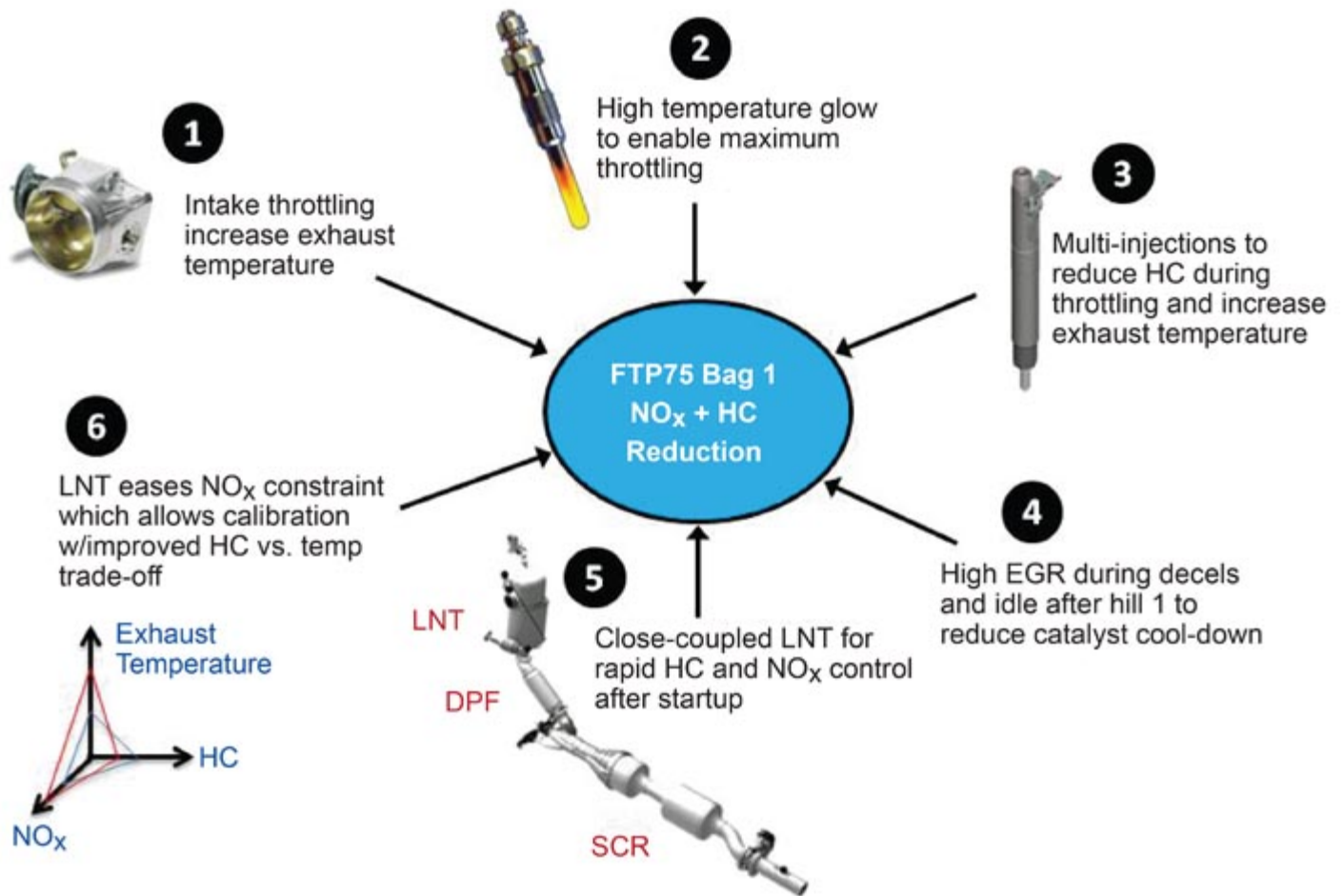


Figure 1. Engine tuning and aftertreatment technologies for SwRI cold-phase emissions control strategy.

Accomplishments — The engine tuning technologies were found to be quite effective in increasing exhaust temperature while maintaining low HC emissions. When the engine tuning technologies were combined with the state-of-the-art LNT, simultaneous NO_x and HC control was achieved within 50 seconds from the start of the FTP75. Cumulative NO_x + HC emissions obtained during the first 160 seconds of the FTP75 are shown in Figure 2. In addition to the SwRI test results, emissions obtained from a production Tier 2 Bin 5 vehicle are shown for comparison purposes. FTP75 Bag 1 weighting factors were applied to both results. Using the SwRI approach, a 52 percent emission margin remained for meeting the future EPA Tier 3/CARB LEV III fleet-average emission requirement compared to only 9 percent for the production vehicle. The potential of achieving the target emission level with the SwRI-developed strategy was confirmed by combining the SwRI results obtained for the first 160 seconds with the production Bin 5 diesel results for the remainder of the test cycle.

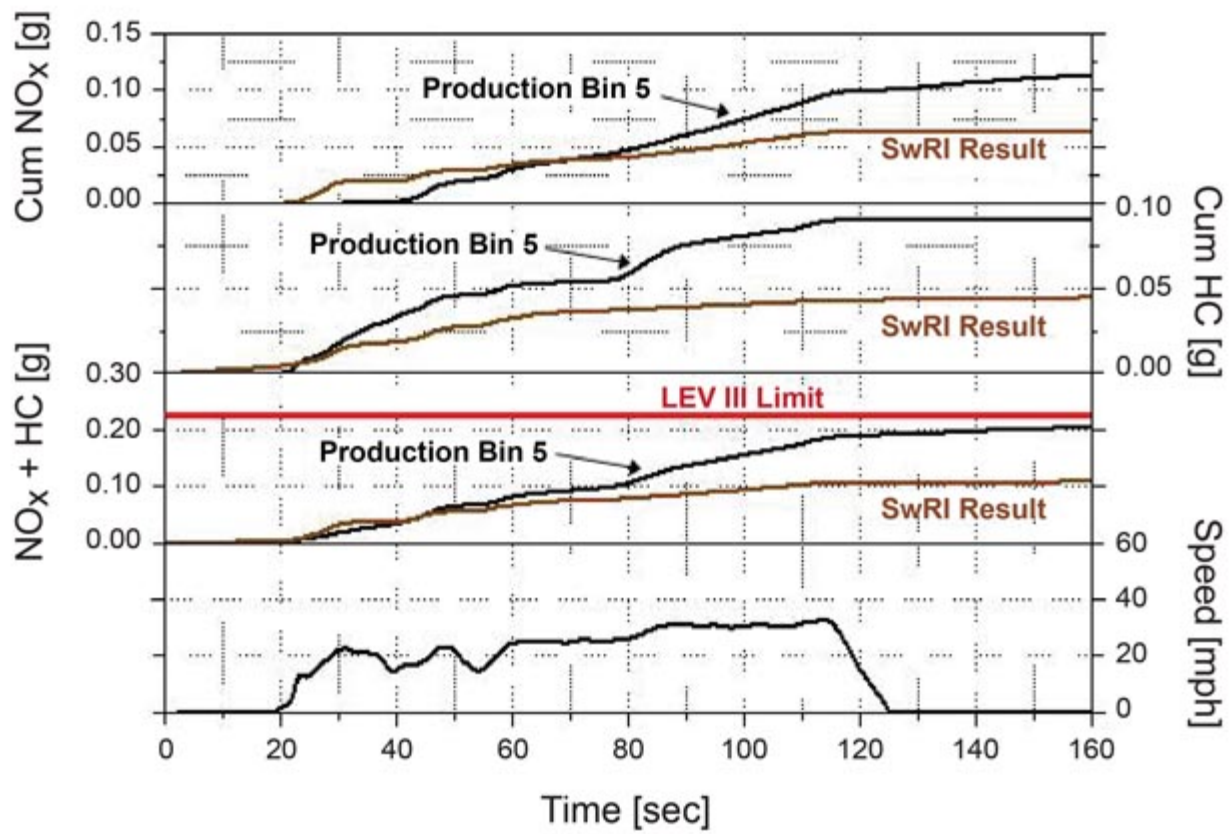


Figure 2. Cold-phase emission comparison between SwRI results and a production Tier 2 Bin 5 vehicle. FTP75 Bag 1 weighting factor applied.

2013 IR&D Annual Report

D-EGR WGS Catalyst Development and Optimization, 03-R8326

Principal Investigators

Gordon J.J. Bartley

Terrence Alger

Jess Gingrich

Raphael Gukelberger

Inclusive Dates: 07/01/12 – 07/01/13

Background — SwRI has been actively developing its dedicated exhaust gas recirculation (D-EGR) concept and system within the HEDGE Consortium. A key to successful application is the amount of hydrogen (H_2) that can be efficiently produced and fed back into the intake mixture. Rich operation of the D-EGR cylinder produces a significant amount of H_2 , but more is beneficial. The D-EGR cylinder exhaust also contains substantial amounts of carbon monoxide (CO) and water (H_2O). A water gas shift (WGS) catalyst reacts CO with H_2O to form H_2 and carbon dioxide (CO_2), but no WGS catalyst had ever been developed for this application or environment. Catalysts that SwRI had used to evaluate the concept were traditional three-way (TWC) exhaust formulations that achieved about 45 percent H_2 production efficiency with minimal durability. If this efficiency could be increased to 70 percent and durability improved, an additional 2 to 3 percent brake thermal efficiency (BTE) is possible, a very significant technological advance.

Approach — Three different catalysts received from catalyst companies had been evaluated on the D-EGR engine. The one that provided the best performance became the reference formulation for this work. The catalyst was analyzed to obtain the overall elemental composition of the catalyst washcoat. Starting with this reference formulation, a matrix of 45 varying formulations was prepared on core samples for testing. SwRI's Universal Synthetic Gas Reactor® (USGR®) was used to perform the testing. Each catalyst's WGS activity was evaluated over a fixed set of test conditions. Sensitivities to individual independent and dependent variables were used in a statistical approach to identify the direction of optimum formulation for WGS reactivity in the anticipated temperature regions. The optimum operating conditions for that formulation were extracted from the data.

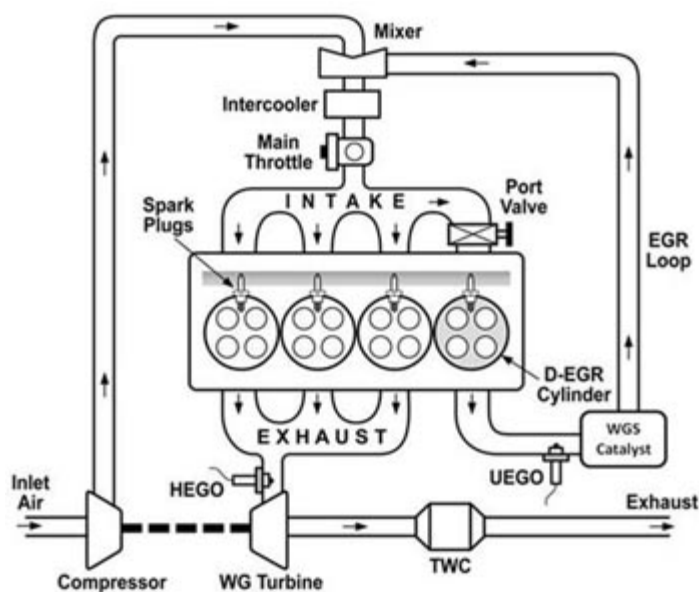


Figure 1. D-EGR Engine Overview Showing WGS Catalyst

Accomplishments — The project work is complete. Four formulations were identified as producing high levels of H_2 , and one in particular was isolated that produced a very high level. The efficiency was somewhere between 65 and 85



Figure 2. SwRI's Universal Synthetic Gas Reactor™

percent, depending on the calculation method and H₂ measurement technique. Two key findings were that rhodium and barium both had a positive effect on H₂ production, and there was a beneficial synergy between the two. This formulation was prepared on full-size substrates and tested under D-EGR conditions on a bench engine. The H₂ production exceeded the 7-percent target, achieving a maximum of 8.35

percent. Unfortunately, the catalyst could not maintain this performance over the long term. In just a matter of hours, the activity, as measured by CO conversion efficiency, fell significantly. It is believed that continuous rich (reducing) operation results in coke build up in the catalyst, reducing the activity. The project was completed before any solutions to this issue were evaluated. One such option would be to operate the catalyst over a perturbed regime with one cycle in eight running lean (oxidizing). The hypothesis is that the lean cycle could oxidize the coke precursors before they have a chance to build up into coke deposits. Further work is needed to address this issue.

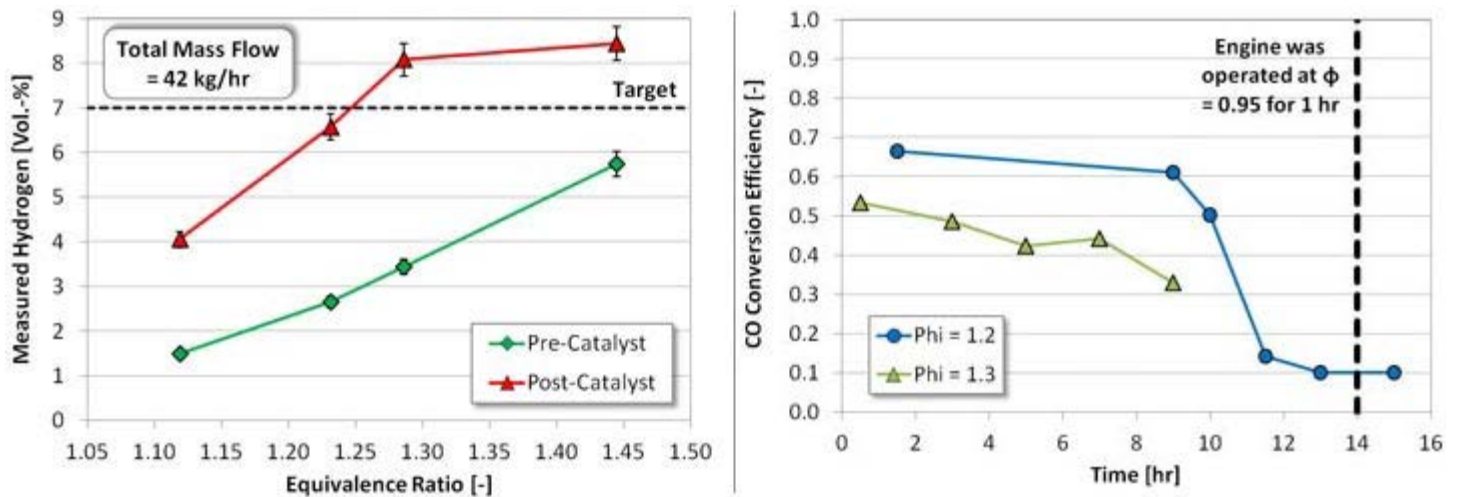


Figure 3. H₂ production (left) and CO conversion efficiency (right)

2013 IR&D Annual Report

Development of Advanced Analysis of Aluminum Cylinder Heads, 03-R8364

Principal Investigators

[George E. Bailey](#)

Anthony J. Megel

G. Mark Jones

Inclusive Dates: 01/02/13 – 06/07/13

Background — The increasing use of combustion techniques such as gasoline direct fuel injection, boosting intake pressures using turbo- or supercharging, and using exhaust gas recirculation as done in the High Efficiency Dilute Gasoline Engine (HEDGE) programs at SwRI, are resulting in increased cylinder head pressures and temperatures. A cost-effective analysis method was required to enable SwRI to rapidly design and develop cylinder heads for its clients. The analysis of cylinder heads made from aluminum alloy is more complex than heads made from cast iron because the loading and thermal fields are in a range where the modulus, strength and fatigue life of the aluminum alloy changes significantly.

Approach — The relative analysis approach was used, which recognizes there will be variability in loading, tolerances and in material properties due to processing. It compares new design analysis results with known designs that have an operating history. Cylinder-head analysis requires a prediction of the stress and temperature fields during operation, then a prediction of durability under these loading conditions. A commercial finite-element analysis program was used to predict stresses and temperatures, and a commercial fatigue analysis program was used to predict durability. A high-performance production four cylinder turbocharged gasoline engine was used as the subject. The thermal fields during operation had been measured in a previous internal research project, 03-R8313. Cylinder heads were purchased from a dealer and their material properties were characterized. Computed tomography was used to create a solid model of the head. An analysis performed by a consulting company was used to calibrate the finite element and durability models because durability testing of the head would have been prohibitively time-consuming and costly.

Accomplishments — Calculation tools were developed to precisely determine the size and location of features from computed tomography scans. A model of the engine block was required so a general parametric model was created that can also be used on future projects. Many finite element analysis variables were investigated, and appropriate target values were defined for these parameters. These include element types, mesh sizes, interference fit contact methods, head gasket material properties and modeling procedures, and head bolt modeling. Thermal modeling guidelines were also established that included partitions for heat transfer from the hot gasses into the exhaust valves and ports, and nucleate boiling curves for the water jacket. Procedures were developed to measure the relevant material properties for aluminum cylinder heads including tensile and compressive properties, and fatigue behavior. Numerical methods were developed to calculate Brown-Miller equation parameters from the tensile and fatigue results for use in durability predictions. The stresses predicted in the head using the methodology developed in this project were within 10 percent of those independently calculated by the consulting company. The modeling methodology and procedures developed in this project have been documented and published as work instructions and are ready for use in client projects.

2013 IR&D Annual Report

Development of a Methodology to Generate On-Board Diagnostic Threshold Selective Catalytic Reduction Catalysts for Heavy-Duty Diesel Applications, 03-R8376

Principal Investigators

[Reggie Zhan](#)

Cynthia Webb

Inclusive Dates: 03/15/13 – Current

Background — The on-board diagnostic (OBD) system monitors engine and aftertreatment components that affect the vehicle's emissions performance. When the malfunction illumination light (MIL), also known as the "check engine" light, is illuminated, at least one emission related problem has been detected, and the driver is notified that vehicle service is needed. For heavy-duty diesel engine and medium-duty diesel vehicle applications, the California Air Resource Board (CARB) mandates that heavy-duty OBD systems be implemented for all on-highway engines offered for sale in California beginning with model year 2013. Even though urea-based selective catalyst reduction (SCR) technology has been used as a primary means to meet the US2010 diesel NO_x emissions requirements in North America, there is no proven method to consistently create OBD threshold SCR catalysts in the laboratory environment.

Approach — The goal of this project is to answer the industry challenge to develop methodology to consistently age zeolite SCR catalysts to the OBD threshold level. The approach is to use SwRI's FOCAS burner technology to thermally age the SCR catalysts to the "worst performing acceptable" (WPA) and "best performing unacceptable" (BPU) levels to meet OBD calibration requirements. An existing US2010 certified MY2012 Ford PowerStroke 6.7L diesel engine is being used for the program. The heavy-duty transient FTP cycle has been replicated using the SwRI FOCAS HGTR system for SCR performance evaluation. An SCR thermal aging cycle has been developed and optimized for aging SCR catalysts to threshold NO_x levels. The FOCAS HGTR system is being used to conduct SCR aging and performance evaluations. The FOCAS HGTR generated WPA and BPU SCR catalysts will then be emissions-tested using the Ford PowerStroke 6.7L diesel engine. These tests will validate the proposed SCR catalyst aging methodology.

Accomplishments — It is expected that a novel approach will be developed to generate OBD threshold SCR catalysts. The technical approach will also be further applied as a generic method to age SCR catalysts under precisely controlled operating conditions.

2013 IR&D Annual Report

Investigation of an Oleophobic Coating Effect on Gasoline Direct Injection (GDI) Engine Components to Reduce Carbon Deposits, 08-R8362

Principal Investigators

[Brent Shoffner](#)

Dr. Terrence Alger II

Dr. Kent Coulter

Carol Ellis-Terrell

Dr. Sylvain Kouame

Eric Liu

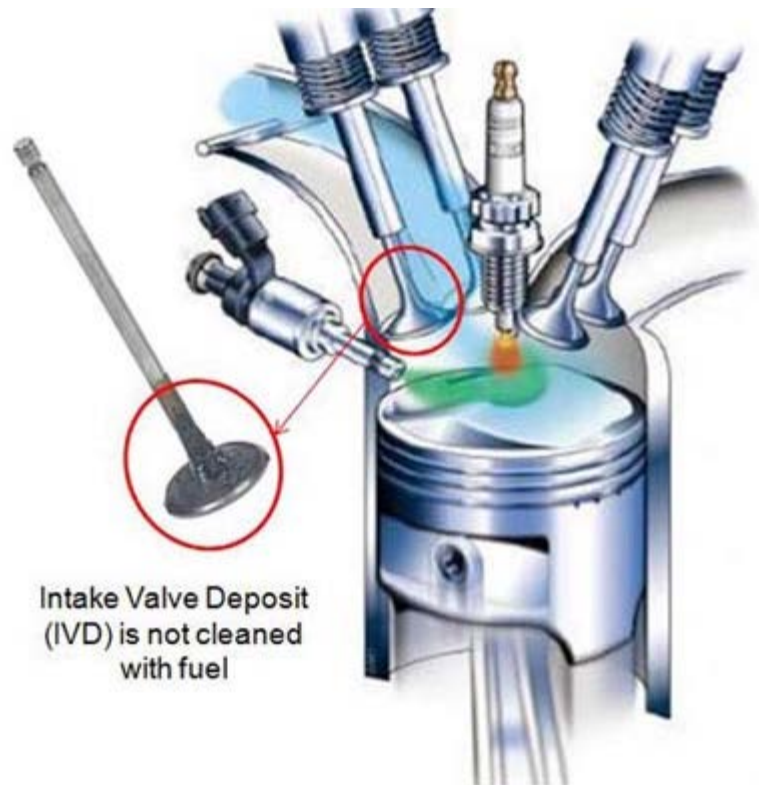
Inclusive Dates: 01/01/13 – 12/31/13

Background — Carbon deposits on the backside of intake valves in light-duty vehicle gasoline engines have always been a durability issue for the automotive industry. In traditional carbureted or port fuel injected engines these deposits have been controlled through the addition of detergent additives to the fuel. Unfortunately, in newer engines using gasoline direct injection (GDI) these additives are ineffective because the liquid fuel is introduced directly into the cylinder and the detergent-carrying liquid fuel has minimal contact with the backside of the intake valve.

Deposits on the tulip area of the intake valves have the potential to restrict air induction and decrease engine performance. With GDI engines the fuel additives will have minimal effect on the intake valve deposit (IVD) resulting in a problem, which does not have an economic solution at this time.

Approach —

- The temperature environment of the intake valves was researched based on previous SwRI data.
- The intake valve surface metallurgy and finish were measured.
- IVD from GDI engines was analyzed.
- Candidate coatings were evaluated for bench properties such as the oleophobic contact angle.
- The original equipment manufacturer (OEM) intake valves and valves with three different coating technologies applied in the “tulip area” were evaluated in a dynamometer based GDI engine test. The IVD weight was determined for each valve at the end of test.



Typical GDI cylinder configuration

Accomplishments —

- A dynamometer-based engine test procedure was developed that can be used to evaluate the potential effects of engine oil, fuel, and coatings on the formation of IVD.
- Concentrations of elements in the IVD and the engine oil are similar.
- Interesting IVD formations were observed that relate to intake valve rotation and injector spray pattern.
- The engine test results indicated that the surface (metal or coating) of the intake valve tulip area does affect the formation of IVD. However, none of the coatings evaluated reduced the IVD weight less than the OEM (uncoated) valves.

2013 IR&D Annual Report

Integrity Management of Nuclear Power Plant Components Subjected to Localized Corrosion Using Time-Dependent Probabilistic Model, 20-R8267

Principal Investigators

[Pavan K. Shukla](#)

Oswaldo Pensado

Jay Fisher

Inclusive Dates: 11/14/11 – Current

Background — The objective of the project is to develop an adaptive-predictive probabilistic model to forecast localized-corrosion-induced pit sites and pit depth distributions. Nuclear power plant (NPP) operators are required to periodically inspect components by visual and volumetric examinations to maintain integrity and ensure safety. However, as nuclear power plants age, more frequent inspections are required to ensure component integrity. A framework to define the inspection schedule based on risk considerations is needed to keep the cost of inspection constrained without compromising safety. SwRI is developing a model to forecast localized-corrosion-induced damage of NPP components based on damage measured at a given time. For example, if a component exhibits pitting corrosion in an environment, the model will be used to estimate the distribution of pit depths as a function of time and an initial state. The model is expected to account for previous inspection data, randomness of pit generation and propagation, and pit growth rate as a function of time. The model could be used to estimate the probability of component failure due to pitting corrosion, and calibrate inspection schedules so that detection of corrosion-induced degradation occurs before failure.

Approach — The approach consists of model development, experiments and data analysis and integration. Probabilities of transition between discrete states that satisfy Kolmogorov's forward equations for a pure birth process can be used to describe the evolution of depths of a population of pits. The discrete state of a pit is defined as a pit falling in a range of depths (e.g., a pit is in state 1 if its depth falls between 0 μm and 100 μm ; it is in state 2 if the depth is between 100 μm and 200 μm ; and so on). Thus, pit growth is conceptualized as a pit that transitions from one state to the next. Parameters to define the transition rate between states can be obtained by measuring the average pit depth as a function of time.

Experiments are being conducted with 304 stainless steel coupons that are exposed to a corrosive environment. The coupons were repeatedly sprayed with a sea salt solution and dried at 95°C for 10 minutes to deposit a layer of sea salt. The coupons were then exposed to an absolute humidity of 30 g/m³ at 50°C. This combination of salt, humidity and temperature environment causes pitting corrosion on the coupons. The coupons are then removed from the environment one by one with time, and analyzed for pitting corrosion using a laser-based microscope. A mathematical algorithm was developed to count the number of pitting corrosion sites and their depth profile. This information was used to exercise the model to forecast localized-corrosion-induced pit population and pit depth distributions.

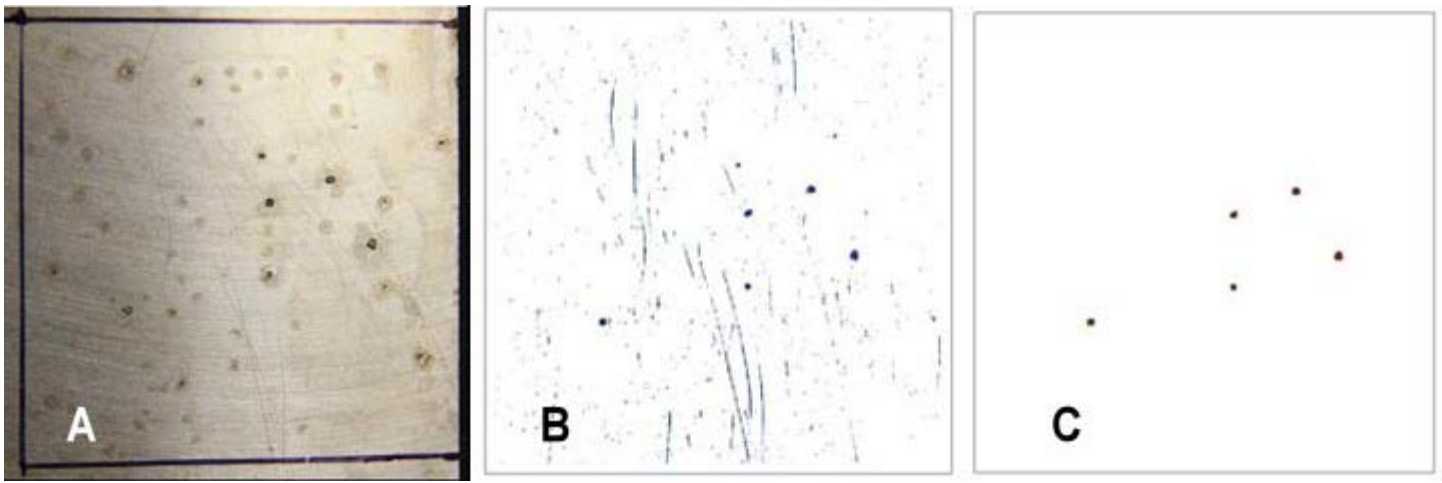


Figure 1. (a) Picture of a 304 stainless steel coupon exposed to salt, humidity and temperature environment for 8 days, (b) laser-microscope output, and (c) pits identified using the mathematical algorithm.

Accomplishments — The model was exercised for pit-depth distribution data collected from the coupons. Figure 2 is a comparison of the measured pit-depth distributions (represented by the dotted lines) to the forecast cumulative pit-depth distribution (represented by solid lines) at several detection times. The plot for eight days in Figure 2(a) includes two dotted curves because two coupons were drawn out for measurements after eight days of exposure. In the subsequent forecasts, the initial distribution was computed as the average of the previous forecast and the previous measurement. Thus, for example, the average of the eight-day curves (measured and predicted) was used as input to the 14-day forecast. Likewise, the average of the 14-day curves was used as input to the 23-day forecast. In this manner, each new forecast carries forward information from all of the previous forecasts and measurements. The data in Figure 2 indicates that the model is able to track the pit depth distribution with a reasonable level of accuracy.

A methodology has been developed to forecast the distribution of damage by pitting corrosion. The 304 stainless steel coupons were sprayed with the sea salt solution to induce pitting corrosion. The coupons showed signs of pitting corrosion within a few hours after the coupons were placed in the environment where absolute humidity was 30 g/m^3 at 50°C . The coupons were removed from the environment at defined intervals, and the coupons were analyzed to measure the pit depth distribution. Pit depth distributions were used as input to forecast distributions at the next detection time. The forecasts are reasonable. The only input in the forecast algorithm is the measured average depth (or another quantile) as a function of time. Forecasts can be used to estimate when the extent of damage of a component by pitting corrosion would not be acceptable. The forecasted information also can be used to determine the inspection schedule based on risk of failure considerations and regulatory constraints for specific components in the nuclear power plants.

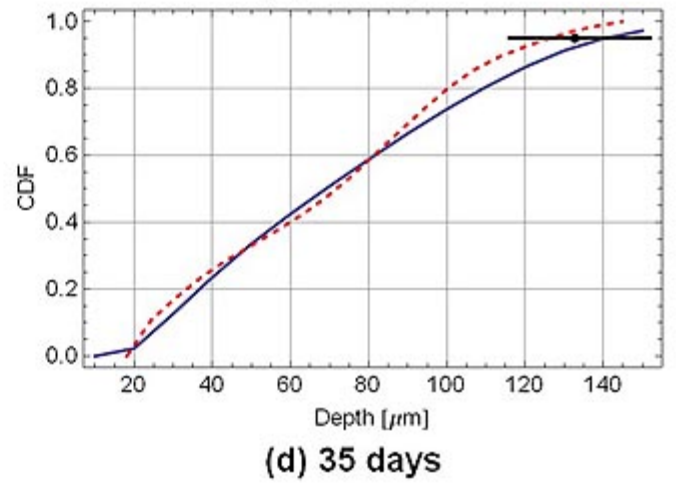
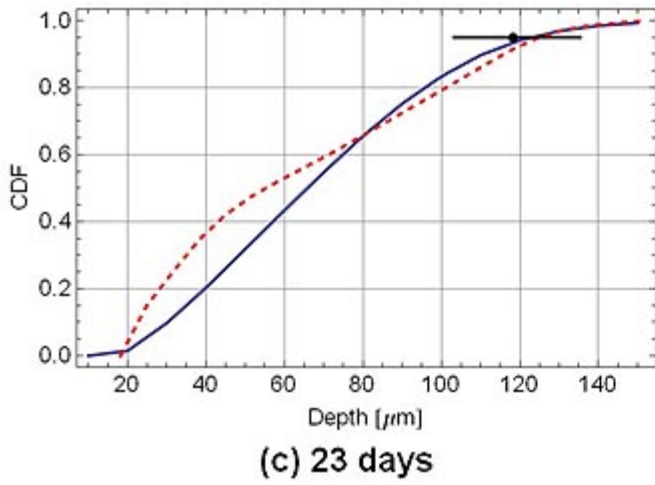
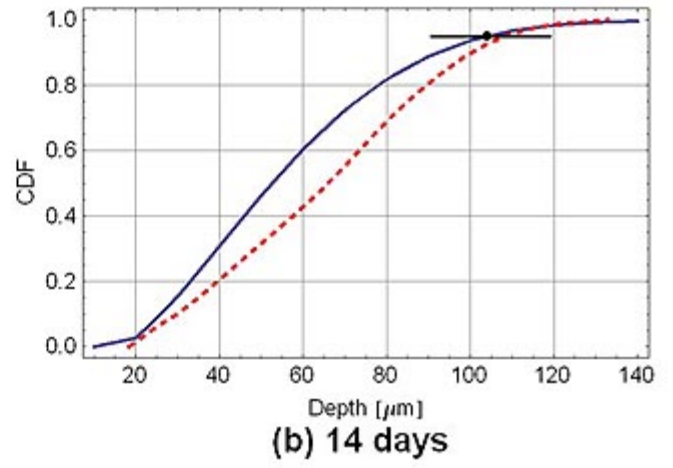
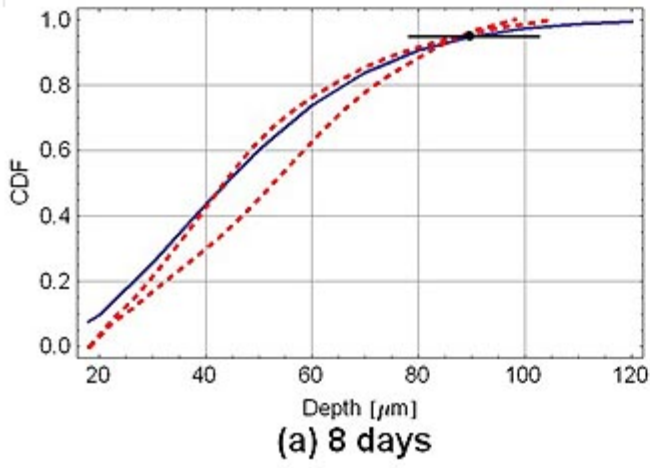


Figure 2. Comparison of cumulative distribution function of the pit depth forecast represented by solid line to the measured depth distribution represented by dotted line after (a) 8 days, (b) 14 days, (c) 23 days, and (d) 35 days.

2013 IR&D Annual Report

Development of an Integrated Numerical Framework for Tsunami Hazard Assessment at Nuclear Installations, 20-R8268

Principal Investigators

Debashis Basu

Kaushik Das

Ron Janetzke

Biswajit Dasgupta

John Stamatakos

Rob Sewell, Consultant

Inclusive Dates: 10/01/12 – 05/15/13

Background — Tsunamis are a series of long ocean waves generated by large-scale earthquakes or landslides that occur along active faults near continental margins or subduction zones. The primary aim of this project was to develop an integrated tsunami analysis method for risk assessment at nuclear installations and other industrial facilities near the coast. The analysis focused on earthquake generated tsunamis. The developed method calculates parameters such as maximum wave runup height, impact velocity and inundation area from an earthquake-generated tsunami. The generation stage of tsunami evolution includes formation of the initial disturbance of the ocean surface caused by earthquake-triggered deformation of the sea floor. Subsequently, this initial disturbance of the water surface evolves into a long gravity wave radiating from the earthquake source. The integrated tsunami analysis method includes predicting the initial wave height that is linked to the earthquake source mechanism and analyzing the fragility of coastal structures affected by the tsunami waves.

Approach — The developed method models the earthquake-generated tsunami source and associated displacement, open-sea wave propagation, and wave run-up, including inundation and onshore effects. The final step in the method — tsunami fragility analysis — computes the dynamic inelastic (damage) response of simple structures to estimated tsunami forces. The two major components of the computational framework developed in this project include generating the earthquake moment magnitude-dependent initial tsunami source displacement field and using the two-dimensional nonlinear Boussinesq form of the Navier Stokes equations to simulate wave progression in far-field and near-field regions. The Boussinesq equations also are used to calculate general wave parameters (wave arrival time, wave height and velocity, and inundation areas) for any specified location(s). Finally, analytical studies using simplified nonlinear structural dynamic models were conducted to determine tsunami fragility functions for a representative coastal structure. Impacts of both hydrostatic and hydrodynamic pressures on the structure were considered in the fragility analysis. The developed computational framework can provide significant assistance in advancing the application and utility of tsunami risk assessment aimed ultimately at systematic decision making and effective implementation of tsunami safety policies.

Accomplishments — An integrated tsunami analysis method was developed that can be used in hazard and risk assessment at nuclear installations and other critical coastal facilities. The methodology not only provides estimates of tsunami wave height and run up for a given earthquake magnitude, it also provides a fragility analysis of coastal structures affected by the wave. Three tsunamis were analyzed and modeled. The first was the 2011 Tohoku-Oki tsunami that took place on March 11, 2011, from a 9.1 magnitude earthquake. Simulated results for the Tohoku-Oki tsunami were compared with the available observations. In addition, two other demonstration tsunami cases were studied: the Indian Ocean tsunami (2004) and a representative hypothetical tsunami on the west coast of the United States. This project has been instrumental in expanding the program in earthquake-generated tsunami modeling, particularly in

support of tsunami risk assessment for coastal nuclear and petrochemical installations. The research can be applied to site characterization studies of nuclear power plants and any medium- and long-term waste storage facility planned near the coast. Although the project focused primarily on hazards from the earthquake source mechanism, the capabilities developed can be extended to other types of tsunami sources (e.g., subaerial and submarine landslides and asteroid impacts), are useful as a launching point for additional capabilities development for tsunamis (e.g., tsunami warning system concepts and designs), and have predicted the potential effects of storm surge and other coastal flooding phenomena, as well as fragility studies for various types of impact wave/hydraulic loading of structures. Abstracts were submitted and accepted for presentation at the 2014 Offshore Technology Conference (OTC2014), 2014 ASME Offshore Mechanics and Arctic Engineering (ASME OMAE) Conference and 2014–PSAM conference.

[2013 IR&D](#) | [IR&D Home](#)

2013 IR&D Annual Report

Soil-Structure Interaction Assessment of New Modular Reactors, 20-R8270

Principal Investigators

[Amitava Ghosh](#)

Kaushik Das

Larry Miller

Todd Mintz

Sui-Min Hsiung

Inclusive Dates: 10/01/12 – 11/01/12

Background — To meet the growing demand for power, the nuclear industry is developing several new, advanced nuclear reactor designs with scalable modules. Each module will produce relatively small amounts of electricity (e.g., one NuScale module can generate only 45 MW of electricity) compared to current nuclear power plants, which are often in the 500-1,200 MW range. As power demand grows, several modules of these reactors can be installed at a given site, as needed. Because the construction is relatively simple and small in size, the lead time to start power generation is shorter. Each of these new reactors consists of an integrated reactor module and a reactor containment vessel. These containment vessels are located below the ground surface and are either fully or partially submerged inside the containment vessel. In addition, these containment vessels are attached to the support structures via seismic damping systems. These new reactor designs pose a complex soil structure-fluid interaction problem from earthquake-induced ground motion. Understanding this soil-structure-fluid interaction phenomenon is essential to the designers and regulators to ensure adequacy of the seismic damping/isolation system for safe operation of the modular reactors during seismic events.

Approach — This project uses a simplified, sequentially coupled analysis methodology for assessing the response of a containment structure housing a small modular reactor during a seismic event using the geomechanical code FLAC and the computational fluid dynamics (CFD) package ANSYS-FLUENT. It was assumed that the nuclear reactor behaves as a rigid body due to large inertia of the massive structure. Additionally, any structural deformation of the reactor from fluid sloshing inside the containment structure will have limited effects on ground motion. The FLAC code analyzes the amplification of the earthquake motion as it propagates upward through the geological medium and to the containment structure. The time dependent forces or velocities at the containment structure wall boundary from the FLAC analysis initiate fluid sloshing, which is simulated in the ANSYS-FLUENT package. The general volume flow approach was used to simulate fluid sloshing and track the air-water interface. The solution process assumed unsteady compressible flow.

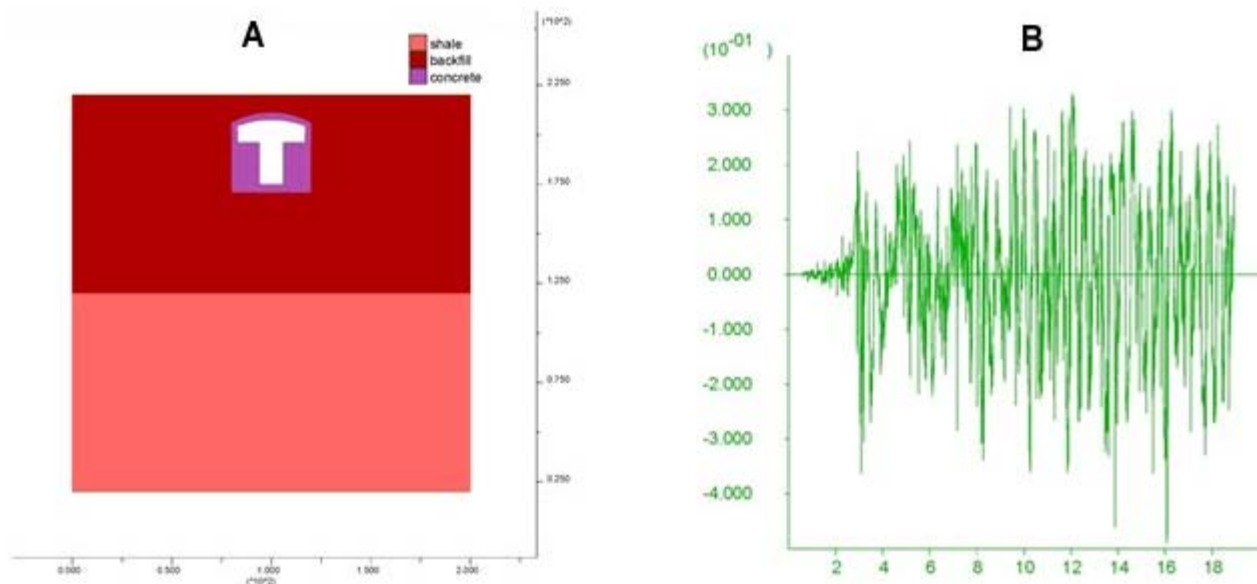


Figure 1. Soil-structure (modular reactor) interaction analysis under seismic load: (a) the model dimension in meters and (b) ground acceleration (m/s^2) calculated at the base of the reactor as a function of time (second).

Accomplishments — A site response analysis was conducted considering a hypothetical site to study the amplification of seismic waves propagating from the bedrock to the ground surface and the resulting soil-containment structure-fluid interaction with a modular reactor. Figure 1(a) shows the model used for soil-structure interaction analysis under seismic excitation. Ground acceleration at the base of the reactor from a strong-motion earthquake in California is shown in Figure 2(a). A simplified CFD model in two-dimensional space was developed to understand fluid sloshing in response to ground motion. At the wall, viscous effects are expected to be negligible compared to fluid sloshing; therefore, grid clustering was not done in the near-wall region. The sloshing motion continued after the input acceleration signal stopped. The vertical force on the reactor caused by sloshing is shown in Figure 2(a) (negative sign because the forces are acting downwards). A representative water surface profile to highlight the sloshing motion in the reactor is shown in Figure 2(b). It shows the free water surface at an angle with the horizontal plane indicating fluid motion and deformation due to ground motion.

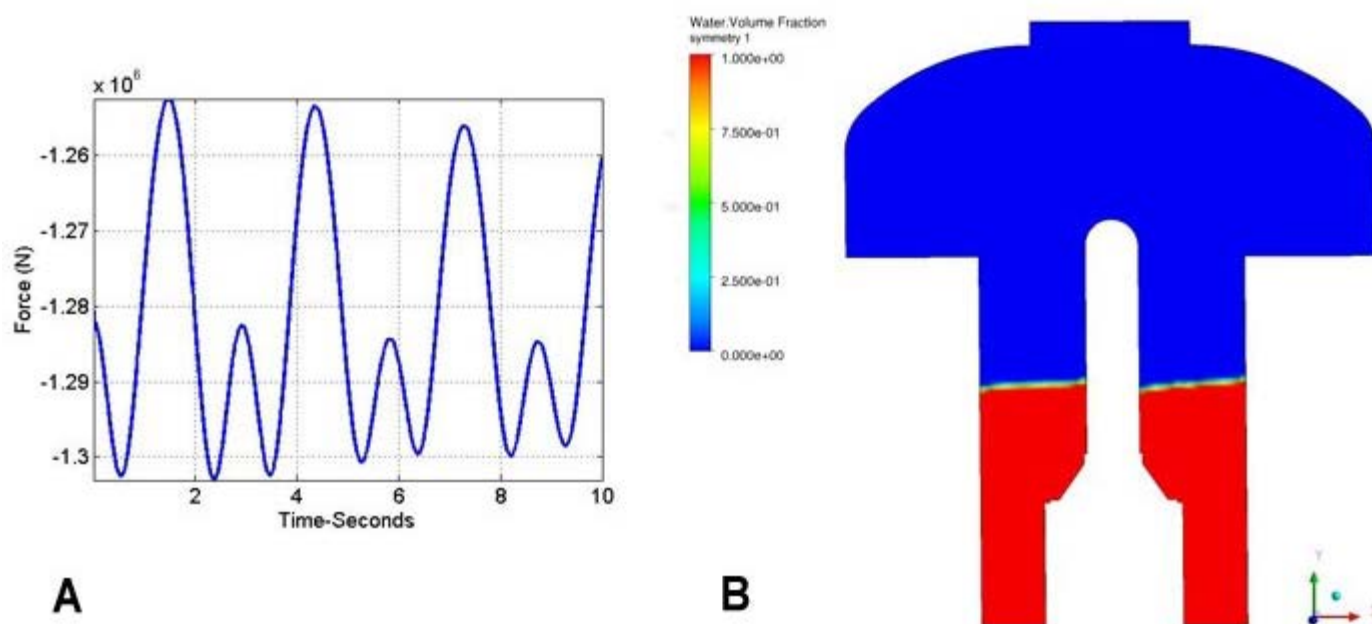


Figure 2. Computational fluid dynamics analysis for sloshing motion in a small modular reactor: (a) vertical forces due to fluid sloshing in response to seismic wave, and (b) contours of water volume fraction at Time = 0.4 s.

2013 IR&D Annual Report

Chemical-Based Tertiary Oil Recovery from Carbonate Rocks, 20–R8348

Principal Investigator

Sitakanta Mohanty

Inclusive Dates: 11/07/12 – 03/07/13

Background — The world average recovery factor from hydrocarbon reservoirs is stuck around 50 percent, even after primary and secondary recoveries, leaving behind a vast amount of oil in mature fields. Tertiary oil recovery (TOR) technologies (e.g., thermal, microbial, chemical) are needed to tap into the oil after secondary recovery (e.g., water flooding) has reached its economic limit. The current sustained higher price of crude oil has presented an economic incentive for implementing inherently expensive TOR technologies. The complexities of the TOR technologies are well recognized by the industry and are considered higher risk (i.e., lower probability of success). If TOR technologies can be improved, they will substantially lower the cost of recovering additional oil, but are fraught with significant technical challenges and many uncertainties. Greater research and development are needed to overcome challenges against significantly improving the recovery of the left-behind oil and reducing uncertainties so investment decisions can be made with greater confidence.

Approach — The objective of this research was to conduct computational studies to develop insights on the interplay of governing chemical TOR (i.e., CTOR) processes in sandstone and carbonate rocks and evaluate several chemical injection modes to potentially maximize oil displacement and ultimate oil recovery using a mechanistic multiphase, multi-component, multi-dimensional computer model. The study requires an appropriate understanding of (i) formation heterogeneity, (ii) constitutive relationships for representing relative permeabilities, (iii) detailed geochemical relationships among the multiphase fluids and the rock, and (iv) the relationship between small and medium-scale fluid flow experiments, all combined in an integrated systems approach that brings various processes together.

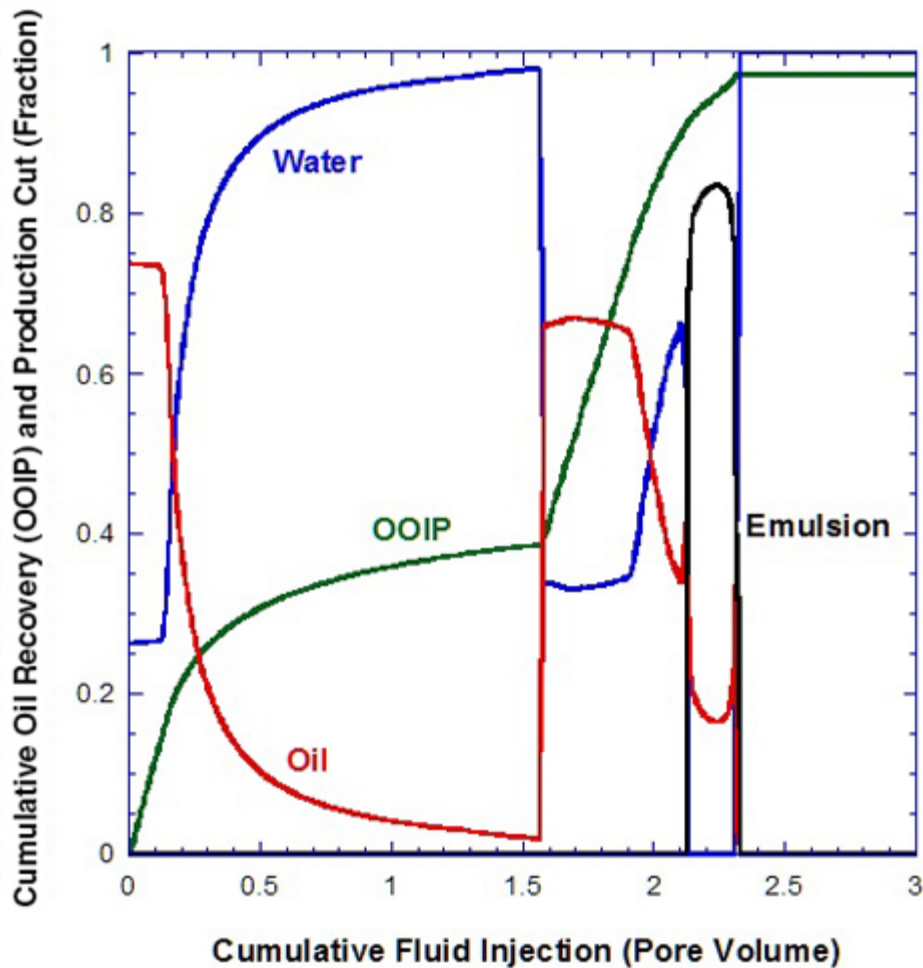


Figure 1. Simulation of alkali-surfactant-polymer (ASP) combination flood. The figure shows cumulative oil recovery expressed in original oil in place (OOIP) and production cuts (water, oil, and emulsion) as a function of cumulative fluid injection expressed in pore volumes.

Accomplishments — Using numerically simulated core floods and some surrogate data, the oil displacement pattern and ultimate recovery from the alkali-surfactant-polymer (ASP) CTOR method were studied (Figure 1). A probabilistic framework was used to propagate uncertainty and conduct sensitivity and uncertainty importance analyses to identify influential parameters. The modeling study identified a variety of factors such as injection slug size and concentration, pre-flushing, salinity level, effective polymer porosity, and other factors that could affect additional oil recovery. The probabilistic framework allowed for ready set-up of a large number of model parameters to be sampled to quickly screen parameters that influence ultimate oil recovery. The method permits the analyst to focus on those aspects that rank high in this screening test (Figure 2). This allows the analysts to determine where additional laboratory experiments, field data collection, and more detailed modeling studies should be conducted on optimal and economical design to increase confidence (i.e., reduce uncertainty) in the oil recovery estimates, which directly affect profitability. The study complements SwRI expertise in a variety of fields to tackle complex, enhanced oil-recovery (EOR) projects in an integrated fashion. With a strong emphasis on rigorous uncertainty quantification, this study enables SwRI to offer unique capabilities to the petroleum industry for making better decisions related to extracting additional oil from mature oil fields.

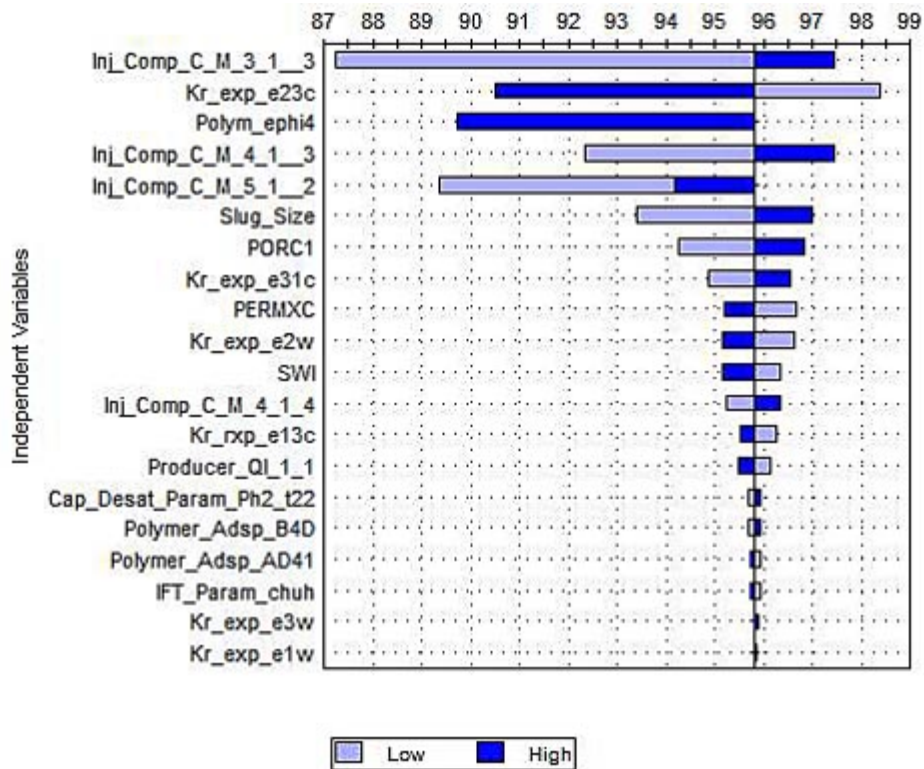


Figure 2. Identification of parameters that predominantly influence oil recovery in numerical simulation of alkali-surfactant-polymer (ASP) chemical combination flood. Such results can support decision making on whether a tertiary oil recovery technique is viable for a specific reservoir.

2013 IR&D Annual Report

Integrated Physical Analog and Numerical Modeling of Geologic Structures, 20-R8368

Principal Investigators

[Kevin J. Smart](#)

Danielle Y. Wyrick

Inclusive Dates: 01/01/11 – Current

Background — One of the major hurdles in structural geology and geomechanics is the ability to accurately model the evolution of complex geologic structures in a reproducible and efficient manner. Whether modeling large-scale crustal deformation or outcrop-scale localized deformation, the ability to create realistic, predictive models remains constrained by the limitations of the modeling approach. Typically, complex geologic problems have been characterized by one of two modeling approaches: physical analog modeling or numerical modeling. Physical analog modeling is currently better suited to simulating three-dimensional structural complexity, including discontinuous deformation such as faulting. However, analog modeling is cumbersome for conducting multiple parametric analyses, and is not amenable to extraction of quantitative stress information. In contrast, finite-element-based numerical modeling can record complex stress and strain fields during model evolution but still struggles with accurately capturing discontinuous processes such as fracturing and faulting. In particular, finite element models are often "too perfect," in that they do not include inherent flaws to accurately model natural geologic structures.

Approach — The objective of this research is to couple physical analog and finite element modeling approaches to leverage the strengths of one approach against the weaknesses of the other, and to quantify the differences in data inputs and outputs between the approaches. To reconcile the inherent limitations in the two modeling approaches, a suite of experiments are being conducted using both modeling approaches with the goal of testing and informing both. This project seeks to perform calibrated, identical (or as near as practical) physical analog and numerical modeling of complex geologic phenomena to quantify and cross-inform these modeling approaches. This project consists of three tasks: constructing and analyzing models to simulate fracturing due to fluid/magma injection; constructing and analyzing models to simulate regional extension; and incorporating project results into peer reviewed publications and presentations.

Accomplishments — A material properties database is being compiled to augment both the physical analog and numerical modeling components. Analog modeling materials must conform to known scaling laws, yet many materials reported in the literature have not been thoroughly tested for strength characteristics. For the numerical models, a mathematical description of the stress-strain behavior is selected and requires input values for material properties. Dry sand has traditionally been used in analog modeling and its material behavior is well-documented. However, to impart heterogeneity to this layering, alternative analog materials will need to be identified that can mimic the scaling behavior of weaker and stronger intervals. A number of promising materials are being tested to find potential materials that scale appropriately to weaker and stronger rocks. The in-progress material database is being used to conduct preliminary numerical simulations that paralleled the geometry and loading conditions of initial physical analog models. These initial numerical simulations provided an assessment of the relative strengths and weaknesses of the available constitutive relationships. Preliminary results suggest that the continuum damage-mechanics-based plasticity material model provides the strain localization behavior needed to simulate behavior observed in physical models.

2013 IR&D Annual Report

Hypothesis Testing for Subfreezing Mass Movements, 20–R8407

Principal Investigators

[Donald M. Hooper](#)

Cynthia L. Dinwiddie

Inclusive Dates: 07/01/13 – Current

Background — Debris flows, some seasonally recurring, are known to be present on dune slopes in several mid- to high-latitude dune fields on Mars. Mass movement signatures are among the best records of historical and ongoing geologic activity on Mars, and suggest the erosive action of water and present habitability — a major investigative theme of the modern Mars Exploration Program. Sand dunes are young, transient features on Earth and Mars; debris flows on Martian sand dunes therefore imply recent alluvial activity and seasonally recurring debris flows imply modern, ongoing alluvial activity. Analogous debris flows consisting of a sand and liquid water mixture that cascaded down leeward dune slopes under subfreezing conditions were observed in March 2010 at the Great Kobuk Sand Dunes, Alaska. Similar mechanisms may be responsible for generating Martian debris flows on dune slopes.

Approach — During winter 2013–2014, SwRI will conduct a field survey of subfreezing debris flow development on sand dunes at the Great Sand Dunes National Park and Preserve (GSDNPP) in Colorado. The hypothesis is that relatively dark sand lying on bright snow may cause local hot spots to form where solar radiation can be absorbed by the sand and conducted into the snow, enabling meltwater to form at subfreezing air temperatures and sand to mobilize through alluvial processes. Measurement of the areally distributed and multilevel subsurface environmental conditions that are associated with initiation of subfreezing debris flows will be acquired to better understand the fundamental processes that may lead to similar alluvial mass wasting events on Mars. Surveys of slope angles, solar radiation, areal and temporal surface temperature distributions, moisture profiles, timing of flow initiation, debris flow velocities, water-to-sediment ratio, and debris flow morphologies will be performed to validate SwRI's conceptual model of the processes that control subfreezing debris flow initiation and development.

Accomplishments — Meteorological data was downloaded from the GSDNPP Remote Automatic Weather Stations (RAWS) site. For the initial analysis, the mean daily values for air temperature and solar radiation were examined. The maximum mean daily total solar radiation was plotted as a measure of the maximum potential total solar radiation that could fall on the dunes at this latitude and time of year. For the temperatures, the focus was on the maximum temperature during the course of the day. During field work, debris flows may be observed when the maximum daily air temperature is subfreezing, but solar radiation is strong. In October 2011, GSDNPP was mapped by LiDAR (Light Detection and Ranging) at 1 laser return per meter to provide a high resolution digital elevation model (DEM). The National Park Service provided this data set at no cost to the project. The LiDAR-based DEM is fundamental for geomorphologic evaluation because it provides topographic detail and the ability to resolve spatial derivatives of elevation, such as slope and aspect. These data were used to identify on an hourly basis the maximum winter solar illumination across dune slopes. Identifying the diurnal maximum total solar radiation levels and the maximum air temperature levels can determine which dune slopes are strongly illuminated during a specific portion of the day and then the most likely period of the day when meltwater-induced debris flows will form during the winter can be estimated.

2013 IR&D Annual Report

An Experimental Facility and Analytical Methodology for Determining Frequency-Dependent Force Coefficients of Foil Gas Bearings, 18-R8189

Principal Investigator

[Aaron Rimpel](#)

Inclusive Dates: 10/01/10 – Current

Background — Accurate knowledge of linearized stiffness and damping coefficients of bearings is a critical aspect in the successful design of high-performance turbomachinery. In recent years, improvements in foil gas-bearing technology have led to their increasing application in the expanding oil-free turbomachinery market (current applications include air cycle machines, auxiliary power units, automotive turbochargers, micro gas turbines, refrigeration compressors, etc.). Foil gas bearings utilize a gas, such as the process gas of a compressor, for example, as the lubricant that separates the rotor from the stationary bearing surfaces. Thus, the need for a separate lubrication circuit with seals, as required for traditional oil lubrication, is eliminated. Foil gas bearings are also not limited by precessing-inertia speed limits as with rolling element bearings, nor do they require expensive control systems as with active magnetic bearings. The relatively low damping of foil gas bearings, when compared to oil lubrication, is mitigated through the use of friction damping mechanisms in the compliant support structures within the bearing. Foil gas bearings of various types are the main focus of gas bearing research today, and they are also the most common gas bearings currently found in commercial applications. Despite the growing popularity of foil gas bearings, there is considerable uncertainty regarding their stiffness and damping coefficients.

Approach — The approach used for this project is both experimental and analytical. An experimental test rig is capable of measuring frequency-dependent stiffness and damping coefficients of foil gas bearings for journal speeds up to 60 krpm. A key component of the test rig is the ability to excite the journal in forward or backward whirl with the use of a bi-directional rotating inner shaft mechanism. A pressure chamber may permit testing of various gaseous working fluids from sub-atmospheric pressures up to 635 psig. The analytical method applies transient fluid-structure interaction (FSI) modeling techniques to simulate the gas film and structural components of the foil gas bearing via coupled computational fluid dynamics (CFD) and finite element analysis (FEA). The transient FSI method can allow modeling of the complex structures of foil gas bearings, and it may be general enough to be applied to a wide range of foil gas bearing geometries and extensible to other turbomachinery components such as seals.

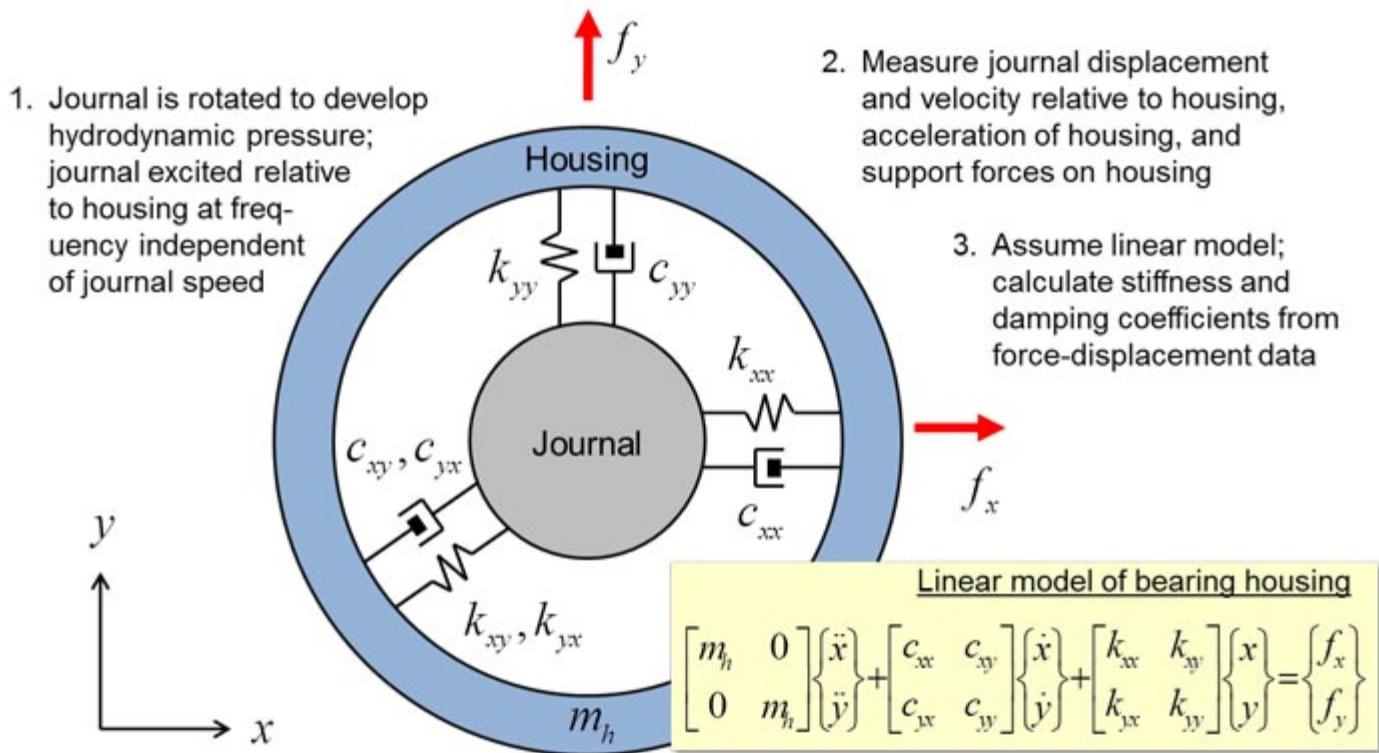


Figure 1. Model of a bearing using linearized stiffness and damping coefficients. Spring and damper elements represent dynamic behavior of lubricating fluid film in series with mechanical structure of top foils and undersprings.

Accomplishments — The design of the test rig was completed, and all features of the rig were fully demonstrated. The algorithms necessary to extract frequency-dependent stiffness and damping coefficients from the measured data have been tested extensively and have been validated with various test cases. The transient analytical method has been demonstrated on a simplified geometry (plain sleeve bearing, centered whirl) for which other established methods are typically applied due to their simplicity. Comparisons of the new and established methods showed excellent agreement for the simple geometry, and parameter studies of transient time-step resolution and mesh density provided insight to optimal simulation settings. A novel “growing rotor” technique for starting a simulation with preloaded foil bearings was developed, and the ability to model compliant, spring-supported bearing foils in a steady-state simulation was demonstrated.

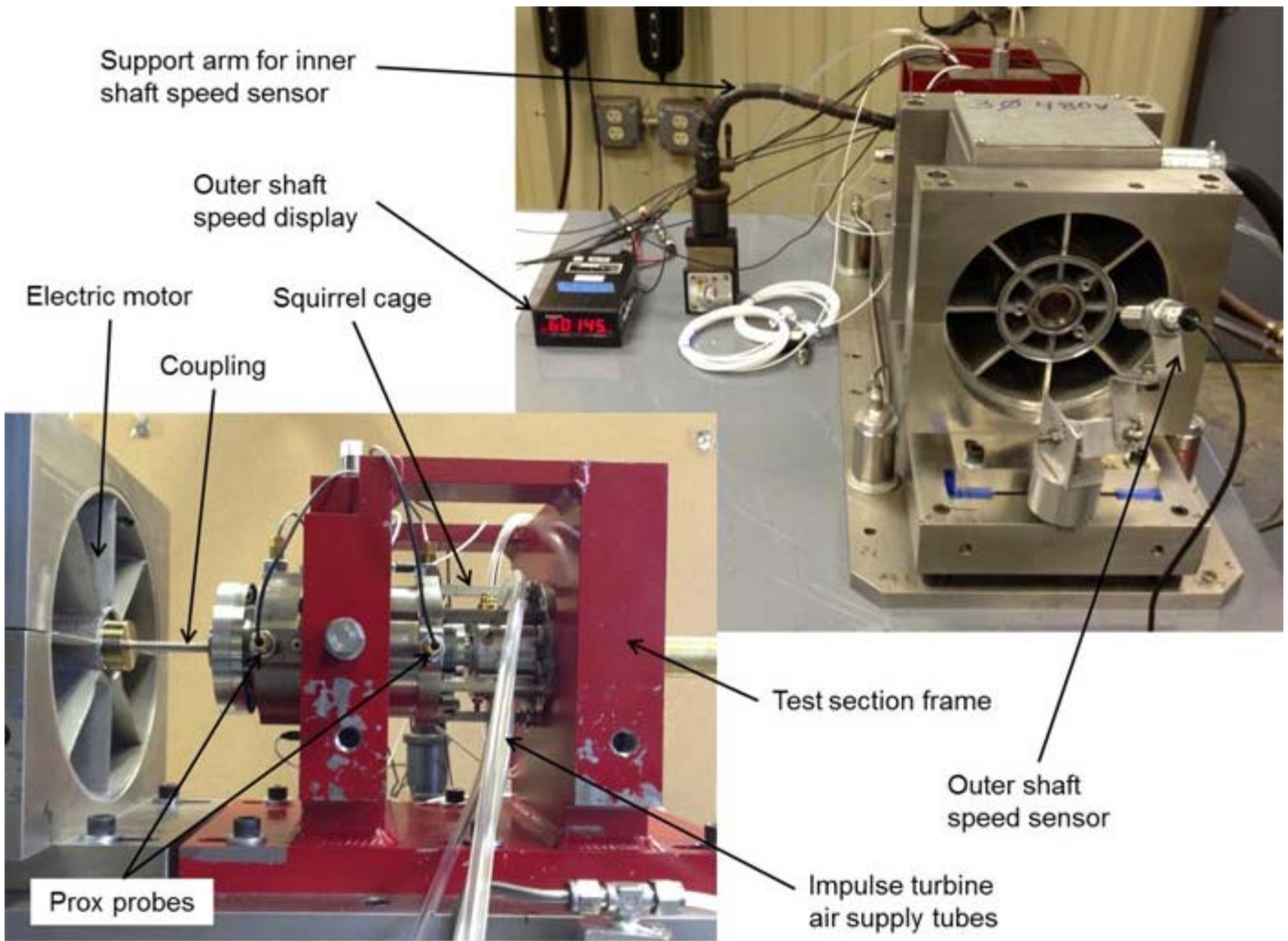


Figure 2. These photos show the test rig demonstration setup. The outer shaft is capable of being driven up to 60 krpm, while the inner shaft is capable of being driven at ± 60 krpm.

CFD Simulation of Fluid Gap

Structural Simulation of Bearing Housing

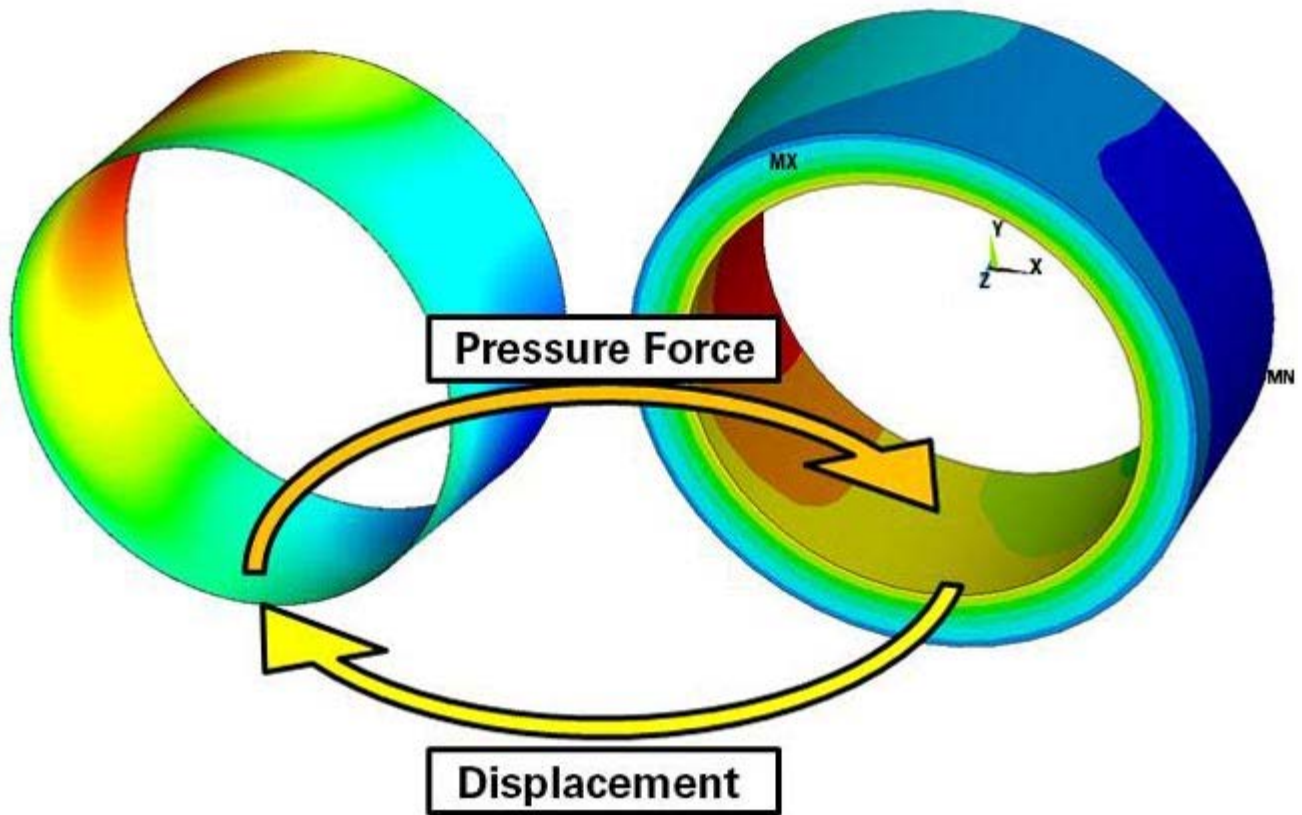


Figure 3. Fluid-structure interaction (FSI) couples the fluid and mechanical simulation results.

2013 IR&D Annual Report

A Comprehensive Approach to Predicting Vortex-Shedding-Induced Pulsation Amplitudes in Piping Systems, 18-R8325

Principal Investigators

[Eugene L. Broerman](#)

Sarah Simons

Rebecca Owston

Aaron McClung

Nathan Poerner

Inclusive Dates: 07/01/12 – Current

Background — One of the major design criteria for centrifugal compressor piping systems is the prevention of piping system vibration and valve failures resulting from vortex-shedding-induced (VSI) pulsations. In recent years, computational fluid dynamics (CFD) has been used to theoretically predict the dynamic shaking forces that cause vibration when the subject phenomenon occurs in piping systems. However, a practical, validated approach to applying these theoretical methods has yet to be developed. SwRI's current approach to address this concern is a screening-type vortex-shedding analysis ("Strouhal analysis") for determining whether there is a coincidence associated with the frequency of the vortex-shedding of the gas flow and the acoustic natural frequency of piping stubs. If a coincidence is predicted based on the screening analysis, piping changes are recommended to avoid the coincidence. These piping changes are typically expensive, time consuming, and possibly unnecessary in some circumstances. There is currently no way to determine the severity of the resulting pulsation amplitudes and, therefore, the severity of possible piping vibration. The lack of an accurate prediction method requires added conservatism that has forced many operators to reduce operating flexibility or make costly piping changes that could otherwise be avoided. VSI pulsation amplitude predictions would allow SwRI to offer a significant cost-saving service to its clients.

Approach — This project is a combined experimental and analytical effort. An experimental Strouhal test program is being conducted in conjunction with a supporting effort that uses a commercial CFD package to provide supplemental pulsation amplitude predictions in order to populate pulsation amplitude response surfaces. The response surfaces will be used as the basis for developing a new boundary condition to be implemented in SwRI's proprietary Transient Analysis Pulsation Solver (TAPS). The new boundary condition will incorporate a source term representing the acoustic excitation caused by Strouhal shedding at a piping stub. This new simulation capability will augment the current SwRI Strouhal screening methods by providing a means of predicting pulsation *amplitudes* when acoustic resonance cannot be avoided. The primary objectives of this project are to develop validated simulation capabilities (i.e., using TAPS and CFD) to accurately predict the amplitudes of vortex-shedding-induced piping pulsation and gain knowledge during the execution of this investigation that will enable the definition of design guidelines for using clamps to restrain shaking forces resulting from acoustic coincidences in small-bore piping.

Accomplishments — An experimental test matrix was developed that included mainline piping diameters ranging from 3 inches to 6 inches, flow conditions associated with Reynolds numbers that range from $2(10)^5$ to $4(10)^6$, and branch piping diameters that range from 1.5 inches to 3 inches. Test sections were fabricated such that appropriate measurements (dynamic pressure, temperature, static pressure, flow, etc.) could be obtained during each data sampling. Laboratory testing was completed at two SwRI test facilities and preliminary results show good agreement between the calculated/predicted acoustic natural frequencies and the measured natural frequencies. Vortex-shedding frequencies have also been observed to be at approximately the predicted frequencies. Some of the measured pulsation amplitudes have been

lower than anticipated; therefore, additional testing is being planned to provide more insight into this unexpected result. In particular, future testing will be performed in a system in which much higher Reynolds numbers can be achieved (approximately $1.7(10)^7$). Appropriate CFD software packages and turbulence models were assessed and model verification was attempted. Investigations determined that the resources (time and software licenses) could not be covered within the scope of this project; therefore, CFD allocated funding will be applied to additional testing.

2013 IR&D Annual Report

Improvement of Wet Gas Compressor Performance Using Gas Ejection, 18-R8327

Principal Investigator

Grant Musgrove

Inclusive Dates: 07/02/12 – Current

Background — During upstream production of natural gas, the gas brought to the surface is compressed so that it can be injected into a pipeline and transported elsewhere. Sometimes the gas brought to the surface is a mixture that includes a small amount of liquid hydrocarbons, up to 5 percent volume fraction, called "wet gas." Because a compressor is designed for dry gas only, wet gas reduces the performance of the compressor to require much more power. Typically, the liquid is removed upstream of the compressor such that compressor performance is unaffected by wet-gas production. However, the capital and maintenance costs of the large separators required to remove the liquid become significant in sub-sea and offshore installations. Therefore, a significant cost savings can be achieved in offshore and sub-sea installations by eliminating the separator and allowing wet gas to enter the compressor. The current approach to investigate the effects of wet gas on compressor performance is to conduct flange-to-flange performance testing of compressors operating under wet-gas conditions. Flange-to-flange tests, however, do not provide a fundamental understanding of how wet gas physically affects compressor operation. With a better understanding of wet-gas effects, it may be possible to improve compressor design and operational control during wet gas conditions.

Approach — The goal of this project is to design and test a concept to eject air from the airfoil to create a gas film barrier that keeps the liquid from coming in contact with the airfoil surface (Figure 1). Airfoil performance is evaluated from measured lift, drag and surface pressure along the airfoil in wet-gas flow, including high-speed images of the gas-liquid flow near the airfoil. This project is conducted in two phases using computational predictions and experimental measurements. In the first phase, the effects of airfoil performance with wet gas over a range of operating conditions are studied with experimental measurements and computational predictions using a lattice-Boltzmann fluid solver, whereby the computational predictions can be directly compared to measurements. In the second phase, a gas ejection concept is implemented using the results from Phase 1, and studied computationally and experimentally for comparison to the baseline configuration without gas ejection.

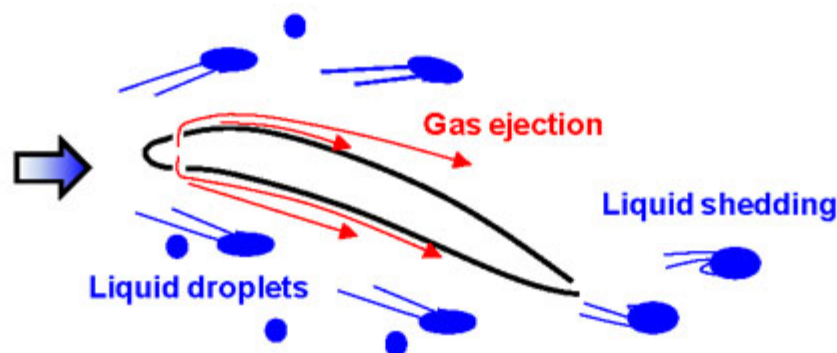


Figure 1. SwRI gas ejection concept.

Accomplishments — A lattice-Boltzmann computational fluid dynamics tool has been developed to

simulate single-phase, turbulent, incompressible flow around an airfoil at variable angle of attack. Multi-phase capability is currently being added to the solver to simulate wet-gas flow around an airfoil. Because the solver is implicitly transient, shedding vortices from the airfoil can be seen from the computational results (Figure 2). Pressure distribution over the airfoil surface is found to agree well with analytical predictions and experimental measurements (Figure 3). An open-loop wind tunnel has been designed and constructed for testing wet gas performance of airfoils (Figure 4). The airfoil is manufactured using 3D printing to allow complex internal features of the airfoil to be constructed. Airfoil measurements from the wind tunnel are validated using analytical predictions of pressure distribution on the airfoil surface. Measurements of airfoil drag have been recorded for wet gas flows with liquid mass fractions up to 10 percent to show that airfoil drag increases with water amount. At this time, the increase in drag is thought to be caused by the complex liquid film interaction at the airfoil surface. Images of the liquid film taken during baseline testing show a wavy liquid interface on the airfoil moving in the upstream direction (Figure 5).

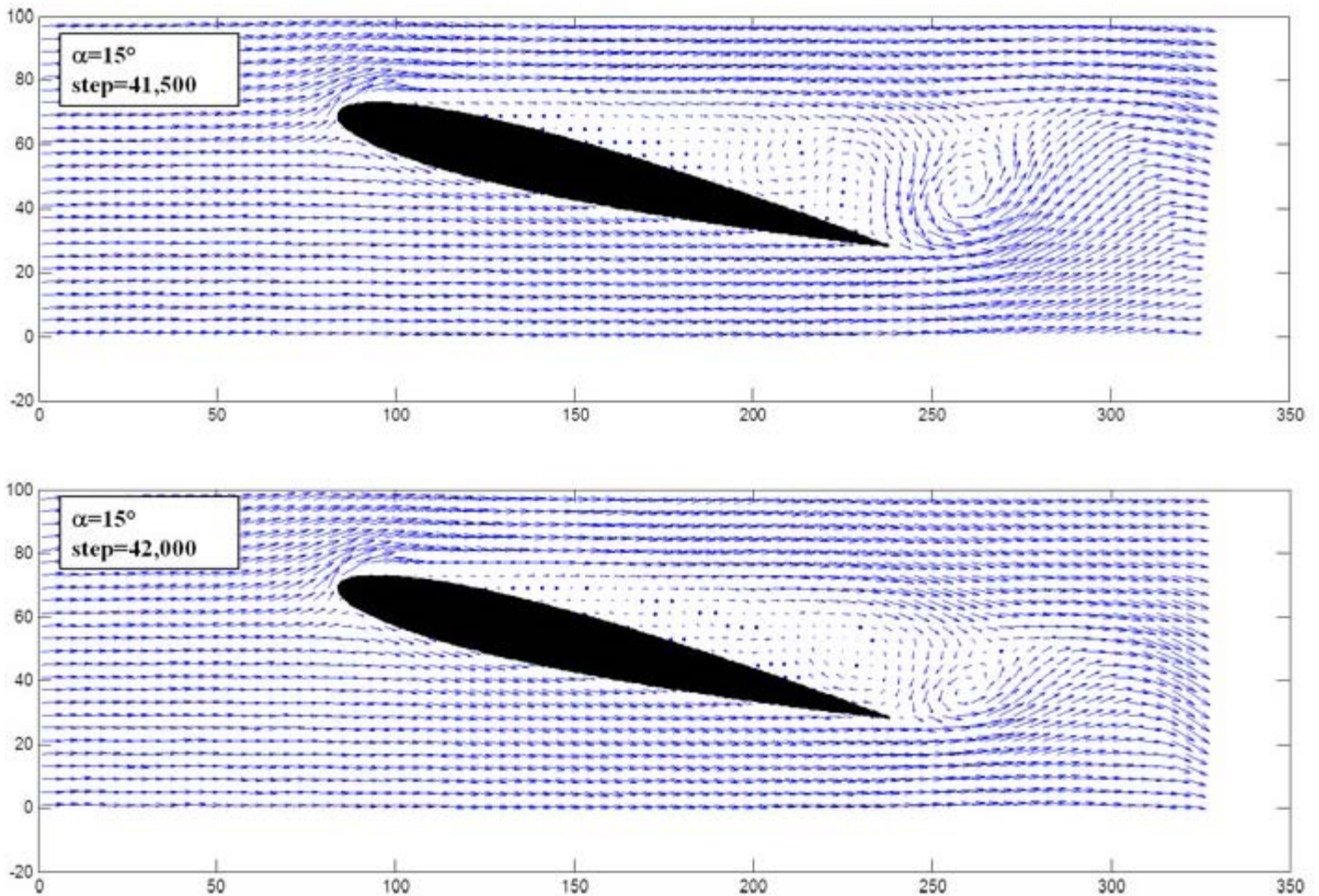


Figure 2. Computational results showing shedding vortices.

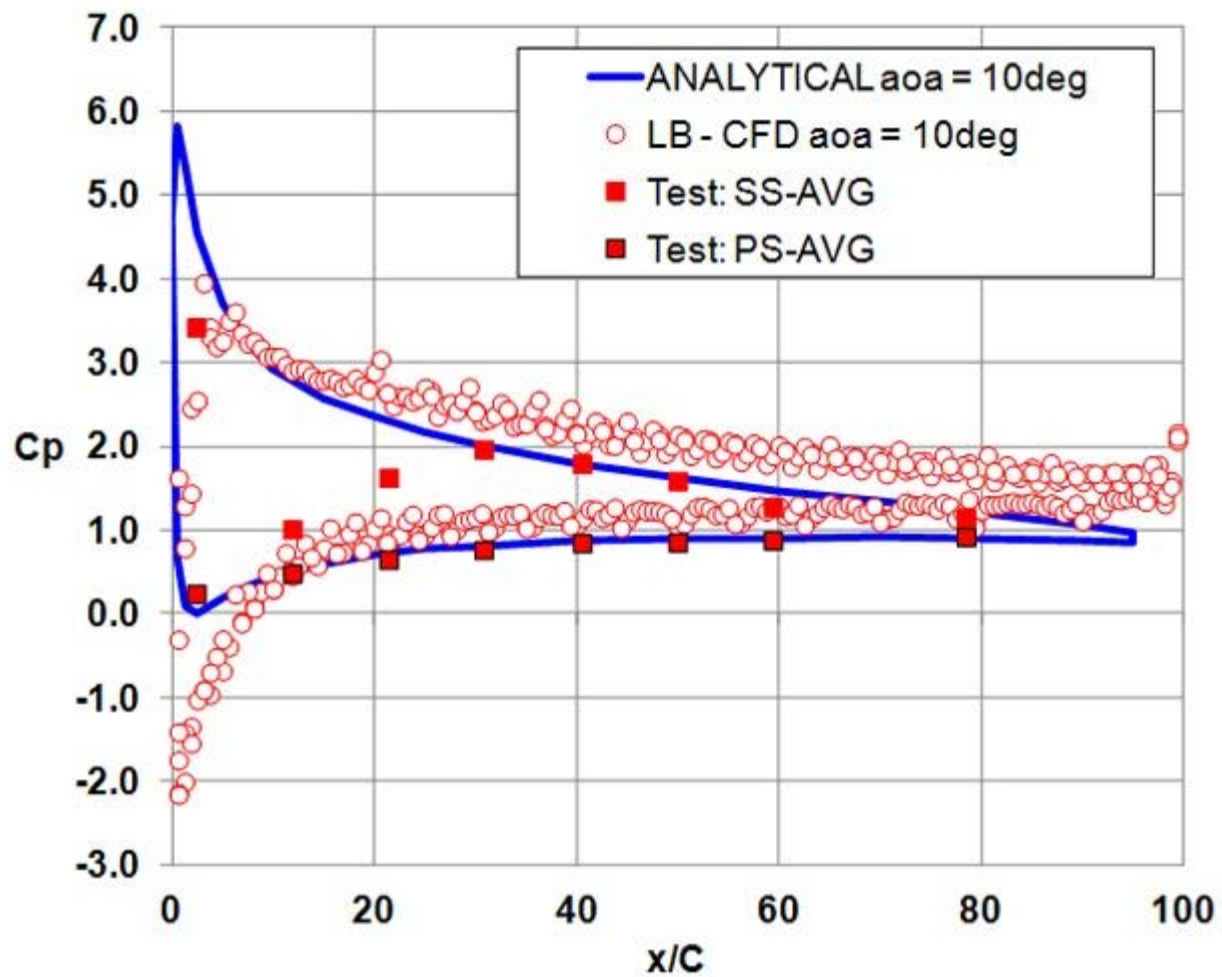


Figure 3. Analytical predictions and experimental measurements of airfoil surface pressure distribution.

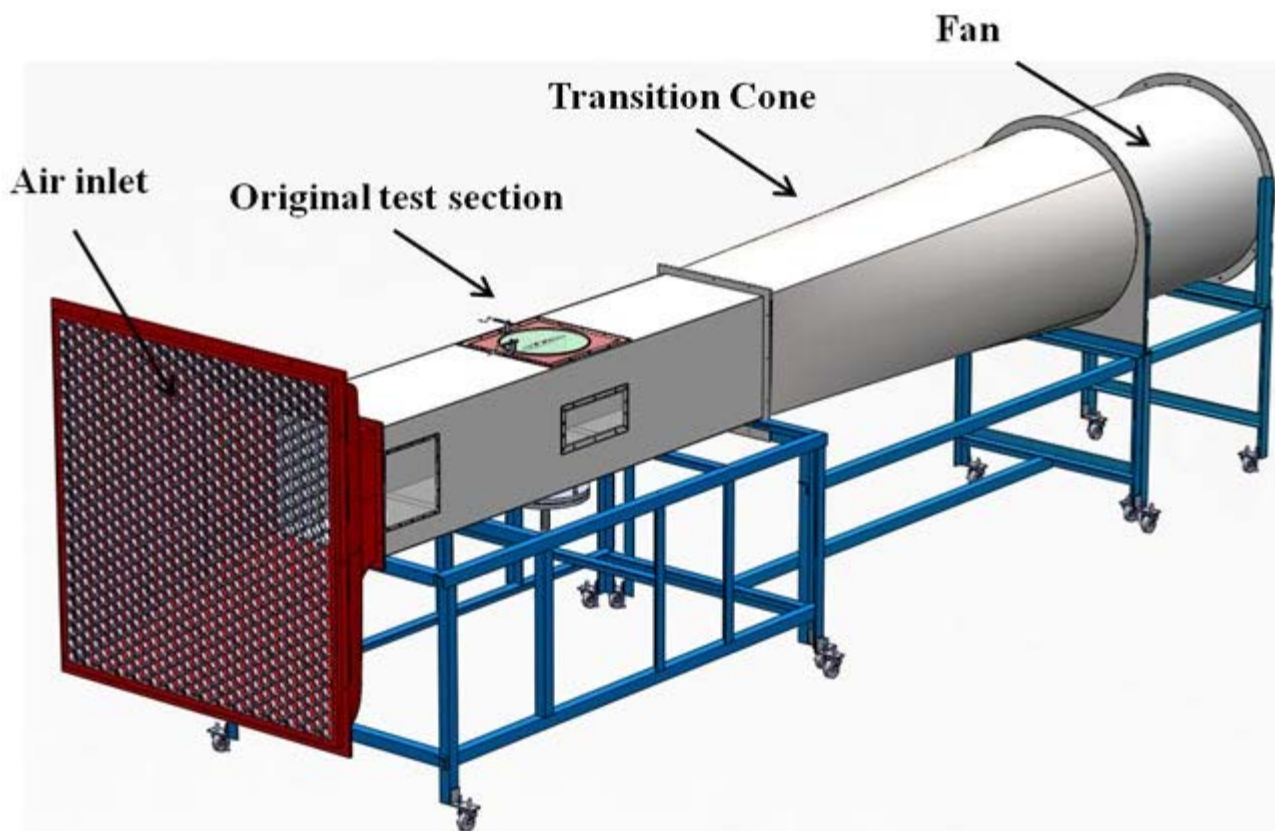


Figure 4. SwRI-designed open-loop wind tunnel.



Figure 5. Baseline testing image shows liquid film interaction.

2013 IR&D Annual Report

Alternative Advanced Electronic Countermeasure Techniques, 09-R8349

Principal Investigators

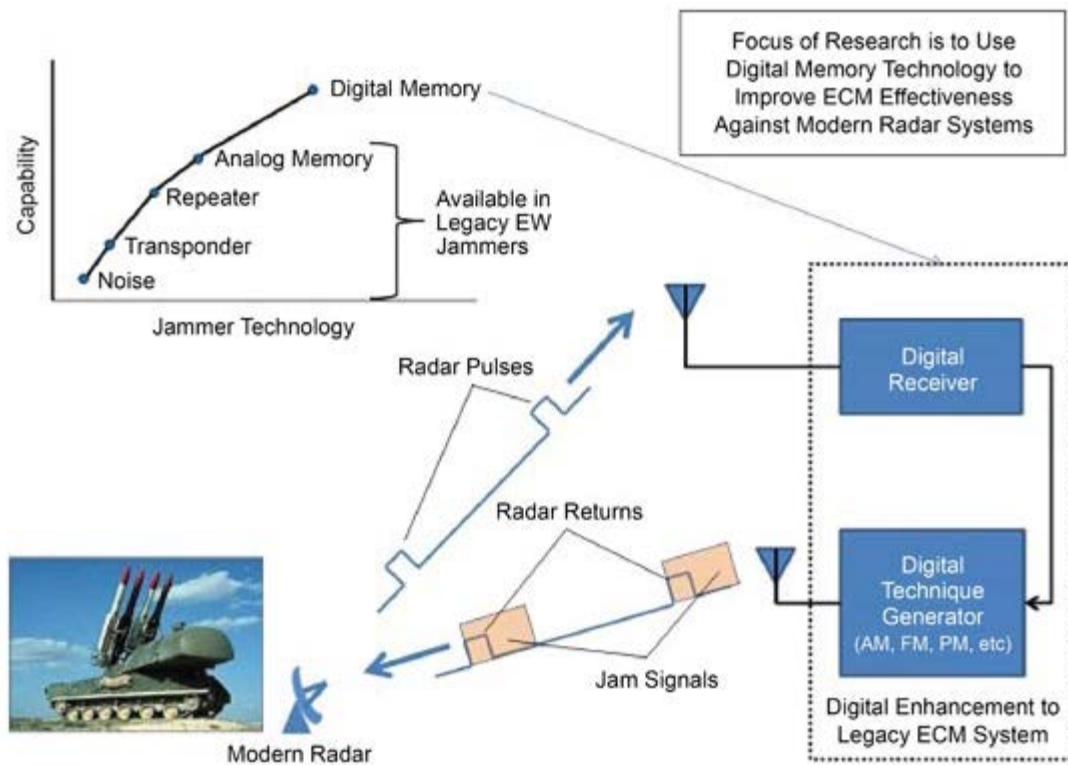
[Finley Hicks](#)

Jeremy Pruitt

Inclusive Dates: 11/26/12 – Current

Background — Radar systems are designed to use transmitted and received radio frequency (RF) signals to compute a target's position and velocity to identify enemy aircraft, track them, and guide weapons to their projected location. Electronic countermeasures (ECM) systems are designed to 'jam' radar signals in a way that deceives or degrades a radar's ability to accurately determine an aircraft's position and velocity. In recent years, radar system improvements, which primarily involve the use of digital hardware, have made legacy ECM systems less and less effective. At the same time, attempts to develop new all-digital ECM systems have been delayed by long development cycles and shrinking defense budgets. As a result, there is a growing need for low-cost, digital enhancements to legacy ECM systems that will make these systems viable until next-generation, all-digital ECM systems can be fielded.

Approach — SwRI has investigated several viable, low-cost alternatives to expensive all-digital ECM systems to protect aircraft against modern radars. The objective of this project has been to develop a prototype capable of enhancing legacy ECM systems to greatly improve their effectiveness against modern digital radars. The prototype includes select digital hardware capable of generating new and enhanced types of jam signals. At the same time, the prototype will illustrate a low-cost approach by demonstrating ways to leverage existing capabilities of legacy ECM systems to the greatest extent possible.



SwRI-developed approach for enhancing legacy electronic countermeasure systems.

Accomplishments — SwRI has successfully investigated alternative approaches to developing digital enhancements to legacy ECM systems. These enhancements include digital receiver and technique generator capabilities. The digital receiver has the capability to digitize an incoming radar signal with an instantaneous bandwidth (IBW) of several hundred megahertz, accurately measure frequency very quickly (< 100 ns) to correlate incoming pulses to specific radar threats, and measure advanced radar intra-pulse characteristics, such as chirp and bi-phase modulation. The digital technique generator has the capability to modulate the digitized radar signal with ECM techniques and transmit the resultant jam signal, providing a very quick response time (measured in ns) from the time the radar signal is detected to the time the jam signal is transmitted. SwRI has successfully developed a design to accomplish these advanced ECM capabilities, and SwRI is currently in the process of completing the prototype hardware to demonstrate these capabilities.

2013 IR&D Annual Report

GPS-denied Localization System, 10-R8248

Principal Investigators

[Kristopher C. Kozak](#)

Christopher L. Lewis

Marc C. Alban

Samuel E. Slocum

Michael O. Blanton

Inclusive Dates: 09/06/11 – 09/06/13

Background — Global Positioning System (GPS) receivers provide a low-cost localization and navigation solution to a wide variety of commercial and military systems. As safety-critical systems come to rely on GPS (and other satellite-based localization systems), concerns have mounted due to its well-known vulnerabilities; GPS has limited accuracy and requires an unobstructed line-of-sight to multiple satellites. Its signals are subject to interference, multi-path, jamming and spoofing. While GPS has become more essential and ubiquitous, few practical alternatives have emerged. The fragility of GPS can be considered one of the limiting factors in the adoption of some cutting-edge technologies such as automated driving. The objective of this project was to develop a camera-based system that provides real-time localization measurements and can serve as a reliable supplement or alternative to GPS.

Approach — SwRI developed two related map-based localization methods that use cameras on a vehicle. Two camera systems were designed: a downward-facing camera with high intensity illumination and a forward-facing stereo pair. The downward-facing camera system allows for extremely high precision localization on pre-driven, mapped routes, while the forward-facing camera system allows for localization using both maps generated on pre-driven routes, as well as maps consisting of readily available aerial imagery. By processing the real-time imagery acquired with the cameras and comparing the image features/landmarks

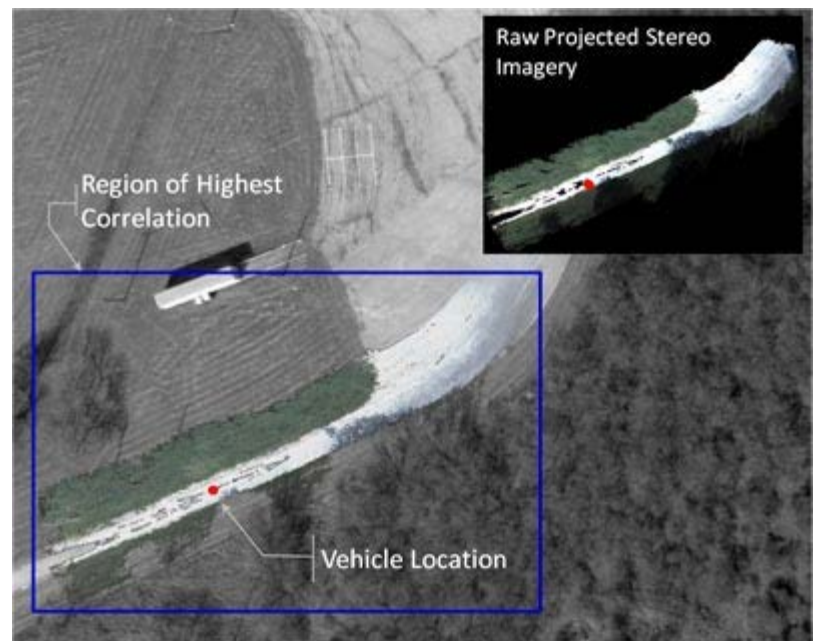


Figure 1. Features of opportunity in ground images are matched by appearance subject to geometric constraints to identify overlapping frames and determine vehicle location.

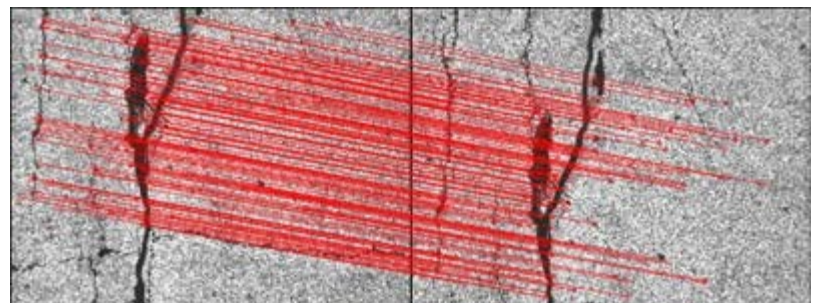


Figure 2. Stereo imagery acquired on a ground vehicle can be used to determine location relative to a georegistered aerial image.

to the geo-referenced imagery that comprises the map, the location of the cameras (and thus the vehicle on which the cameras are mounted) can be determined. In addition, either camera system can be used to compute differential motion between camera frames, and thus can fill in gaps when the live imagery from the vehicle cannot be confidently matched to the map.

Accomplishments — For the ground-facing camera localization approach, a full-hardware system, which includes a camera and synchronized high-intensity illumination, was designed and installed on an SwRI vehicle. An algorithmic framework based on feature matching with geometric constraints was developed as the basis of the localization approach. This approach has been shown in a subsequent analysis to have a very high success rate for positively identifying location (on a variety of road surfaces), with a very low rate of incorrect matches. A map representation and optimization scheme was developed to facilitate live localization and to improve the overall consistency and accuracy of the localization. Finally, the full ground-facing system was implemented and operated successfully in real time on the vehicle. The precision of this system was measured versus a high-accuracy GPS, and found to perform comparably, on the order of 1 cm. For the forward-facing stereo camera localization approach, two separate algorithmic frameworks were developed, a feature matching approach and an image correlation approach. Both methods have been demonstrated to yield successful localization on several types of data, including real projected stereo imagery.

2013 IR&D Annual Report

Microwave Methods for Enhanced Combustion in Natural Gas Engine Applications, 10-R8408

Principal Investigators

[E. Sterling Kinkler Jr.](#)

Jess W. Gingrich

Barrett W. Mangold

Russell K. Barker II

Inclusive Dates: 07/01/13 – Current

Background — Internal combustion engines (ICE) are used to convert energy stored in fossil fuels to usable power for transporting people and accomplishing work in an astonishing array of applications and industries. Planes, trains and automobiles have been the most visible platforms using ICE technologies since the early 1900s, and the energy crises of the 1970s initiated much interest in higher fuel efficiencies. Accompanying the vast growth of operating ICE products, environmental issues are also major concerns. Current and especially future, economic, regulatory and social pressures are fueling significant research in cleaner, higher efficiency combustion processes. Exhaust gas recirculation (EGR) techniques are frequently found in modern gasoline engines to help reduce harmful emissions and improve efficiency. High levels of EGR dilution can result in slower combustion and related ICE performance problems. Enhanced combustion of gaseous fuels has long been observed when electric fields are applied. Microwave (MW) techniques can produce very high intensity electric fields within an enclosed volume and are often used to develop intense electric fields that accelerate sub-atomic particles to near-speed-of-light velocities for modern physics research. International regulations allocate multiple MW frequency bands for use in industrial applications. Previous work at Southwest Research Institute, coupling MW power into an existing spherical chamber during combustion of gasoline/air mixtures, has produced promising experimental results.

Approach — The objective of the project was to effectively couple MW power into an enclosed metallic chamber emulating the combustion chamber (CC) of modern ICE products. Design and test of fundamental methods and techniques to develop intense electric fields within a modern ICE CC is an enabling step toward implementing running ICE platforms that can facilitate performance testing with MW enhanced combustion (MEC) techniques applied. The approach to this project is to research, fabricate and test experimental MW coupling methods that can achieve significant MW fields within a CC and accommodate the many constraints imposed by the design and operation of modern commercial ICE products. The ICE CC is generally in the shape of a cylinder with variable height and contains a harsh internal environment, including cyclic high temperatures and pressures. Project research goals include implementing high-intensity internal electric fields for a range of ICE products and operating conditions. The large-bore natural gas ICE class was chosen due to physical and dimensional characteristics and the potential for relatively significant economic and environmental impact of improvements in efficiency and emissions, as engines in this class typically run 24/7 at high loads.

Accomplishments — A preliminary list of features and attributes was established for MW methods related to program goals and ultimate applicability to commercial ICE products. Research and preliminary design and analysis were performed for a number of experimental MEC implementation methods and an initial design was selected that uses a coaxial MW delivery system coupled to a small circular dielectric-filled MW waveguide. The filled waveguide is intended to couple and excite a desired MW field structure within the CC, maintain the necessary pressure envelope of the CC, and facilitate future MEC integration within commercial ICE products. The preliminary design of a laboratory CC fixture was also completed

that mimics selected commercial CC shapes and sizes, and can facilitate MW system function, performance and sensitivity experiments. Materials required for the initial experiment designs of the MW system and CC test fixtures have been acquired, and final design and fabrication are under way. An agreement with a major engine manufacturer is currently being negotiated. Teaming with a large original equipment manufacturer will provide realistic constraints on the design of the MEC system to accelerate acceptance of MEC technology in the large bore natural gas engine industry.

2013 IR&D Annual Report

Development of a Wireless Power Transfer Technique for Quick-Charging Inaccessible Electronic Devices, 14-R8363

Principal Investigators

[Monica Rivera](#)

Richard D. Garcia

Joseph N. Mitchell

Grahm C. Roach

Jeffrey L. Boehme

Inclusive Dates: 01/01/13 – Current

Background — Many system- or mission-critical electronic devices are located off the electrical grid and, as a result, on-board energy storage units in the form of batteries are typically used to supply power to the devices. Because of finite energy storage limits, the energy storage units within these devices must be periodically replaced or replenished. While the completion of this task is relatively straightforward for devices that are easily accessible, difficulties arise when the devices are located in areas that are inaccessible due to work-force limitations, inhospitable terrain, adverse weather, hazardous environmental conditions, mission constraints or the presence of hostile adversaries. While energy-harvesting systems are often incorporated into off-grid, system-critical devices, the magnitude and consistency of the energy generated by these systems are still a concern. The primary objective of this research effort is to develop a wireless power transfer technique capable of quick-charging electronic devices located in inaccessible locations. To accomplish this goal, a portable wireless power transfer technique will be developed and the appropriate design parameters will be determined to minimize charge time while maximizing power transfer efficiency, the feasibility of quick-charging electronic devices from a mobile delivery platform will be demonstrated, and credible data about the wireless transfer process and overall system performance will be generated.

Approach — In this project, power will be transferred wirelessly to an inaccessible electronic device via a narrow-band light source. The wireless power transfer process is unique from existing light-based wireless power transfer systems in that it can supply power to electronic devices in a recurrent, non-continuous fashion, store the delivered energy quickly in supercapacitors for abbreviated charge durations and enable power transfer beyond the operator's line-of-sight via the use of an unmanned aerial system (UAS).



Unmanned Aerial System (UAS) with gimballed eye-safe payload. A flashlight of comparable size and weight was used during initial tests to simulate the laser payload in the wireless power transfer system.

Accomplishments — During the project, power was successfully transferred via a laser-based system over a separation distance of one meter. In an effort to expedite the charging process, a multi-phase supercapacitor charging circuit was designed and constructed, and the parameters that influenced overall charge time were investigated. To comply with current Federal Aviation Administration (FAA) regulations while still accomplishing the work outlined in the project, an indoor test area with a six-camera motion capture system was used. The UAS hardware and software were also modified to increase the hovering and pointing stability of the platform and payload during autonomous flight mode.

2013 IR&D Annual Report

Scaling Kinetic Inductance Detectors (KIDs), 15-R8311

Principal Investigator

Peter W. A. Roming

Inclusive Dates: 05/07/13 – 09/07/13

Background — For approximately the last three decades, charged coupled devices (CCDs) and hybrid complementary metal-oxide-semiconductor (CMOS) detectors have dominated the field of optical and IR imaging. Despite their dominance, they lack simultaneous timing and spectral information, and only have good quantum efficiencies over a narrow wavelength range. The development of superconducting tunnel junctions (STJs) and transition edge sensors (TESs) has alleviated these shortcomings. However, STJs and TESs suffer from the major challenge of constructing large format arrays, which are required for most imaging applications. Kinetic inductance detectors (KIDs) are a relatively new alternative superconducting technology that have many of the same desirable characteristics of STJs and TESs, but have great promise for creating large-scale formats like current CCDs and CMOS detectors.

The largest current working KID-based instrument has an ~2,000 pixel array, a far cry from the needed 64 kpixel to 4 Mpixel KID-based arrays. Multiplexing such large arrays has been challenging. Because of SwRI's experience with several detector technologies, extensive electronics background, and radio frequency expertise, SwRI is positioned for making large format KID arrays a viable alternative to CCDs and CMOS detectors in such areas as precision scientific, military, and medical imaging.

The current approach for multiplexing arrays relies on detecting changes in resonance by injecting a signal with multiple frequency components as the source signal. The frequency components within the source signal are designed to match the resonant frequency of each sensor element. If the array has N elements, then N frequencies are required to stimulate all of the elements in the array. The output of the array is a signal with multiple frequency components, ideally one for each sensor element. The spectral response of the array is measured with no photons present. When photons are absorbed by an element, its resonant frequency will change, and detecting the change in frequency indicates detection of photon absorption.

While this method has been proven to enable detection of photons, it has two key drawbacks that limit its utility in remote and in size-constrained applications. The first is in device characterization. Each element is designed with a different resonant frequency, but because of manufacturing tolerances and variation due to temperature, the exact frequency is unknown. Each element of the array needs to be individually characterized to identify its resonant frequency under precisely controlled conditions. Then, combining all resonant frequencies generates a single source signal. A second, even greater challenge is that the resonant frequency of each element changes with micro-Kelvin changes in temperature. This necessitates in-system re-calibration of the resonant frequency of each element with and without photon absorption. After re-calibration, the electronics that generate the source signal need to be modified with the new set of frequencies, as do the electronics and signal processing for sensing the changes in resonant frequency due to photon absorption. The large number of elements in arrays required for many sensing applications exacerbates the problem.

Approach — The multi-frequency source signal is replaced with white noise, a signal that contains equal power within every frequency across the band of interest. The constant power spectral density enables every element in the array to resonate, as long as its resonant frequency is within the band of interest. Measurement of the array output is very similar to that of the multi-frequency source. The white noise causes each sensor element to resonate, and the spectral response of the array will contain a notch at the resonant frequency of each sensor element. Instead of needing to calibrate each element to determine its

resonant frequency, a measurement of the response is taken during dark conditions, and only changes in resonances need to be detected for detection of photon absorption.

Accomplishments — The basic design of the output electronics for detecting frequency shifts has been completed.

2013 IR&D Annual Report

Capability Development for Extreme Ultraviolet Imaging and Calibration, 15-R8322

Principal Investigators

[Michael W. Davis](#)

G. Randall Gladstone

Jerry Goldstein

Thomas G. Greathouse

Kurt D. Retherford

Gregory S. Winters

Bill R. Sandel (University of Arizona)

Inclusive Dates: 07/01/12 – Current

Background — SwRI has a nearly 20-year history of designing, integrating, testing and launching ultraviolet spectrographs. Beginning with the EUVS rocket in 1993 and continuing through four iterations of the Alice line of spectrographs, SwRI's UV spectrographs have successfully returned data from comets, asteroids, the Moon, planets and even stars. However, virtually all of these observations were made in the far ultraviolet (FUV) range, longer than 100 nm. The next step in advancing this technology is to expand SwRI's capabilities to even shorter UV wavelengths.

Approach — The objective of this project is to develop the capability to build and calibrate instrumentation that operates solely in EUV wavelengths. An improved version of the IMAGE-EUV imager will be designed. Upon selection by NASA, the imager will be built and calibrated at SwRI. Along with a notional design, some of the technical risks in building and testing an EUV imager will be reduced in preparation for the next appropriate NASA mission opportunity. Finally, calibration of an existing detector system at EUV wavelengths will be conducted using all of the steps that would be performed in a real flight EUV instrument calibration. By the conclusion of this project, SwRI will be positioned to be the leader in EUV instrument design and calibration.

Accomplishments — A baseline imager design was developed that increases the field of view 43 percent while increasing the collecting area by 20 percent over the previously built imager. A multilayer mirror coating that doubles reflectivity over the previously built imager and a vendor experienced with the coating have been located. FUV-blocking filters were measured and it was confirmed that their EUV transmission matches the manufacturer specification. Also the EUV performance of a spare detector was measured.

2013 IR&D Annual Report

Develop Transplantable Vascularized Cell Constructs to Accelerate Wound Healing, 01-R8214

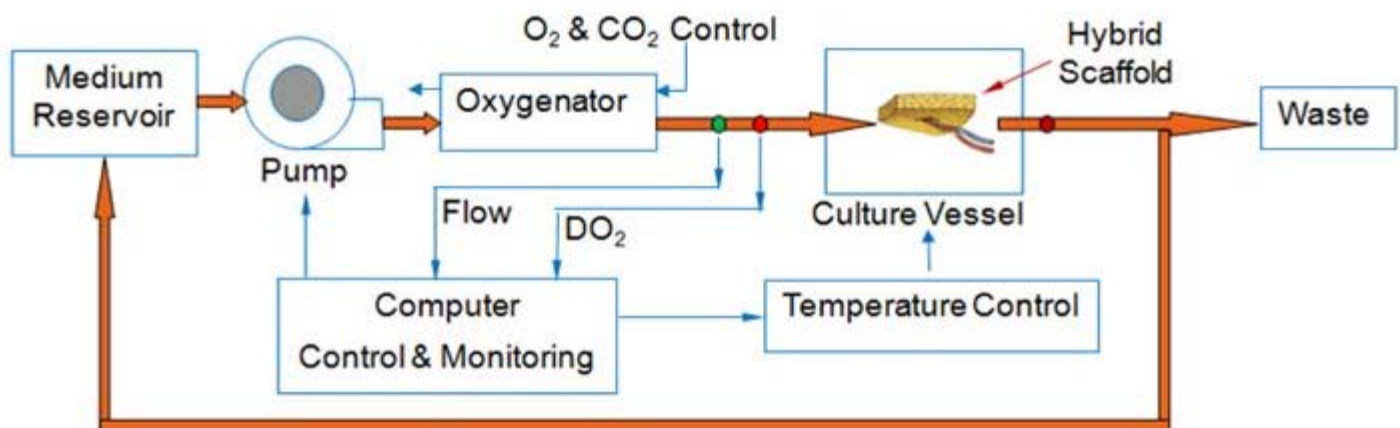
Principal Investigator

Jian Ling

Inclusive Dates: 04/01/11 – 12/01/12

Background — One of the most promising treatments for both chronic and combat wounds is tissue transplantation, especially the microsurgical free-flap reconstruction. This procedure completely detaches skin and fat, including arteries and veins, called the flap, from one part of the body and moves them to the wound sites. This procedure has shown to be 95 percent successful in many wound treatments. However, free-flap reconstruction is limited by the availability of the tissue flaps from either autograft or allograft due to donor-site morbidity. The objective of this project was to develop engineered "tissue flaps" to accelerate the wound healing process.

Approach — A hybrid scaffold was developed to mimic a free flap. The hybrid scaffold was composed of a three-dimensional, cylindrical porous scaffold wrapped around a membrane material in tubular shape. The cylindrical porous scaffold is made of composite materials including polycaprolactone (PCL), collagen and fibrin. While PCL enhanced the mechanical properties of the overall scaffold for *in vivo* implantation, the collagen and fibrin can promote cell growth and vascular formation. The tubular-shaped membrane material formed a flexible perfusion chamber that allows the 3D scaffold to be perfused *in vitro*, as well as *in vivo*, through connections to host blood vessels. A dynamic perfusion system (see illustration) was developed to perfuse the hybrid scaffold to supply nutrition and oxygen to cells cultured on the hybrid scaffold. Traditional static culture through diffusion makes it difficult to deliver nutrition and oxygen to cells residing inside a scaffold greater than 3mm in thickness. Human umbilical vein endothelial cells (HUVECs) and human bone marrow mesenchymal stem cells (hMSCs), were co-cultured on the hybrid scaffold to convert the scaffold into a cell construct with initial vascular system.



An in vitro perfusion system to mimic blood flow to convert the hybrid scaffold to a cell construct that mimics an engineering flap with initial vascular system before in vivo implantation.

Accomplishments — This project proposed a new idea of a tissue-engineered composite scaffold to mimic free flaps used in reconstruction surgery. The composite scaffold is expected to be implanted *in vivo* and directly anastomosed with host blood vessels like a free flap for wound healing. Based on

preliminary data, two patent applications were submitted: "Engineered Tissue Implants and Methods of Use Thereof" and "Hybrid Tissue Scaffold For Tissue Engineering."

[2013 IR&D](#) | [IR&D Home](#)

2013 IR&D Annual Report

Metabolomics of Radiation Exposed Rats, 01-R8259

Principal Investigators

[Kristin A. Favela](#)

Mike Dammann

Inclusive Dates: 10/01/12 – 06/30/13

Background — In the event of a radiological disaster, the mass screening of a population (civilian or military) to determine the amount of absorbed dose will allow for the correct level of care to be delivered. This triage approach requires methodology that is accurate, rapid and minimally invasive. Biomarkers that are present in human breath or saliva are attractive targets; recent studies have shown definitive evidence of radiation biomarkers in urine, but these studies have not examined breath or saliva.

Approach — This project used an animal model (male Agouti rats) and a metabolomics approach in an attempt to identify novel biomarkers in plasma, breath and saliva using comprehensive two-dimensional gas chromatography time-of-flight mass spectrometry (GCxGC-TOF MS). GCxGC-TOF is well-suited for the discovery of trace components in complex biological matrices. Neither breath nor saliva had been previously identified for indicators of radiation exposure. Specifically, groups of four rats were exposed acutely and chronically to low doses of radiation. Control groups were administered a sham dose. Breath, saliva and plasma were collected over a period of time and assayed by GCxGC-TOF MS.

Accomplishments — A total of 1.8 million individual data points were collected on the breath, saliva and plasma samples representing a massive data mining challenge. A sophisticated data reduction program reduced the data set to the most meaningful 450,000 signals for processing by principal components analysis (PCA). Complex trends were observed in the saliva and plasma data, indicating differences in metabolomics expression among the test and control groups. Analysis of the breath was limited by the sampling time and low lung volume. This project has benefitted external projects in numerous and synergistic ways. The informatics gains made by this project have resulted in a significant increase in sample load for this technology.

2013 IR&D Annual Report

Combined Laser and Medicated Scar Therapies, 01-R8276

Principal Investigators

Gianny Rossini

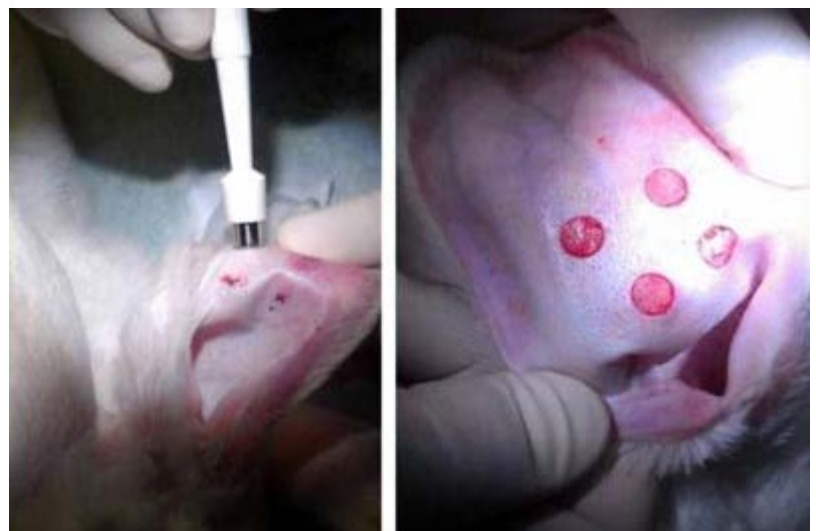
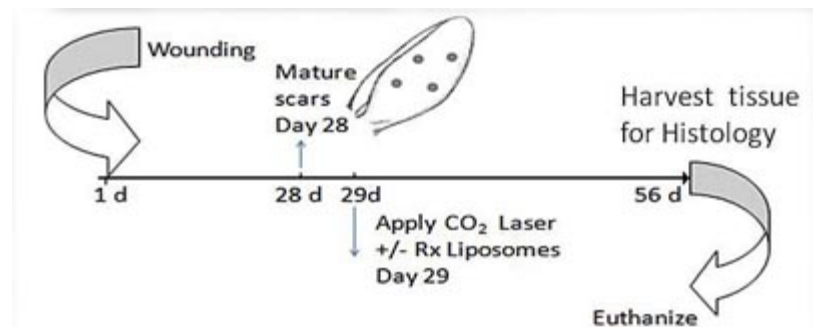
Gloria E. Gutierrez

Inclusive Dates: 01/01/12 – 12/01/13

Background — Large dermal scars on the skin, in particular on the face, represent a difficult problem in terms of treatment options and a major morbidity not only functionally but also in terms of psychological effects due to social stigmatization. The current development of a fractionated, CO₂ laser for scar treatment has created a considerable opportunity for not only scar treatment but also for dermal drug delivery in general, as the laser procedure itself creates transient microchannels in the skin leaving a perfect route for dermal drug delivery to the otherwise impermeable skin barrier. To develop a formulation able to penetrate the tissue modified by laser microporation, such a formulation needs to carry a large payload and be flexible to navigate the transient and narrow walls left after the laser procedure. The main goal of this project was to develop a transdermal formulation using flexible liposomes loaded with a common scar medication: triamcinolone acetonide (TCA) as well as another FDA approved drug, a proteasome inhibitor known to have an effect on reducing scar formation. Developing these transdermal formulations with enhanced skin penetration can increase the number of potential therapeutic applications, not only for the treatment of scars, but also for many other dermatological diseases and conditions.

Approach — The approach used consisted of formulating flexible liposomes (ethosomes, transferosomes, and cubosomes) as carriers for the FDA-approved drugs: corticosteroid Triamcinolone acetonide and bortezomib (Velcade) for scar mitigation. Liposomes were characterized in terms of particle size, surface charge, drug loading and release, followed by skin permeation studies on synthetic skin and full-thickness human skin (obtained from tissue banks) to study drug absorption using Franz cell system together with confocal imaging to confirm liposomes permeation. In the last part of this project, SwRI's dermal formulation was tested in combination with a laser microporation procedure using an established rabbit hypertrophic scar model.

Accomplishments — TCA and Velcade were successfully formulated using conventional and non-conventional liposomes, and controlled-release was demonstrated over a 17-day time period needed for the intended use. Skin



To study the efficacy of the therapy, researchers performed a rabbit-ear model pilot study.

permeation of TCA formulated in
ethosomes using full-thickness human
skin was three times higher than current TCA cream, which is commercially available. Using confocal
imaging microscopy, skin penetration was demonstrated down to 30 microns in depth consistent with
penetration of the stratum corneous, the most impermeable portion of the skin. A rabbit-ear model pilot
study was performed, and this model was established up to day 56 well beyond the standard 28 days (see
illustration), which was a key element for testing the formulations after laser treatment using the
established scar model. The final efficacy study using this extended scar model is still pending; however,
preliminary measurements using a caliper indicate positive results consistent with the goals of scar
improvement and prevention.

2013 IR&D Annual Report

Applied Dermal Delivery Nano-Formulations, 01-R8321

Principal Investigators

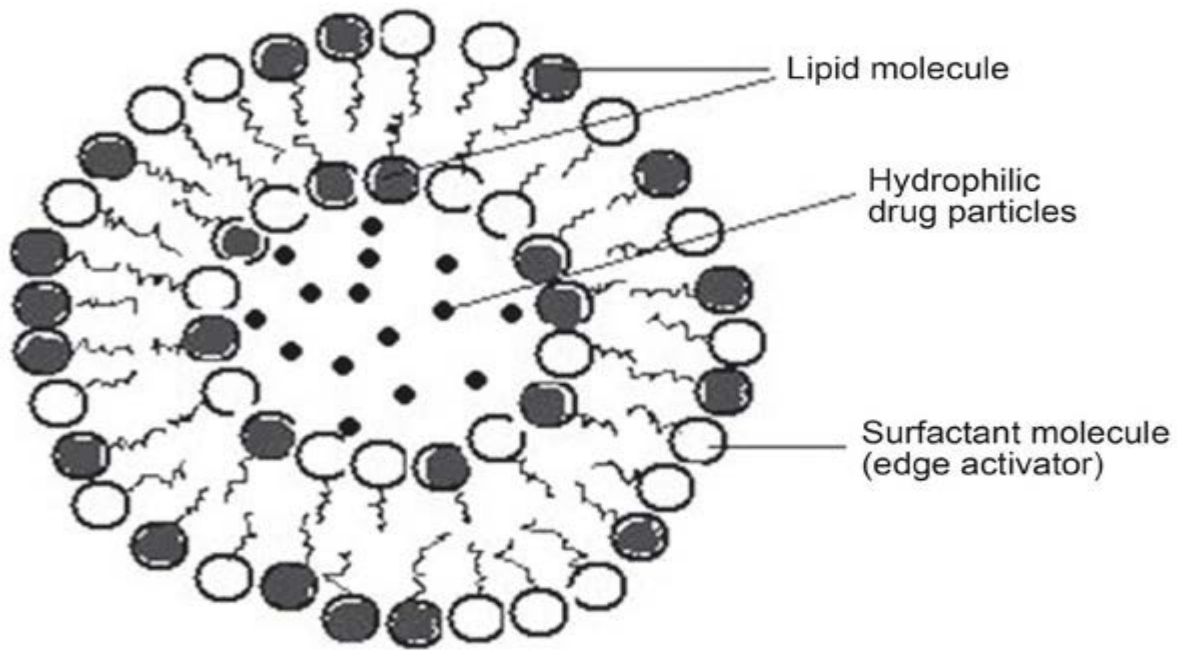
Gianny Rossini

Lucy De Leonibus

Inclusive Dates: 07/11/12 – 11/11/12

Background — Skin is a formidable barrier that protects us from environmental exposures. Water-soluble compounds cannot permeate the skin barrier; however, small-molecular-weight, lipid-soluble compounds have shown significant skin penetration. The lipid-soluble drugs estrogen, scopolamine and nicotine have already been formulated as easy-to-use dermal patches. Up to 2010, the list of transdermal or local use drugs on the U.S. market was limited to 25 drugs plus nine additional drugs in clinical trial. Also, ongoing clinical trials involving microporation techniques are expanding the opportunities for transdermal delivery to a new level. The first goal of this project was to formulate drugs for the treatment of dermal parasites, such as Leishmaniasis, which have a wide range of water-solubility. For this purpose, ethosomes and cubosomes were used because they are excellent in masking the water-soluble portion of the drug, while at the same time being flexible and around 200 nm in size. Our second goal was to test compounds of interest for the expression of bone morphogenetic protein (BMP), a potential target of interest.

Approach — This project was based on dermal drug delivery using flexible liposomal formulations, known as ethosomes, transferosomes, and cubosomes (see illustration), for which SwRI has significant past experience. Flexible liposomes were prepared for a variety of compounds provided by SwRI collaborators. New preparation methods were developed based on the solubility properties of the compounds, and these formulations were tested on a Franz cell apparatus loaded with synthetic skin to determine skin permeability. Particle size was measured using Photon Correlation Spectroscopy (PCS). Flexibility was measured using extrusion across a small pore-sized membrane under constant nitrogen pressure and, the weight ratio of extruded and non-extruded was used to calculate the apparent permeability. Bone morphogenetic protein levels were measured using real-time-polymerase chain reaction (RT-PCR).



Representation of flexible liposome loaded with hydrophilic drug.

Accomplishments — A pilot study was conducted for each of the seven drugs in consideration plus appropriate controls using the above-mentioned flexible liposome technologies. Each formulation was fabricated at multiple drug loadings, with the aim of testing the best technology before scaling up. After evaluating the pros and cons of each technology, the best option was to use ethosomes as the most likely to perform well *in vivo*. Also, this formulation was the only one able to load the highest amount of drug needed for this project (close to 5 percent drug loading). As a final product, ethosomes were prepared with loading between 1 percent and 5 percent, particle size close to 200 nm for lower drug concentrations and zeta potential of -30 mV. To improve sample viscosity, a thickening agent, Carbopol 940, was used with pH close to neutral. In short, 30 mL of each drug was prepared for a total of seven drugs plus controls. The final dermal formulation was based on the ethosome technology, which demonstrated several-fold improved permeability over controls in a Franz cell testing device. Selected compounds were tested *in vivo* showing promising results in the treatment of Leishmaniasis.

2013 IR&D Annual Report

Photoresponsive Polymeric Composites Utilizing UV Light Harvesting from Upconverting Nanoplatelets, 01-R8334

Principal Investigators

Benjamin R. Furman

Kelly L. Nash (UTSA)

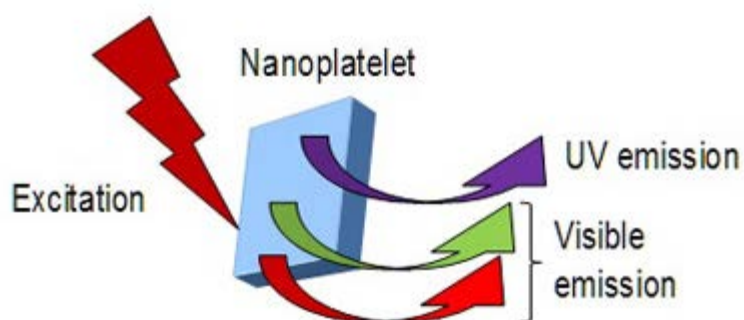
Inclusive Dates: 09/01/12 – 08/31/13

Background — This project was initiated with the aim of developing breakthrough capabilities in the areas of photoresponsive nanomaterials and photoacoustic detection methods. Highly luminescent upconverting nanocrystals (UCNCs) were developed that can initiate the depolymerization of crosslinked hydrogels. The UCNCs are promising for the initiation of high-energy photochemistry using safe and inexpensive near-infrared laser sources.

Approach — UCNCs were synthesized at SwRI and incorporated into a photochemically adaptable hydrogel matrix. Physical characterization of the luminescence and photoacoustic properties of the composite were conducted at UTSA. A thiolated polyethylene glycol (PEG) system was selected for the nanocomposite matrix due to its commercial availability and unique responsiveness to long-wavelength ultraviolet light. Filler materials were selected from materials based on NaYF_4 and its analogs (e.g.

LiYF_4 , NaYbF_4 , NaGdF_4 , etc.). The upconversion luminescence of these crystalline structures is especially strong owing to their unique combination of hexagonal symmetry and crystal field behaviors. The materials possess both monovalent and trivalent cation sites that facilitate the manipulation of the intrinsic photoluminescence behaviors through ion substitution. Extensive use of microwave methods allowed the team to shorten the development cycle for new UCNC compositions and significantly extend the formulations beyond those originally proposed.

Accomplishments — During the course of the project, a new ionothermal microwave synthesis was discovered that provides unprecedented control over particle size, size distribution, crystallinity and photoluminescence intensity of UCNCs. The program yielded new hydrogel-based nanocomposites with photoemissive and photoresponsive capabilities. These capabilities can be integrated into drug-releasing, wound-care and dental materials and are useful for applications involving antimicrobial and photodynamic biomedical therapies. They also bear relevance to calls within the U.S. Department of Defense for developing game-changing, multifunctional, autonomic and shape-responsive materials.



Schematic of multi-wavelength emissions from a nanocrystal by upconversion luminescence processes.

2013 IR&D Annual Report

A New Generation of Bone Cements/Grafts Based on Magnetic Calcium Phosphate Nanoparticles (MCP NPs) Using a Magnetic Field-Triggered-Polymerization (MFTP) Process, 01-R8370

Principal Investigators

[XingGuo Cheng](#)

Qingwen Ni

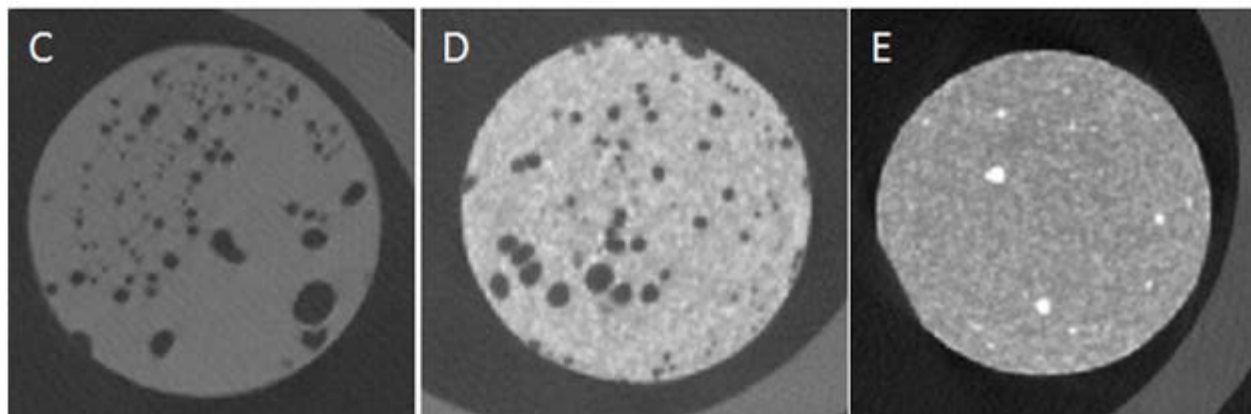
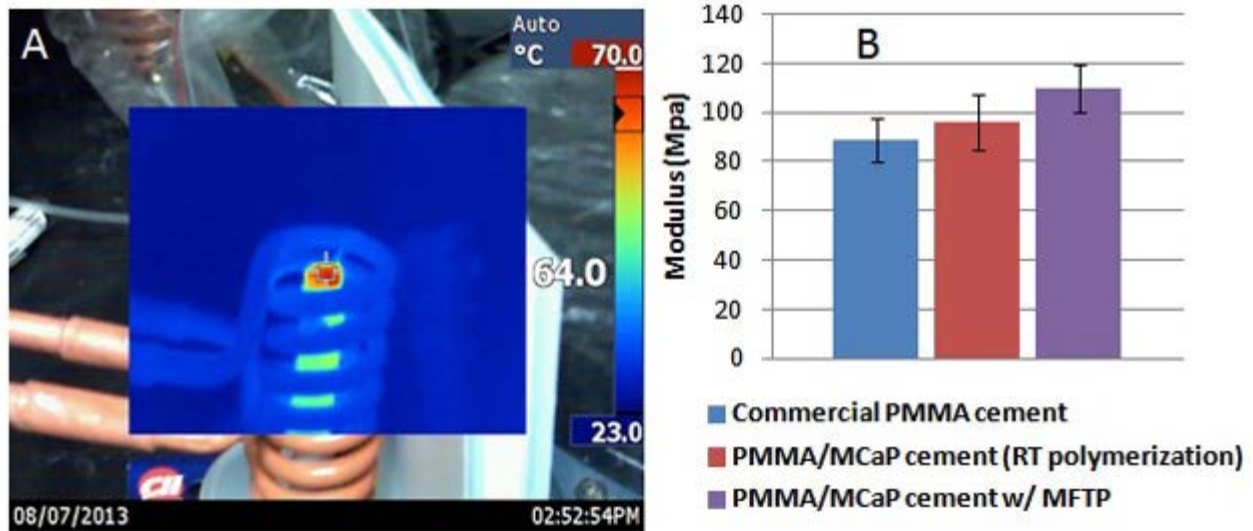
Todd Bredbenner

Daniel Nicolella

Inclusive Dates: 02/11/13 – 08/30/13

Background — Traditional bone cement prepared by spontaneous polymerization of acrylic monomer has several drawbacks such as poor cell attachment, nondegradability and poor radio-opacity. The addition of radio-opaque material such as BaSO₄ or ZrO₂ in the cement further deteriorates its mechanical properties due to weak interfacial bonding. New MCP NP-containing bone cements were investigated using either the traditional process or the MFTP process compared with the PMMA bone cement without MCP NPs. It is thought that new bone cements will have improved radio-opacity, cell attachment and mechanical strengths, due to the incorporation of highly biocompatible MCP NPs and strong interfacial bonding.

Approach — First, MCP NPs were mixed with an organic matrix composed of a monomer (i.e., methyl methacrylate, MMA), a free radical initiator (i.e., benzoyl peroxide, BPO), PMMA beads, and a small amount of activator (i.e., N,N-dimethyl-4-toluidine, NDMT) to form a uniform mixture (dough-like or gel-like). Second, the mixture was injected into a mold and placed inside a coil, which elicited median-level alternating magnetic field (AMF). MCP NPs generated heat and trigger the controlled polymerization and hardening of the organic matrix (Figure 1A). Finally, the new bone cement was characterized by micro-CT, biomechanical testing following ASTM F451-08 and *in vitro* cell testing. Moreover, MCP NPs-containing new bone cement was prepared using the traditional method (i.e., spontaneous polymerization).



A. Infrared thermo image showing the formation of new bone cement inside the coil due to the heat generated by MCaP NPs under an alternating magnetic field (AMF). B. Compressive modulus of various bone cements. C-E. Micro-CT cross sections of the traditional PMMA bone cement, PMMA/MCaP cement w/ RT polymerization, and PMMA/MCaP cement w/ MFTP process.

Accomplishments — New MCaP NPs-containing bone cements had significantly higher modulus (Figure 1B, $p < 0.05$), higher ultimate strength, improved radio-opacity (Figure 1C-E), and improved attachment of pre-osteoblasts, compared to pure PMMA bone cement that contains only PMMA beads, but no radio-opaque material. It was demonstrated that new MCaP NP-containing bone cement/grfts with improved properties could be prepared using the MFTP process or traditional spontaneous polymerization. MCaP NP-containing bone cements/grfts can be used as replacements of traditional bone cements/grfts, thermo-responsive treatments or triggered drug release (e.g., bone cancer, infections), and bone repair and regeneration.

2013 IR&D Annual Report

Drug-loaded Magnetic Calcium Phosphate Nanoparticles (MCaP NPs) for Cancer Therapy, 01-R8400

Principal Investigators

[XingGuo Cheng](#)

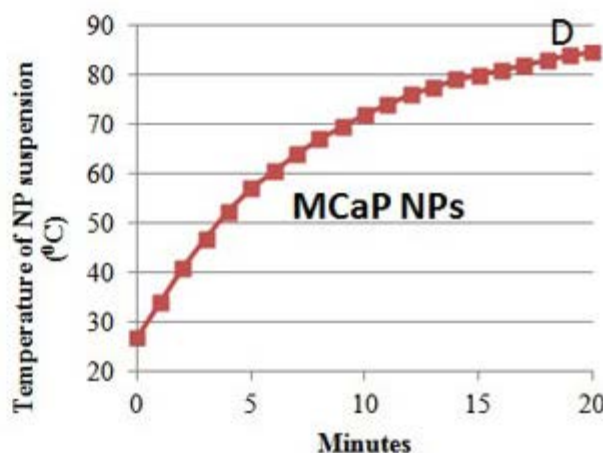
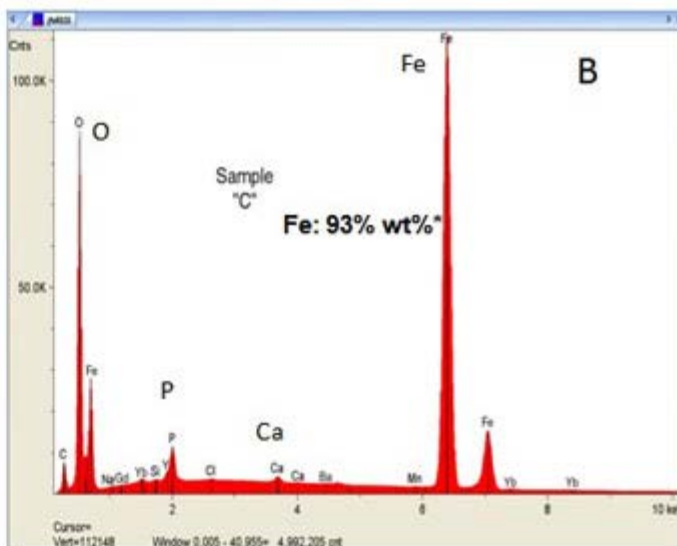
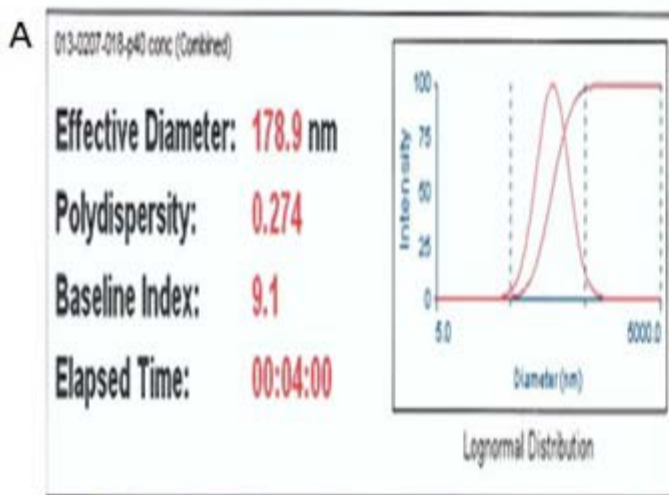
Qingwen Ni

Hakan Basagaoglu

Inclusive Dates: 07/01/13 – Current

Background — One in four deaths in the United States is attributable to cancer, with prostate and breast cancers the most common forms. The current systemic chemotherapy drug treatment of cancer has two major disadvantages: severe side effects and drug resistance. There is a clear need to develop a novel cancer therapy to effectively treat cancer with fewer side effects. The objective of this project is to develop newly formulated MCaP-based magnetic NPs as a combinational therapy for advanced breast/prostate cancer treatment. Both magnetic induction heating (hyperthermia-based therapy) and NP chemotherapy will be used to kill cancer. Targeted dual therapy can effectively treat cancer because of its possible synergistic effect and unique targeting mechanism.

Approach — This project has three objectives: synthesize and characterize MCaP NPs and investigate drug loading and release; evaluate the efficacy of MCaP NPs combination therapy *in vitro* and determine the minimum concentration of MCaP NPs required for tumor hyperthermia; and evaluate MCaP NP accumulation in a xenograft tumor mice model and treatment efficacy *in vivo*.



A. Particle size of a MCAp NP formulation. B. EDX analysis of a MCAp NP formulation that has high loading of iron oxide inside the CaP. *Note: Results do not include elements with $Z < 11$ (Na). C. Purchased bench top IHG061A induction machine (coils of different sizes are available). D. The induction heating capabilities of our prepared MCAp NP suspension in water (18.6 mg/mL). The MCAp NPs can be heated to 60°C within 6 min.

Accomplishments — The MCAp NP formulation was improved by fine-tuning the amount of CaP encapsulating the iron oxide magnetic NPs. As shown in Figure 1A-B, at similar NP size (~180 nm), MCAp with iron loading up to 94 wt percent can be formed. By reducing the amount of CaP, more iron oxide was encapsulated inside and thus the magnetic heating capability will be increased. NP formulation with the highest Fe loading was heated up using alternating magnetic field (AMF). As shown in Figure 1C-D, MCAp NPs can be heated up to 60°C within six minutes. Drug-loaded NPs were magnetically separated and analyzed by UV-vis. In the next phases, these targeted, drug-loaded NPs will be tested *in vitro* and *in vivo* to ascertain if they are viable for cancer treatment.

2013 IR&D Annual Report

Determination of PAHs in the Rubber by GC/MS, 08-R8402

Principal Investigator

Joseph Pan

Inclusive Dates: 07/01/13 – 06/30/14

Background — On May 29, 2007, The European Commission of the European Union issued 1906/2007/EC (by REACH under EC, Registration, Evaluation, Authorisation and Restriction of Chemicals). The European Union law requires that as of January 1, 2010, the total concentration of eight specified polycyclic aromatic hydrocarbons (PAHs) must be less than 10 ppm and benzo(a)pyrene, BaP, must be less than 1.0 ppm in the oils isolated from the tire rubbers. The specified official method for meeting the REACH standards is ISO 21461, which is an NMR method. ISO 21461 does not produce PAH data that allows direct comparison with the specific PAH limits in the original REACH standards. A method that determines PAH levels in the rubber and allows direct comparison with the specific PAH limits in the REACH standard is needed. Most car/truck tires have carbon blacks in them to enhance tire performance. However, most carbon blacks contain moderate to high levels of PAHs. The European Union law does not limit PAH contents in the carbon blacks being put into the tires. This project will demonstrate that the PAHs contained in the carbon blacks will easily throw the total PAHs (including BaP) in the rubber over the EU limits set for the tire rubbers even though the process oils prior to being put into the tire contain PAHs within the EU limits set for the process oils.

Approach — The project had five objectives.

- Test and find the most effective solvent and find a better extraction technique for the extraction of PAHs from rubber samples that contain process oils and carbon blacks.
- Develop a robust rubber extract cleanup method that will produce clean rubber extracts for the PAH determination by GC/MS.
- Apply the SwRI-developed GC/MS method for the accurate and precise determination of the PAHs in rubber extracts from rubber samples. This GC/MS method will be validated by analyzing the rubber made with process oils previously doped with known amounts of NIST PAH SRM 6620a (National Institute of Standards and Technology, Standard Reference Materials).
- Demonstrate that the SwRI-developed GC/MS method is superior to the ISO 21461 NMR method by analyzing PAHs in the rubber using both methods. On the same rubber samples, compare the GC/MS produced PAH results against the "original REACH PAH standards" and compare the ISO 21461 produced results against the "proxy REACH PAH standards."
- Demonstrate the significant contributions of carbon blacks to the PAH levels in the rubbers by analyzing rubber compounds with and without the carbon blacks in them.

Accomplishments — Extraction tests of a custom-made rubber with acetone, carbon disulfide, carbon tetrachloride, cyclohexane, 1,4-dioxane, and toluene indicate that toluene has the highest PAH extracting efficiency from the rubber. A previously developed cleanup method for the process oils works well on the rubber extracts for the PAH GC/MS analysis. The size of the rubber bits has bearing on the PAH extraction efficiency: the smaller the rubber bits, the higher the PAH extraction efficiency. However, if the small rubber bits (0.1 to 1.0mm) were generated by a liquid nitrogen cryo-mill milling the rubber by impact, this trend may not hold.